Ollscoil na hÉireann, Corcaigh
The National University of Ireland, Cork
University College Cork

School of Food and Nutritional Sciences
Head of School: Prof. Mairead Kiely
Supervisors: Prof. James A. O'Mahony and Dr. Tom F. O'Callaghan

Characterisation of the changes in the physicochemical properties of high-solids skim milk during thermal processing, and their relationship with fouling

Thesis presented by
Tara R. Murphy
B.Sc. Food Science, University College Cork
for the degree of
Master of Science
in
Food Science and Technology
September 2023

Table of Contents

Declaration

I hereby declare that the work submitted is entirely my own and has not been submitted to any other university or higher education institute, or for any other academic award in this university.

Signature:

Tara Murphy

Date: 21st September 2023

Acknowledgements

I would like to express my appreciation and thanks to my academic supervisors, Prof. Seamus O'Mahony and Dr. Tom O'Callaghan, for the opportunity to pursue my research MSc at University College Cork, and for their patience, guidance, and supervision throughout my studies.

I would like to thank Enterprise Ireland for funding my research through the Dairy Processing Technology Centre. I would also like to express my gratitude to the technical and administrative staff in the School of Food and Nutritional Sciences, including Theresa Dennehy, Avril McCord, Johann Scollard, Dave Waldron, Dr Therese Uniacke-Lowe, Anne Cahalane, and Anne Fenton.

I would like to thank all my colleagues and friends in the Food Ingredients Research Lab – Amrutha, Francesca, Mestawet, Nadia, Niamh, Nicolas. A particular mention to Eoin, Tessa, Jasper, and Tom. Eoin, Tessa, and Jasper – thank you for always looking out for me, both inside and outside the lab, you have all helped me get through these past two years and I will always be grateful for that.

A special thanks to my Mom and Dad for being my constant source of support and for shaping me into the person I am today. I am beyond fortunate to have you as my parents, and I will carry your love and guidance with me in all my future endeavours.

Finally, I would like to express my gratitude to Tom. Meeting you has made this whole experience worth it; you have changed my life for the better and I feel so lucky to be starting the next chapter of life with you.

This thesis is dedicated to my parents,

Sean and Marie, and my grandparents,

Bill and Phil.

Abstract

Fouling of thermal processing equipment during production of dairy products and ingredients is a challenge for the dairy industry, with evaporator fouling during the production of skim milk powder being an area of particular focus. The build-up of foulant mass deposit within different regions of the evaporator technology has significant economic, operational, and environmental consequences for the dairy industry, as the decline in the heat performance of the equipment results in more frequent cleaning required and increased energy and water consumption, in addition to potential deterioration in product quality as the required product temperature may not be achieved. The objectives of the work reported in this thesis were to study the effect of pH on the heat stability and physicochemical properties of concentrated skim milk during thermal processing to assess their contributions to evaporator fouling. Heating concentrated skim milk (30%, w/w, total solids; pH 6.0, 6.1, 6.2, 6.3, 6.4, 6.5, 6.6, 6.7) using a high temperature short time thermal treatment (90 °C x 3 min), using a rheometer, showed that as the pH of the samples decreased, both viscosity and particle size distribution increased after heating, coinciding with an increase in sedimentation. Heat treatment (90 °C x 2 h) of concentrated skim milk at pH 6.2 on the fouling rig resulted in severe fouling. Moreover, when the concentrated skim milk was analysed for particle size and sedimentation after heat treatment using the fouling rig, the findings aligned with the initial analysis conducted during the rheometer based HTST thermal treatment. Further characterisation of evaporator fouling was carried out by heat treating concentrated skim milk samples at pH 6.1, 6.3, 6.5 and 6.7 on the fouling rig while in-line measurements of pH, conductivity and temperature were conducted, followed by analysis of the concentrated skim milk samples, cleaning-in-place chemicals and foulant material adhered to the heat exchanger after the fouling experiments. It was observed that samples of concentrated skim milk that caused fouling also displayed increased viscosity, particle size and sedimentation when compared to the samples that resulted in no fouling. The adhered foulant formed at pH 6.1 and 6.3 was found to consist predominantly of protein on a total solids basis, with protein profiling showing that the most prominent proteins were denatured β-lactoglobulin and α-lactalbumin, as well as a strong presence of caseins. It was found that by maintaining the pH of concentrated skim milk above 6.3, fouling during heat treatment could be successfully avoided. Furthermore, through pH adjustment to achieve no fouling to extensive fouling, it was possible to analyse physicochemical properties such as viscosity, particle size, and sedimentation, to provide a practical approach to predict the potential for fouling in concentrated skim milk. These findings contribute significantly to

our understanding of the impact of protein stability on the formation of fouling deposits caused by concentrated skim milk, allow us to develop/validate predictive tools and to develop/test mitigation strategies for fouling.

Chapter 1

Literature Review

Methods for measuring and predicting fouling during thermal processing of thermal dairy solutions

Tara R. Murphy, Eoin W. Finnegan, Tom F. O'Callaghan, James A. O'Mahony

School of Food and Nutritional Sciences, University College Cork, Cork, Ireland

Declaration

This chapter was written by author Tara R. Murphy (TRM) and reviewed by all co-authors. TRM co-designed the study and performed all of the experimental work.

1.1. Introduction

Thermal processing is a key unit operation in the processing of many dairy products and ingredients. Milk is thermally processed in order to tailor its functionality, kill pathogens, and improve the overall shelf life by eliminating any other deteriorative organisms (Chandan *et al.,* 2015). These thermal processes include pasteurisation, ultra-high-temperature (UHT) processing, evaporation, sterilisation, and pre-heating, in a number of formats ranging from direct and indirect heating mechanisms. Fouling during thermal processing is defined as the build-up of foulant mass deposit in different areas of the thermal processing equipment, such as in pipes, on the heat exchange surface, and in any other fittings in the apparatus (Milanovic *et al.*, 2006). The formation of deposits can cause challenges during production by increasing the overall thermal resistance, resulting in a decline in the heat performance of the equipment. This can lead to corrosion, obstructions to fluid flow, increased pressure drop, and reduced heat transfer coefficient (Grijspeerdt *et al.*, 2003), which causes increased operating costs. There is also a possibility of deterioration in product quality, as the required product temperature may not be achieved (Mahdi *et al.*, 2009), as well as the possibility of deterioration in microbial quality of subsequent processing runs due to biofilm formation (Mérian & Goddard, 2012). In the dairy industry, fouling can be split into two categories (Huppertz & Nieuwenhuijse, 2022); 'Type A' is primarily caused by denaturation of the whey protein β-lactoglobulin (β-Lg) (Lalande *et al.,* 1984), and 'Type B' is due to mineral precipitation (particularly calcium phosphate) (Foster & Green, 1990).

It would be valuable for the dairy industry to have the ability to measure or predict the presence, type, and/or intensity of fouling that occurs in a thermal process when designing, improving, or adapting production processes in order to avoid unnecessary product or capital loss (Wallhäußer *et al*., 2013). However, fouling is a complicated process that depends on several often difficult-to-measure parameters, meaning it is challenging to achieve an accurate

quantification of overall fouling resistance (Bott, 2001). Several diverse approaches have been investigated to measure and/or predict fouling, and this review will outline and compare these different techniques. Furthermore, this review will explore the intricacies of fouling modelling and predictive algorithms, fouling simulators, in-process monitoring of fouling, and alternative rapid techniques for identifying fouling.

1.2. Heat-induced changes in milk

Thermal processing of milk results in biological, chemical, and physicochemical changes that can have significant effects on its organoleptic, nutritional, and functional properties (Fox *et al.,* 2015). Heat treatment leads to the denaturation of whey proteins, which involves the disruption of the protein's native structure, resulting in changes to their functional properties. Whey proteins, being globular proteins, are more susceptible to denaturation compared to the caseins, as casein lacks secondary and tertiary structure (Mulvihill & Donovan, 1987). The denaturation process in milk can be reversible or irreversible depending on the physicochemical conditions (Hoffmann & vanMil, 1997). In the reversible denaturation, whey proteins undergo partial unfolding, resulting in the loss of helical structure. However, in the irreversible denaturation, an aggregation process takes place, involving sulfhydryl (–SH)/disulphide (S–S) interchange reactions and other intermolecular interactions such as hydrophobic and electrostatic interactions (Anema & Li, 2000; McMahon *et al.*, 1993; Vasbinder & De Kruif, 2003). Typically, the aggregation of whey proteins occurs through the interaction of a free -SH group with the S-S bond found in cystine-containing proteins like β-lactoglobulin, κ-casein, α-lactalbumin, and bovine serum albumin. These interactions involve -SH/S-S interchange reactions and result in irreversible protein aggregation (Considine *et al*., 2007). The aggregated proteins form complexes of different molecular sizes, which depend on the heating conditions and the composition of the proteins involved (Ndoye *et al*., 2013).

Calcium phosphate plays a crucial role in the stability of casein micelles and the interaction between casein and whey proteins. Skim milk is a two-phase system of casein colloidal calcium phosphate in equilibrium with a serum phase of salts and proteins (Holt, 1985; Gaucheron, 2011). During the heating process, the solubility of calcium phosphate diminishes, causing its transfer to the colloidal phase, where it becomes associated with the casein micelles (Wang & Ma, 2020). This transfer is accompanied by a reduction in the concentration of calcium ions and a decrease in pH (On-Nom *et al.,* 2010). Both whey proteins and casein have calcium-binding sites, and they compete for calcium ions during heating (Morr & Josephson, 1968).

The pH of milk changes during heating due to several factors and reactions that occur as a result of the heat treatment. The primary factors influencing pH changes in milk during heating are related to the dissociation of certain components and the production of acidic or basic compounds (Chaplin & Lyster, 1988). Milk is a complex biological fluid containing various components that can act as acids or bases. The pH of milk is initially ~6.7, however, heating can alter the acid-base equilibria in milk, resulting in pH shifts (Salaün *et al.,* 2005). For instance, the dissociation of weak acids, such as lactic acid, can increase, leading to a decrease in pH. Conversely, the dissociation of weak bases, like phosphate ions, can decrease, resulting in an increase in pH (Gaucheron, 2005). As mentioned earlier, heat treatment can cause denaturation of proteins in milk. When whey proteins undergo denaturation, their native structure and conformation are disrupted, resulting in the exposure of previously buried ionizable amino acid residues. These exposed amino acids, particularly acidic residues such as glutamic acid and aspartic acid, can contribute to the release of hydrogen ions (H+) in the surrounding solution, decrease the pH of milk (Anema, 2021). Changes in the mineral equilibrium on heating causes a decrease in the pH of milk; Primary and secondary calcium phosphate precipitate as tertiary phosphate, releasing H+ ions, and organic phosphate,

specifically in the form of casein phosphate, undergoes hydrolysis and subsequently precipitates, leading to the release of H+ ions (Fox, 1985). The Maillard reaction, which occurs between reducing sugars (such as lactose) and amino acids, can also influence the pH of heated milk (Van Boekel, 1998). Lactose undergoes a conversion to organic acids, primarily formic acid, resulting in an increase in H+ concentration, decreasing the overall pH of the milk (Berg, 1997). It is important to note that the specific pH changes observed during heating can depend on the temperature, duration of heat treatment, composition of the milk, and any other factors that may influence the reactions mentioned above. Additionally, variations in starting pH and buffering capacity of milk can also affect the extent of pH changes during heating.

1.3. Properties of dairy foulant

Dairy fouling is a complex process that involves both aggregation of whey protein and formation of calcium phosphate in the bulk of the fluid (Mahdi *et al.,* 2009). Figure 1 shows the protein and mineral reactions that contribute to dairy fouling; Georgiadis & Macchietto (2000) proposed that the protein reaction takes place in the bulk and at the thermal boundary layer of milk. A first order reaction causes native protein to unfold, followed by a second order reaction causing the unfolded protein to aggregate, with only the aggregated protein forming deposits on heat transfer surfaces (Sava *et al.,* 2005). Initially a protein monolayer adsorbs onto the heat transfer surface at room temperature and as temperatures exceed 65˚C, β-Lg molecules begin to denature and unfold in the bulk of the fluid (Mahdi *et al.,* 2009). Aggregation of β-Lg occurs, and particles of calcium phosphate are formed in the bulk which are continually transported to the heat transfer surface; the activated molecules adsorb onto the heat transfer surface, forming fouling deposit (Simmons *et al.,* 2007). The deposition rate is proportional to the amount of aggregated protein adhering at the thermal boundary layer; the thicker the deposit, the higher the thermal fouling resistance (Georgiadis & Macchietto, 2000). Another important aspect of the dairy fouling process is mineral deposition as there is an inverse

relationship between mineral solubility and temperature that results in further fouling deposition. As calcium phosphate becomes less soluble in milk with increasing temperature, it precipitates out of solution and can produce deposits in the form of crystals on the heat transfer surface (Visser & Jeurnink, 1997). Some calcium ions can become entrapped within the protein deposit, stabilising the structure (Huppertz & Nieuwenhuijse, 2022). If the heat treatment exceeds 85˚C, calcium phosphate becomes the main component of the fouling deposit, with this type of deposit being able to entrap small aggregates of protein due to its open network structure (Mahdi *et al.,* 2009).

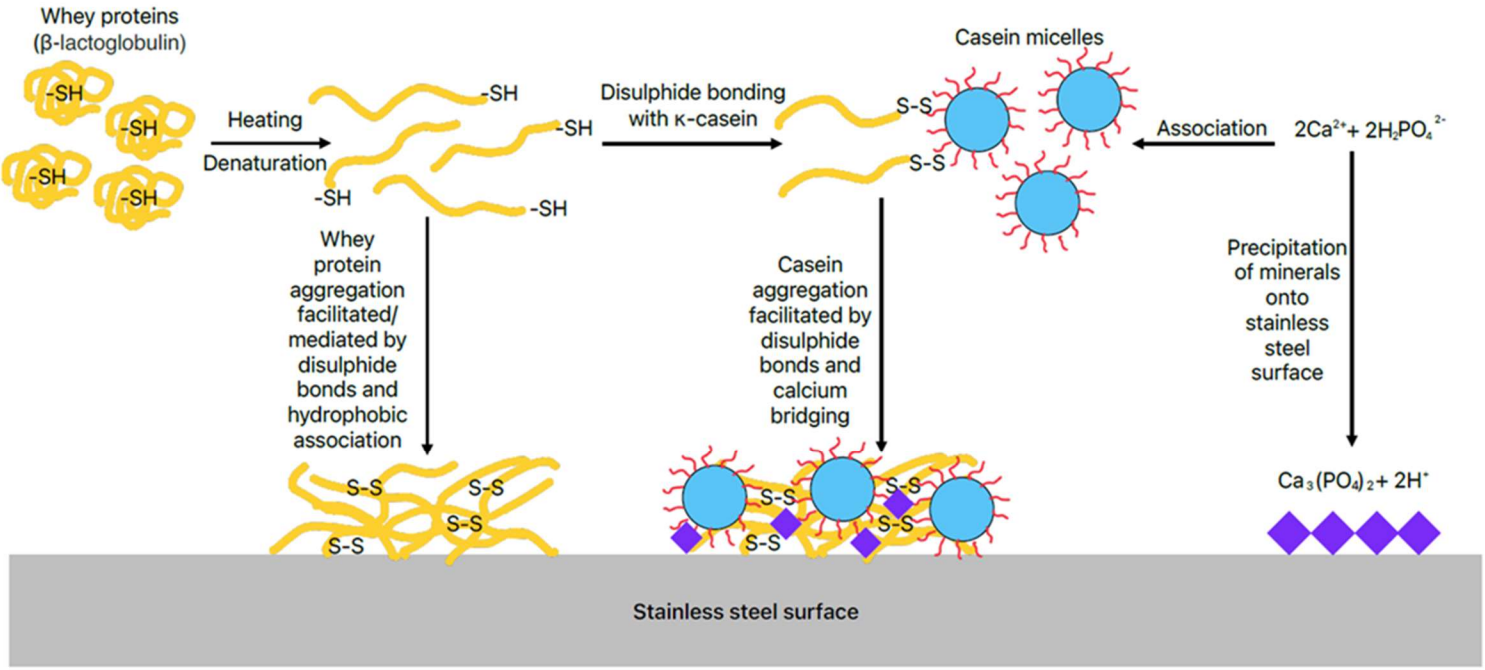

Figure 1.1.*: The protein and mineral reactions contributing to the formation of fouling deposit during thermal processing of milk.*

The extent of dairy fouling deposition is dependent on many different parameters, including protein concentration, flow velocity, pH, calcium content and temperature. Increasing protein concentration has been reported to enhance fouling as the aggregation rate of protein increases with concentration, resulting in a fast forming fouling deposit (Fickak *et al.,* 2011). In addition, a higher protein concentration forms a firmer deposit which is more

difficult to remove. Dairy fouling is also related to flow velocity; when dairy solutions are processed at turbulent flow there is a less severe occurrence of fouling, whereas a more laminar flow results in a greater build-up of fouling deposit (Belmar-Beiny et al., 1993). Heat stability of dairy proteins was shown to decrease with decreasing pH, meaning a higher degree of whey protein aggregation would occur at lower pH values (Law & Leaver, 2000) contributing to the occurrence of dairy fouling. Variations in calcium content of milk, either increasing or decreasing, generally lowers heat stability, which in turn increases the fouling prevalence (Roefs & deKruif, 1994). Temperature is one of the most important parameters impacting fouling during thermal processing, with the extent of fouling increasing with temperature (Belmar-Beiny *et al*., 1993). By understanding the various factors that contribute to dairy fouling, robust methods of measurement and prediction can be established and implemented.

1.4. Measurement and monitoring of fouling

A wide range of analytical approaches and devices have been used to measure and/or predict fouling in thermal processes (Table 1). The techniques reported include ultrasonic, acoustic, thermal, and electrochemical methods, and each have their own advantages, disadvantages, and specificities (Cheng *et al.* 2016; Milanovic *et al.,* 2006; Mairal *et al.,* 1999; Crattelet *et al.,* 2013). Adapting these techniques into in-line process analytical technologies (PAT) formats that can detect the onset and subsequent build-up of fouling for early operator intervention to mitigate/reduce fouling and optimise scheduling of the cleaning operation to minimise downtime and product loss (Withers, 1996).

1.4.1. Fouling thermal resistance

The overall fouling thermal resistance (FTR) is a measure of the resistance to heat transfer due to the thickness of a fouling layer (Asadi & Khoshkhoo, 2013). Therefore, the

higher the value of FTR, the greater the thermal resistance in the system. This value is commonly used as a measure of fouling across many different production processes. The calculation of the overall FTR can vary depending on the system, but generally it is calculated using a version of the following equation (TEMA Standards, 1988):

$$FTR = \frac{1}{U_M} - \frac{1}{U_c} \qquad (1)$$

Where U_M is the mean overall heat transfer coefficient U_c is the overall heat transfer coefficient for the heat exchanger with clean (unfouled) heat transfer surfaces. Both heat transfer coefficients were calculated by the dividing the heat flux by the difference in temperature between the heat transfer surface and surrounding fluid. The above equation was used by Milanovic *et al.,* (2006) to calculate the change in the FTR from experimental measurements of water passing through a double-pipe cooler. The experiment was carried out over 90 d, and changes in temperature at the inlet and outlet of the heat exchanger were recorded every 5 min. The initial value of the overall heat transfer coefficient was 1160 W/(m^2 K), decreasing linearly over time to 650 W/(m^2 K) after 90 d, and the overall fouling thermal resistance increased from 0 to 0.615×10^{-3} m^2K/W over the course of the experiment. The change in overall fouling thermal resistance was caused (primarily) by a mineral scale, previously shown to present linear fouling behaviour (Zubair *et al*., 2000). As mineral fouling is a key aspect of dairy fouling, this approach may be applicable to the dairy industry. This study demonstrates how the fouling resistance can be used as a simple monitoring system, but this value can also be used in more advanced modelling methods (Kern & Seaton, 1959; Gao *et al.,* 2021) described in further detail in Section 4.

1.4.2. Ultrasonic, acoustic, and electrochemical techniques

With technology advances in recent years, fouling can be detected with sensors that can process signals faster than the rate of fouling occurs allowing for early detection before the degree of fouling becomes too severe (Hay & Rose, 2003; Lohr & Rose, 2003). Many of these sensors are based on ultrasonic, acoustic, and electrochemical signals (Withers, 1996). The principle of ultrasonic sensors is based on the use of sound waves to detect the location of a stationary or moving interface. The waves travel through the media, with the velocity of the waves dependent on the medium they travel through, allowing observations on the medium's physical characteristics to be obtained (Bond *et al.,* 2003). The acoustic impedence is calculated by ρc; where ρ is the density of the medium and c is the wave velocity through the medium (Dalmont, 2001). When the ultrasonic wave comes into contact with an interface between two media (e.g., a fouling deposit), the energy is partitioned in a way that results in a reflected wave. The amplitude of this reflective wave is a function of the acoustic impedence difference between the media and topography of the fouling deposit (Ensminger & Bond, 2011).

Mairal *et al.* (1999) developed a novel approach for the measurement of fouling of reverse osmosis desalination membranes in real time and *in-situ* using ultrasonic time-domain reflectometry (TDR). The measurements obtained through ultrasonic TDR were compared with more traditional fouling indicators such as changes in permeate concentration, flux decline, and degree of membrane surface coverage and a good correlation (r=0.73) was reported between decline in ultrasonic signal amplitude and growth of the fouling layer. Ultrasonic TDR was found to be particularly sensitive for monitoring the initiation of the fouling layer, as well as its removal during cleaning, implying that it could be a useful tool in early real-time detection of fouling to prevent product loss, as well as a tool in quality control to check the efficiency of cleaning. It was also possible to measure the fouling layer thickness

by calculation of the time delay between the initiation of the emitted and received transducer signals, when the velocity of the medium was known; after analysis of the entire data set obtained during the fouling experiment by Mairal *et al.* (1999), it was concluded that there was a statistically significant correlation between flux decline and surface coverage, and between amplitude decline and surface coverage. This indicates that amplitude changes work just as well as flux-decline measurements for tracking fouling behaviour. Even though variation in some of the amplitude decline data was high due to its complex nature, this study shows that ultrasonic sensors are a promising option for monitoring fouling due to their low cost and ability to operate non-invasively in opaque systems (Wang, 2015).

The presence of a fouling layer can be detected by an acoustic sensor through measurements of amplitude and the natural frequency of vibration, with a decrease in these values indicating the build-up of a fouling deposit (Prakash *et al.,* 2005). An acoustic sensor was specifically designed for use in plate heat exchangers by Dam Madsen (1994), consisting of a small transducer placed on the inside surface of one plate within the plate heat exchanger. During processing, the presence of a fouling film coats the surface of the transducer, dampening the amplitude of its vibrations and reducing its natural frequency. The sensor was designed to ensure it would foul in the same way as the rest of the plate heat exchanger, allowing the measured amplitude and frequencies to be related to the degree of fouling. The sensor was able to detect fouling thickness ranging from 0.1-0.4 mm and could gradually detect the build-up of fouling through an increasing trend in its resonant frequency. Merheb *et al.* (2007) used multiple acoustic sensors to monitor dairy fouling in a plate heat exchanger in real time. Analysis of low-frequency acoustic waves that were propagated through the plates, via comparison of the development of the acoustic wave parameters, allowed for a fouling rate to be obtained for each zone inside the exchanger. This use of multiple fouling detection sensors in a thermal process would be a valuable asset to the dairy industry, as it could be used to non-

invasively identify ‘hotspots’ for fouling build-up in processing equipment in order to develop targeted adaptive strategies for the mitigation of fouling.

The use of electrochemical devices in industrial fouling detection has been studied with a particular emphasis on biofilm fouling and the use of voltammetric sensors (Kang *et al.,* 2012; Muthukumaran *et al.,* 2016). While the literature regarding the detection of dairy fouling using voltammetry is not as well established, a study by Fysun *et al.* (2020) showed promising results for the use of cyclic voltammetry and square wave voltammetry in dairy fouling monitoring. Voltammetry measures the current of a sample with changing potential, as the current results from oxidation or reduction of the electroactive species in the sample (Thévenot *et al.,* 2001). Cyclic voltammetry correlates the concentration of a chemical species to oxidation and reduction peaks caused by the redox reaction of the species on the electrode, whereas square wave voltammetry determines concentration using square wave pulses of increasing potential with the waves being superimposed on a staircase ramp (Bard *et al.,* 2022). The study on dairy fouling by Fysun *et al.* (2020) compared the efficacy of these voltammetric techniques by determining the change in current between clean and fouled microelectrodes. For both voltammetry techniques, microelectrodes covered with foulant had the lowest current responses due to additional resistance caused by the fouling layer. This is in agreement with the study of Roscoe *et al.* (1993), which determined that absorption of β-Lg and α-lactalbumin (the key whey proteins in dairy fouling) results in a significantly reduced current response. However, square wave voltammetry was found to be less effective in distinguishing dairy fouling of a dairy emulsion system as no oxidation peak currents could be detected. Previous literature has reported that square wave voltammetry is better suited to a low concentration of the electrochemically active species (i.e., proteins), therefore it may be applicable at lower frequencies as the longer duration of the measurement allows for more structural changes in the sample (Mirceski *et al.,* 2007). While more research into the development on an in-line

microelectrode sensor for monitoring of dairy fouling in industrial settings is required, this study demonstrates the potential of voltammetry to be suitable for this purpose.

1.4.3. Thermal properties

Simple measures of thermal properties are often used as indirect indicators of fouling in heat exchangers and other piping surfaces. As the build-up of fouling decreases the heat transfer efficiency, the temperature of the heating medium must increase in order to maintain product temperature; therefore, this temperature increase can be used as an indirect measure of fouling (Prakash *et al.,* 2005). This concept was implemented and adapted by Hill *et al.,* (1997) when investigating the impact of different genetic variants of β-lg on fouling in ultra heat treated (UHT) milk. The temperature difference between the hot water entering the system as the heating medium and the treated milk leaving the system was monitored with an increase in this temperature difference indicating fouling deposit build-up.

The presence of fouling deposit reduces the overall heat transfer coefficient of a heat exchange system; therefore, this thermal property can also be used to monitor fouling. The calculation of the overall heat transfer coefficient considers temperature and flow rate changes with build-up of fouling deposit, making it a more rounded indication of fouling. Jones *et al.* (1996) studied fouling of a whey protein solution using a heat flux sensor, which detected changes in heat flux caused by the build-up of a fouling deposit:

$$Q = UA\Delta T_{lm} \qquad (2)$$

where U is the overall heat transfer coefficient, A is the area of the heat exchange surface, and ΔT_{lm} is the log mean temperature difference. The fouling apparatus was a simple heated

copper block with the milk protein solution flowing through a copper tube, with the heat flux sensor recording changes in voltage output, which were transformed into heat flux readings using a data logger. The value of ΔT_{lm}, measured by thermocouples, and the value of A were substituted into equation 2 to give U; the variation of U with time was monitored as an indicator of fouling.

Differential thermal analysis can be used as an advanced analysis of thermal properties in order to determine fouling status of a heat exchanger. In a study conducted by Crattelet *et al.* (2013), an *in-situ,* on-line fouling sensor based on local differential thermal analysis was applied to an ohmic cell jet heater used for dairy product pasteurisation. The sensor measured local thermal pulses to determine the fouling status of the equipment. The thermal sensor measured the heat flux and temperature of the equipment wall (T_W) and the bulk of the fluid (T_b), with the sensor including a platinum hot wire connected to a direct current generator. By calculating the electric resistance (determined through measurement of electric current and potential), the average temperature of the hot wire could be determined. At the midpoint of the platinum wire, a thermocouple measured the wall temperature at the deposit interface, and another temperature probe determined the bulk temperature. Each signal received by the sensor was converted into a heat generation equation to establish the expression of temperature versus time and position. The sensor could monitor fouling at an intermediate electric current (5-50 mA), with the monitored change in temperature ($\Delta T = T_w - T_b$) being a direct consequence of the heat transfer coefficient (U) and flux. Therefore, at constant flux, the heat transfer coefficient and temperature would change with the formation of fouling deposit. By combining product knowledge with heat transfer analysis, detailed observations of the fouling phenomena can be made. The sensor could also measure thermal conductivity using a periodic temperature field throughout the entire equipment wall. The dampened temperature signal was dependent on frequency, therefore adjusting the frequency allowed a temperature signal to be recorded at

a specific point on the equipment wall (Lahoucine & Khellaf, 2004). To conclude, this study by Crattelet *et al*. (2013) demonstrated the potential of this thermal sensor to evaluate the properties of a fouling deposit *in-situ.* The sensor was shown to accurately detect and measure fouling, as well as displaying low thermal inertia. It could be readily implemented into any thermal process in the dairy industry to enable *in-situ* monitoring of fouling.

1.4.4. Spectroscopic techniques

Spectroscopy is the study of the production or interactions of electromagnetic radiation with matter (Pavia *et al.,* 2014). Spectroscopic techniques are used widely across dairy research for both qualitative and quantitative analysis. These techniques generally characterise, identify, or measure the concentration of particular molecular species, such as protein (Siegel & Saukko*,* 2012), and the ability of these techniques to characterise dairy foulant has been reported in literature, with particular emphasis on Raman spectroscopy and Nuclear Magnetic Resonance spectroscopy.

Raman spectroscopy is a technique capable of providing information on the conformational changes and molecular structure of proteins, taking the peptide backbone conformation and side chains into consideration (Nonaka *et al.,* 1993). As described in Section 2, dairy fouling is primarily caused by the denaturation and aggregation of β-Lg; these reactions are due to heat induced changes in the secondary protein structure, and this secondary structure can be analysed using Raman spectroscopy by studying the amide bands produced by the spectra (Li-Chan, 1996).

This was shown to be useful for fouling evaluation in a study by Blanpain-Avet *et al.* (2011), where Raman spectroscopy was used to analyse the structure of whey protein fouling deposits in a plate heat exchanger. The fouling solution (reconstituted whey protein isolate with

added calcium chloride) was heated from 60 to 85˚C in order to induce β-Lg denaturation in the plate heat exchanger. The nature of β-Lg (i.e., native, denatured, or aggregated) present at the interface between the fouling deposit and the stainless steel surface was determined from Raman signatures of the thermal denaturation processes, as well as analysis of aggregates in the spectral range of 800–1800 cm^{-1}. This spectral range is in the amide I and amide III bands region, which is where changes in the secondary structure of β-Lg can be observed (Stephani *et al.,* 2017). A shift in the frequency of the amide I band and a decrease in the intensity of the 940 cm^{-1} band was observed at the interface between the fouling deposit and the stainless steel surface over the course of the fouling experiment, this indicates a loss of α-helix structures within the molecular conformation of β-Lg. The spectral data showed no evidence of aggregation, meaning the fouling deposit primarily consisted of denatured protein. This study shows the application of Raman spectroscopy in analysing mechanisms governing the dairy fouling deposit, and by elucidating the specific protein reactions that are causing the occurrence of deposit, targeted prevention strategies can be developed.

Recent developments in the use of Raman and Fourier transform infrared (FT-IR) spectroscopy in hyperspectral imaging to study dairy residues (Caponigro *et al.,* 2019) shows great promise in fouling monitoring applications. This study used the two aforementioned spectroscopic techniques to automatically distinguish between different dairy residues (whole milk, skimmed milk, protein milk, butter milk and butter) on surfaces commonly used in the food industry. For both Raman and FT-IR spectroscopy, principal component analysis showed a good separation between the spectra of the different dairy products, with FT-IR spectroscopy results being more precise at recognising different products. The findings of this study could be adapted to automatically monitor the build-up of fouling deposit on food production surfaces, by using milk compositional data to relate the hyperspectral images of the fouling surface to fouling type – i.e., Type A or B as mentioned in Section 1.

Nuclear Magnetic Resonance (NMR) spectroscopy is an increasingly prominent technique in dairy research. The principle of NMR relies on resonance transition between magnetic energy levels, due to immersion of atomic nuclei in an external magnetic field where electromagnetic radiation is applied with specific frequency; the absorption signals give an NMR spectrum with resonance peaks of varying intensities, positions, and structure, that coincide with molecular structure that can be studied quantitatively (Belloque & Ramos, 1999). NMR has more recently been considered as a promising non-invasive detection method for various deposits, with one such application being demonstrated by Fysun *et al.* (2019) in the detection of biofilm and dairy fouling for UHT and pasteurised milk in flexible tubing using low field NMR. The fouling experiments involved pumping the milk through silicone tubing for 4 d at 30˚C for biofilm fouling, and for 4 d at 80˚C for dairy fouling. NMR measurements of the silicone tubing were taken before, during, and after the fouling experiments in order to monitor the change in transverse relaxation time with the build-up of deposit. It was shown that this technique could differentiate between biofilm and dairy fouling, with longer transverse relaxation times being observed for biofilm fouling (100 ms) compared to dairy fouling (50 – 60 ms). Shorter relaxation times are expected in solid or gel-like structures typical of dairy foulant, due to the restricted movement of protons trapped within the gel (Belton, 1997). This demonstrates the potential of NMR for monitoring fouling and implementing more specific preventative measures, as the specific type of fouling can be differentiated.

***Table 1.1.**: Overview of fouling measurement and monitoring methods reviewed.*

Method	Principal	Equations	Equation symbols	System used to test method	In-line monitoring	Combined with other measures of fouling	Authors
Overall fouling thermal resistance	Resistance to heat transfer due to thickness of fouling layer.	$R = \frac{1}{U_M} - \frac{1}{U_c}$	R: Thermal resistance (m^2K/W) U_M: Mean overall heat transfer coefficient (W/(m^2 K)) U_c: Overall heat transfer coefficient for the heat exchanger with clean (unfouled) heat transfer surfaces (W/(m^2 K))	Double-pipe cooler	✓		Milanovic *et al.* (2006)
Ultrasonic sensor	Use of sound waves to detect location of an interface (i.e., the fouling layer), and monitor changes in thickness.	$\Delta s = 12c\Delta t$	Δs: distance between the interface and the transducer (m) c: wave velocity through the medium (m/s) Δt: arrival time (s)	Reverse osmosis desalination membrane	✓	✓	Mairal *et al.* (1999)
Acoustic sensor	Measurements of amplitude and the natural frequency of vibration, with a decrease in these values indicating the build-up of a fouling deposit.	$x = A \sin(\omega t + \phi)$ $f = \frac{\omega}{2\pi}$	x: displacement of wave (m) A: amplitude ω: angular frequency (rad/s) t: time period (s) ϕ: phase angle f: natural frequency	Plate heat exchanger	✓		Dam Madsen (1994); Merheb *et al.* (2007)
Voltammetric sensor	Measures the current of a sample with changing potential, additional resistance caused by a fouling layer would result in a lower current.	$I = V/R$	I: current (A) V: potential difference (V) R: resistance (Ω).	Well-plates with microelectrodes	✓		Fysun *et al.* (2020); Roscoe *et al.* (1993)

Temperature difference	The temperature of the heating medium increases as fouling builds up on the heat transfer surface. This temperature increase is an indirect measure of fouling.	$\Delta T = T_{hm} - T_p$	ΔT: temperature difference (°C) T_{hm}: temperature of heating medium (°C) T_p: temperature of product leaving the system (°C)	Plate heat exchanger	✓	✓	Hill *et al.* (1997)
Heat transfer coefficient	The presence of fouling deposit reduces the overall heat transfer coefficient of a heat exchange system.	$Q = UA\Delta T_{lm}$	Q: heat flux (W/m^2) U: overall heat transfer coefficient ($W/(m^2 K)$) A: area of the heat exchange surface (m^2) ΔT_{lm}: log mean temperature difference (°C)	Copper heating tube	✓		Jones *et al.* (1996)
Differential thermal analysis	The difference in temperature between the sample and a reference material is monitored against time or temperature while the temperature of the sample, in a specified atmosphere, is programmed.	$\Delta T = T_w - T_b$ $K = \frac{Qd}{A\Delta T}$	ΔT: temperature difference (°C) T_w: temperature of equipment wall (°C) T_b: temperature of bulk of the fluid (°C) K: thermal conductivity ($Wm^{-1}K^{-1}$) Q: amount of heat transferred (W) d: distance between the two isothermal planes (m) A: area of surface (m^2)	Ohmic cell jet heater	✓	✓	Crattelet *et al.* (2013)
Raman spectroscopy	Analysis of heat induced changes in the secondary protein structure, caused by the denaturation and aggregation of β-Lactoglobulin.	N/A	N/A	Plate heat exchanger			Blanpain-Avet *et al.* (2011)

Raman and Fourier transform infrared spectroscopy	The observation of how light is scattered or absorbed upon reaching a material, allowing for hyperspectral imaging to study fouling material.	N/A	N/A	Stainless steel slides			Caponigro *et al.* (2019)
Nuclear magnetic resonance spectroscopy	The resonance transition between magnetic energy levels, due to immersion of atomic nuclei in an external magnetic field where electromagnetic radiation is applied with specific frequency can be used monitor the change in transverse relaxation time with the build-up of deposit.	N/A	N/A	Silicon tubing			Fysun *et al.* (2019)

1.5. Fouling modelling and prediction algorithms

There have been many models and algorithms developed over the years for prediction of fouling during thermal processing. Several of these models and algorithms have been primarily based on empirical methods or dynamic heat exchanger models for waste water (Sundar *et al.,* 2020). Early analytical models of water and crude oil fouling were based on rate equations (Epstein, 1988), where the rate of fouling deposit accumulation was either a deterministic function, meaning the function always gives the same answer when it has the same inputs (Ritter, 1983; Watkinson & Martinez, 1975), or a stochastic approximation (Zubair *et al.,* 1997), which finds the extremes of functions that are unknown, when only noisy observations are obtainable (Kushner & Yin, 1997). One of the earliest fouling models was the Kern-Seaton fouling model (Kern & Seaton, 1959), which defined the overall amount of water fouling as the difference between the rate of deposition and removal of the fouling layer. Many researchers have since built upon this model and have applied it to dairy, with improvements in the length indices (Gao *et al*., 2020), computing precision, area indices, and efficiency indices (Li & Webb, 2002). Others have also used the Kern-Seaton model to develop a series of semi-theoretical fouling prediction models (Li *et al*., 2016). Mechanistic models founded on differential mass, energy and reaction balances, and computational fluid dynamics models (CFD) have also been applied to predict fouling of whey protein concentrate in plate heat exchangers (Gu *et al*., 2019). Some researchers have proposed a computer based iterative model for the precise estimation of the heat transfer coefficient to monitor fouling of whole milk (Sahoo *et al.,* 2003), and to monitor the decline in the outlet temperature of milk due to fouling of tubular heat exchangers (Nema & Datta, 2005). The remainder of this section will systematically review the suitability of the principal approaches to modelling and prediction of fouling during dairy processing (Figure 2).

1.5.1. Kern-Seaton classical fouling model

One of the simplest fouling models was developed by Kern and Seaton (1959):

$$R_{ft} = R_{f\infty}(1 - e^{\beta t}) \quad (3)$$

where R_{ft} is fouling thermal resistance, $R_{f\infty}$ is fouling resistance at infinite time (asymptotic value), β is a constant dependent on system properties, and t is time. Although this model provides a simple mathematical explanation of fouling, extensive research is required to determine the values of $R_{f\infty}$ and β as they are dependent on operating conditions and fouling type. Many researchers have used this basic model as the foundation for more detailed models that are more readily applicable to predict fouling in various thermal systems. Gao *et al.* (2021) developed two models to predict waterside fouling for enhanced tubes in a shell and tube condenser. Both models were based on the principles of the Kern-Seaton model, with Model 1 in the form of a ratio of fouling resistance of an enhanced tube to that a plain tube ($R_f^*/R_{f,p}^*$), and Model 2 in the form of fouling resistance of an enhanced tube (R_f^*),. The variables considered in the models were tube geometry, water velocity and water quality. The parameter defined for water quality was valid concentration (C_{com}) of the cooling water, which represents the amount of potential components that could cause fouling. The impact of water velocity on sticking probability (P) and deposit bond strength (ξ) (two critical parameters of fouling) were investigated experimentally. It was found that with increasing water velocity, the sticking probability decreased continuously with the deposit bond strength increasing initially, and thereafter decreasing. Models 1 and 2 presented comparatively accurate predictions, however Model 1 had a higher accuracy in predicting fouling resistance. The fouling prediction in Model 1 took combined fouling into consideration, making it more applicable to predict the

asymptotic fouling resistance in industry. The principles used here for water fouling could be easily adapted and implemented into dairy systems.

1.5.2. Dimensional analysis

Dimensional analysis (DA) is perhaps one of the most powerful approaches for modelling fouling during thermal processing. This is due to the fact that it can be applied when detailed and precise descriptions of physiochemical changes occurring in the process (e.g., denaturation of β-Lg, mineral precipitation, adhesion to the surface) are not available, which is the case for fouling (Delaplace *et al*., 2015). DA is mathematically based on the π-theorem (Buckingham, 1914) and the principle of DA is to use experimental data to define the relationship between a set of dimensionless numbers representative of influencing and target parameters. These dimensionless groups represent commands accountable for the advancement of the system, which in turn could enable the detection of process relationships between fouling deposit mass and other influencing parameters (Gibbings, 2011). DA is relatively easy to implement and has been shown to be efficient in linking operating conditions to product characteristics or equipment performance, as well as being a useful aid in the scale-up of heat transfer.

In a study by Gu *et al.* (2019), DA was used to identify the effects of a range of parameters on total whey protein fouling mass, whereby experimental data was collected from a pilot scale plate heat exchanger, and the total fouling mass was used as the target variable. The model developed to predict total fouling mass covered a wide range of variables including fouling solution flow rate, whey protein solution concentration, total fouling surface area, calcium concentration, outlet temperature, running time, and differences in whey protein concentrate powders. Besides temperature dimensionless parameters, the two main parameters in the model were Reynolds number and calcium to β-Lg molar ratio (Ca:β-Lg). The Reynolds number

serves as a criterion for distinguishing between laminar and turbulent fluid flow. It stands as a key factor governing viscous flows, influencing the choice of a numerical model based on a pre-calculated Reynolds number (Rapp, 2017). The calcium/protein molar ratio was included as a main parameter because Khladi *et al.* (2018) demonstrated that fouling mass is strongly related to this ratio, rather than the protein concentration alone. A large number of influencing parameters reflecting the variables mentioned above were significantly reduced using the π-theorem by grouping influential dimensional parameters into dimensionless numbers based on units (Delaplace *et al.,* 2015). In brief, it was found that there was a linear correlation between fouling and protein mass, and β-Lg aggregation and the calcium to β-Lg molar ratio. The intercept and slope of these correlations/equations depended on fouling side Reynolds number and the type of WPC powder used, with similarity observed between the predicted and experimental values. Further fouling runs were carried out to verify the process relationship and showed that with an outlet temperature of 85˚C, the predictions were strong. However, the model could not predict the correct fouling mass for experiments with an outlet temperature of 82˚C and therefore the model was adjusted for temperatures between 85 and 97˚C, demonstrating the importance of using data within the valid range of the model.

The rate at which protein is deposited and removed from the fouling layer determines the overall extent of fouling (Szirtes, 2007). As both of these rates are functions of Reynolds number, it can be assumed that the total fouling mass is a non-monotonic Reynolds function – meaning it increases or decreases for some time on different intervals of its domain (McDermott & Doyle, 1980). Gu *et al.* (2019) demonstrated that the predicted fouling mass increased with turbulence intensity and Reynolds number, after which the predicted fouling mass decreased; it is assumed that this behaviour is associated with the particular type of heat exchanger plate, possibly shape, used in this study. In summary, DA modelling approaches

could be used to achieve fouling mitigation and control, or to help understand the success of anti-fouling solutions.

1.5.3. Classification models

Generally, a classification model, or algorithm, is a function that evaluates the input features so that the output is divided into two classes: one for negative values and one for positive values (Theodoridis, 2015). In a study by Wallhäußer *et al.* (2013), two classification methods were compared for detecting the presence of protein and mineral dairy fouling in a glass acrylic experimental setup, based on ultrasonic measurements. The classification methods compared were an artificial neural network (ANN) and a support vector machine (SVM). An ANN is a simulation of a biological network that can form a relationship within the data by developing models between input and output vectors (Basheer & Hajmeer, 2000). Cortes & Vapnik (1995) first introduced the SVM, a decision machine that classifies objects in such a way that a clear divide is found between them using a hyperplane, with the hyperplane characterized by support vectors from the individual classes.

The aim of the study by Wallhäußer *et al.* (2013) was to develop a decision method independent of foulant type (i.e., protein or mineral). A combination of specially chosen acoustic and signal parameters, as well as a pattern recognition or a classification method were used to detect fouling on stainless steel. Reconstituted skim milk powder (for protein fouling) and reconstituted milk permeate powder (for mineral fouling) were heated and the acoustic and signal parameters used to determine if fouling had occurred. These parameters included characteristic acoustic impendence, short-time energy, temporal crest factor, spectral crest factor, and spectral smoothness. By understanding how each of these parameters respond to fouling, and by comparing the values of these parameters for protein and mineral fouling, the

classification models could be built. Three ANNs were built, with one for mineral fouling, one for protein fouling, and one for both together. The ANN for protein fouling displayed the best results, with a detection accuracy of almost 100%, followed by mineral fouling with an accuracy of 93.5%, and for both fouling types combined, the detection accuracy was 71.9%. The SVM for protein fouling showed an accuracy of 100%, while for mineral fouling the accuracy was 98.2% and for both fouling types combined, the SVM had an accuracy of 97.6%. Both classification models had comparable results for mineral and protein fouling, but the SVM was more accurate for detecting both fouling types. Seeing as protein and mineral fouling differ greatly in terms of layer structure (spongy and thick for protein; brittle and thin for mineral), variations in calculated features and errors in detection may occur. In the study of Wallhäußer *et al.* (2013), the SVM dealt with this variance better than ANN, as it had ability to determine the absolute maximum of the error function, whereas ANN only found a local one. The data produced by SVM seemed to be independent of fouling type and thickness, and was more robust than ANN.

An ANN was developed by Riverol & Napolitano (2005) to estimate fouling in a plate heat exchanger for pasteurisation of milk. The ANN was designed to predict fouling deposit thickness, the overall heat transfer coefficient, and the time at which the unit must be stopped for cleaning. The model inputs were heat flux and temperature, measured by sensors in the plate heat exchanger, which gave an output of the fouled deposit thickness. Like the heat flux sensor used by Jones *et al.* (1996) in Section 3.3, the data collected by the sensors was used to calculate the overall heat transfer coefficient. The model continually processes this data to calculate an error expression; this being a value between 0 and 1 that indicates when fouling has reached a critical level and the process needs to be stopped for cleaning. The error has a value of 1 at the start of the process, and as the fouling layer becomes thicker the error move closer to 0, at which stage the pasteuriser should be cleaned. The ANN was shown to produce

theoretical fouling deposit thickness values that were similar to actual measurements, indicating that the ANN was successful in predicting fouling.

1.5.4. Models for fouling based on heat transfer properties

A mathematical model for intricate plate heat exchanger arrangements subjected to milk fouling was developed by Georgiadis & Macchietto (2000). A plug flow model was adapted to include the effects of axial convection and radial dispersion. However, this model was based on a 1D hydrodynamic performance of the plate heat exchanger, which does not take into consideration all the effects of plate geometry in industry. In addition, the 1D model produced large prediction errors. A similar 2D model that considers the hydrodynamics of fluid flow could predict temperature distribution of flow more accurately than this 1D model (Jun *et al.,* 2003). This model followed the trends of experimental data more accurately than the 1D model, regardless of the plate dimensions. The 2D model could also detect regions most susceptible to milk deposits, by identifying when cold and hot streams surpassed the threshold values.

Taking all of this into account, a study was conducted by Jun & Puri (2006) that applied the model developed by Georgiadis & Macchietto (2000) to a 2D dynamic model designed to predict the patterns of milk deposit on the surfaces of a plate heat exchanger with more accuracy. Prediction was based on thermodynamic and hydrodynamic performances of the plate heat exchanger in a 2D environment. The model was validated by visual inspection and quantification of milk deposit present in the fluid channels. The simulation results determined that fouling growth becomes more dominant across the whole plate surface when flow rate is decreased. The predicted deposit mass values in each channel corresponded well to the experimental data, with an average prediction error of 10.9%. The predicted temperatures of fluid milk were also in good agreement with the measured values, resulting in a maximum

prediction error of 2.1%. This model is a good option for analysing thermal and hydraulic performance of a heat exchanger during fouling. A good correlation between the operating conditions (i.e., flow rate and fouling layer formation) was shown by the prediction model, which advances on limitations of previous studies (e.g., Georgiadis & Macchietto, 2000). However, description of the fouling layer in this case is limited as the hypothesis considers only aggregated protein as the fouling source, not taking into consideration the influence of calcium content on protein denaturation and deposition rate, salt precipitation, the corrugated pattern of the plate, or the thickness of the deposit. The model is also limited as it is challenging to obtain data for certain parameters that influence the fouling layer, such as thermal conductivity, density, and specific heat capacity of the deposit (Gu *et al.,* 2019).

The fouling of falling-film evaporators was analysed by a set of dynamic models developed by Díaz-Ovalle *et al.* (2017). These models considered several key operating variables; temperature, mass fraction of solids, fouling thickness and film thickness. The dynamic models were developed from simple mass and energy balances that considered thermo-physical properties of the product, as well as thermocompression, as functions of composition and temperature. The model was designed to predict the thickness of the falling-film, as well as to evaluate the effect of fouling on heat transfer performance. A set of ordinary differential equations make up the models, and these are numerically solved using a specially developed software with the modelling of heat transfer using a calculation of the overall heat transfer coefficient, taking fouling thermal resistance into consideration. The user of the software can input the number of effects in the evaporator, and the features of each effect, such as: number of tubes, length and diameter of tubes, number of liquid passes, and output vapour fraction. The model developed in the work of Díaz-Ovalle *et al.* (2017) was tested by comparing predictions to in-process measurements obtained from an evaporator with four effects used to concentrate whole milk. It was found that the models outputs for the overall

heat transfer coefficient and falling-film thickness matched with the experimental data throughout the evaporation process. By relating these values back to fouling, this model can be used in the prediction of fouling in evaporators taking various process and product parameters into consideration.

1.5.5. Deep learning

A fouling resistance prediction model based on deep learning was developed by Sundar *et al.* (2020). This accurate and scalable model can predict fouling resistance (i.e., resistance to heat transfer due to foulant build-up) using commonly measured heat exchanger parameters and utilizing feed-forward ensemble neural network architectures based on deep learning. The neural network was used to understand the non-linear functional relationship that exists between fouling resistance (target variable) and heat-exchanger operational data (casual variables) (LeCun *et al.,* 2015). The network inputs were inlet fluid temperatures, ratio of fouled fluid flowrates to flowrates under clean conditions and outlet fluid temperatures, with these inputs relatively quick and simple to measure *in-situ* using established process monitoring sensors. The neural network architecture of the fouling resistance module required training using deep learning techniques. A deep neural network is a very specific function, usually with millions of parameters, that can estimate complicated nonlinear maps by calculating the correct parameters; the function 'learns' these parameters using training data (Montavon *et al.,* 2018). For each data sample, the predicted target variable (fouling resistance) was compared with the observed fouling resistance in order to diminish the prediction error. This procedure was repeated numerous times for each data sample until the network was capable of precisely predicting the fouling resistance for every data sample in the training dataset. Once the neural network was trained with a dataset that covered the entire operation of the heat exchanger, it was used to predict fouling resistance for new samples. The test data accuracies for the

prediction model was over 97% for a training dataset with over 5000 points, demonstrating that this model was effectively and accurately trained to predict fouling resistance and could therefore be used to make real-time predictions in an industrial setting by obtaining inputs with numerous temperature and flowrate sensors at the inlets and outlets of the heat exchanger. The model could be adapted to any heat exchanger by modifying the layers of the network. The network could also be adapted to instantly identify regions of the heat exchanger that are most impacted by fouling by inputting region specific temperature and flow-rate data into the prediction model. This would be useful for conducting region specific corrective action.

1.6. Small-scale simulation of fouling

1.6.1. Fouling microsystems

As fouling studies are often based on trial-and-error approaches involving measurement of parameters such as pressure drop and destructive equipment studies post-fouling, there is a requirement for more tools that involve microscopic and visual observations of fouling, non-destructively, *in-situ* and in real-time (Flemming, 2003). A range of fouling microsystems have been designed in order to analyse fouling on a smaller scale and evaluate the suitability of different measurement and prediction approaches to measure fouling.

Vrouwenvelder *et al*. (2006) designed a membrane fouling simulator (MFS) for the characterization of fouling potential of feed water, early warning indicators of fouling and for the evaluation of potential control strategies for fouling. Several requirements were identified to ensure the system was successful, which are applicable to the development of future fouling systems for thermal processes. First of all, it was determined that the tool must have elements identical to the equipment used in practice, which in this case was a spiral wound membrane. These elements include spatial dimensions, materials used and hydraulics. Secondly, the data

obtained from the system must be reproducible and accurate. Thirdly, the system must be able to monitor fouling quantitatively using operational parameters (e.g., pressure drop), and real-time, in-situ, non-destructive observations (e.g., microscopic). The MFS has multiple ways of detecting fouling rapidly and precisely. A sensitive pressure analyzer acted as an early warning system by measuring pressure drop over the MFS and triggering an alarm when the pressure drop exceeded a certain value. The MFS also had a transparent window to allow visual inspection of fouling. Vrouwenvelder *et al.* (2006) compared the MFS with a membrane module and observed the same pressure drop development and the same accumulation of biomass. Although this specific example highlights membrane fouling, the concepts of using pressure drop and visual inspection to monitor fouling a can be extended and applied to thermal fouling studies.

A micro-scale heat exchanger (MSHE) system was designed and constructed by Magens *et al.* (2017) to study fouling under wall shear stress and surface temperature conditions representative of a high-temperature-short-time pasteuriser. The system consisted of a 650 x 2000 μm flow channel that allowed 2 litres of raw milk to be studied for fouling. Like Vrouwenvelder *et al*. (2006), the pressure drop across the unit was measured over time. In this system, the fouling cell guided the flow of the process fluids, heated the square test plate, and allowed for microscopic imaging. Confocal laser scanning microscopy was incorporated into the system to analyse the fouling layer, particularly the distribution of protein and calcium phosphate, with pictures of deposits on fluoropolymers taken *in-situ.* The temperature of the thermal boundary layer (~ 60˚C) coincided with beta-lactoglobulin (β-Lg) being in the molten globule state, where β-Lg is partially unfolded with its free thiol group exposed, allowing intramolecular disulphide linkages to occur, making this change irreversible (Tolkach & Kulozik, 2007). Pressure drop steadily increased as deposition occurred. Unexpectedly, the thermal resistance did not change significantly within the conditions and timescales of the

experiment. The surface mass coverage was determined from the mass of the fouling deposit after drying overnight. There was substantial deposition on all surfaces, even with the bulk temperatures maintained at ≤ 72˚C, indicating that milk fouling was driven by aggregation and chemical reactions in the hot boundary layer. After 120 min of processing at a surface temperature of 85˚C, there was strong adhesion of a mineral-rich sub-layer (i.e., calcium phosphate). This system is an excellent example of all-encompassing fouling analysis tool, with several fouling monitoring techniques incorporated to obtain the full picture of the development of dairy fouling in a heat exchanger.

A concentric tube fouling rig designed by Khalid *et al.* (2013) is an interesting and promising example of introducing a fouling microsystem into a production process. This fouling deposit monitoring device can be attached to any food processing equipment; in this study it was attached to a lab-scale concentric tube pasteuriser processing pink guava puree at temperatures of 90-95˚C. The rig functions as a sampler for fouling deposit, which can be dismantled at any time for analysis of the fouling deposit material without dismantling the entire food processing equipment it is attached to. The fouling rig was attached to the last tube of the concentric tube lab-scale pasteuriser, as this is where the most fouling was occurring. The rig was removed after every hour of pasteurisation to observe the fouling thickness, and temperature changes were continually recorded in order to correlate the heat transfer properties with the build-up of fouling deposit. A rig of this design has potential to be a useful monitor dairy fouling of a processing line where frequent dismantling is not possible.

1.6.2. Computational fluid dynamics

Computational fluid dynamics (CFD) is a robust numerical tool that is increasingly being used to imitate several processes in the food industry (Norton & Sun, 2006). CFD is a type of fluid mechanics that utilises data structures and numerical analysis to study and solve challenges involving flow. CFD can be applied to simulate and predict fouling, as fluid flow is

a key factor in the occurrence of fouling. CFD models can analyse the contribution of specific mechanisms to fouling, such calcium phosphate reactions (Ojaniemi *et al.,* 2021) and protein denaturation (Jun & Puri, 2005), or it can evaluate the combined effect of several parameters such as the study by De Bonis & Ruocco (2009) that used CFD to analyse the mutual effects of flow, heat transfer and local transport of β-lg on heat exchanger fouling.

In a study by Grijspeerdt *et al.* (2002), 2D and 3D CFD was used to conduct a comprehensive calculation of the flow pattern of milk between two plates of a plate heat exchanger. The calculations conducted were used to identify regions of turbulent backflow, as these regions are very sensitive to fouling. The 2D and 3D simulations conducted using CFD demonstrated that the flow in the centre of the flow channel was quite straightforward. Regions of reverse flow were shown to be the most susceptible to fouling as the extended residence time of the fluid particles caused more intense heating. The validation experiments conducted by Grijspeerdt *et al.,* (2002) showed results similar to that of the simulated flow in CFD, demonstrating that this numerical simulation could give trustworthy results. Two temperature scenarios were simulated to demonstrate the impact of temperature on fouling. It was suggested by Hiddink *et al.* (1986) that the difference in temperature (ΔT) between the heating medium and the milk impacts fouling when it surpasses 10–15 ˚C. Therefore, for the first simulation the plates had a consistent temperature of 110 ˚C, and for the second simulation the plate temperature was increased to 140˚C. For the simulation with a lower ΔT, the highest temperature regions, and thus the regions most prone to fouling, were located at the downside of the corrugations. For the simulation with the higher ΔT, the most fouling was observed at the end of the corrugations, where the temperature was highest. Although a ΔT of 40˚C is not likely to occur in industry, the results demonstrate the accuracy of the simulation and identify potential weak spots in plate design.

1.7. Conclusion

The purpose of this review was to outline the key aspects of dairy fouling during thermal processing in order to identify and analyse the key advancements in fouling measurement, monitoring, and prediction. It is clear from the research reviewed that many methods have been explored to quantify and predict fouling, as fouling continues to be a key challenge in the dairy industry. The monitoring methods range in approaches used, including thermal resistance, ultrasonic properties, acoustic properties, electrochemical properties, temperature measurements, continuous calculation of the heat transfer coefficient, and spectroscopic analysis. The monitoring methods reviewed provide an insight into the wide variety of options available for *in*-situ measurement of fouling through the use of inline sensors. The ability to obtain real-time data for the progression of fouling is an extremely valuable asset to the dairy industry, as it provides information that can minimise downtimes and maximise operational efficiency. The ability to predict the onset and progression of fouling during production is even more valuable to the dairy industry, hence a range of prediction models and algorithms for fouling have been developed based on dimensional analysis, classification methods, classic fouling models, heat transfer properties and deep learning. The use of modelling for prediction of fouling presents a possible way forward for the dairy industry, however further research is required into the development of an all-encompassing model or algorithm that can address all aspects of fouling, as the models reviewed here often focus on specific aspects of fouling rather than accounting for all the contributing factors. Small scale fouling simulations based on fouling microsystems and computational fluid dynamics continue to enable lab-scale research into fouling, which is key in developing the above mentioned monitoring techniques and prediction algorithms. The area of fouling studies is vast and complex, as many of the underlying mechanisms of fouling are still not fully understood, however the research reviewed here demonstrates the key advancements in the monitoring and prediction of fouling over the

years, which aid in the design and implementation of strategies to control fouling during dairy processing.

1.8. Acknowledgements

The authors would like to acknowledge the Dairy Processing Technology Centre (DPTC), an Enterprise Ireland initiative, for financial support of this work (Grant Number TC/2020/0028).

1.9. References

Anema, S. G. (2021). Heat-induced changes in caseins and casein micelles, including interactions with denatured whey proteins. *International Dairy Journal*, *122*, 105136.

Anema, S. G., & Li, Y. (2000). Further studies on the heat-induced, pH-dependent dissociation of casein from the micelles in reconstituted skim milk. *LWT-Food Science and Technology*, *33*(5), 335-343.

Asadi, M., & Khoshkhoo, R.H. (2013). Investigation into fouling factor in compact heat exchanger. *International Journal of Innovation and Applied Studies*, *2*(3), 238-249.

Baghoth, S. A., Sharma, S. K., & Amy, G. L. (2011). Tracking natural organic matter (NOM) in a drinking water treatment plant using fluorescence excitation–emission matrices and PARAFAC. *Water Research*, *45(2),* 797-809.

Bard, A. J., Faulkner, L. R., & White, H. S. (2022). *Electrochemical methods: fundamentals and applications*. John Wiley & Sons.

Basheer, I. A., & Hajmeer, M. (2000). Artificial neural networks: fundamentals, computing, design, and application. *Journal of Microbiological Methods*, *43(1),* 3-31.

Belmar-Beiny, M. T., Gotham, S. M., Paterson, W. R., Fryer, P. J., & Pritchard, A. M. (1993). The effect of Reynolds number and fluid temperature in whey protein fouling. *Journal of Food Engineering, 19(2)*, 119-139.

Belloque, J., & Ramos, M. (1999). Application of NMR spectroscopy to milk and dairy products. *Trends in Food Science & Technology*, *10(10),* 313-320.

Belton, P. S. (1997). NMR and the mobility of water in polysaccharide gels. *International Journal of Biological Macromolecules*, *21(1),* 81-88.

Berg, H. E. (1993). *Reactions of lactose during heat treatment of milk: a quantitative study*. Wageningen University and Research.

Bilaniuk, N., & Wong, G. S. K. (1993). Speed of sound in pure water as a function of temperature. *The Journal of the Acoustical Society of America*, *93(3),* 1609-1612.

Blanpain-Avet, P., Hédoux, A., Guinet, Y., Paccou, L., Petit, J., Six, T., & Delaplace, G. (2012). Analysis by Raman spectroscopy of the conformational structure of whey proteins constituting fouling deposits during the processing in a heat exchanger. *Journal of food engineering*, *110(1),* 86-94.

Bond, L. J., Morra, M., Greenwood, M. S., Bamberger, J. A., & Pappas, R. A. (2003, May). Ultrasonic technologies for advanced process monitoring, measurement, and control. In *Proceedings of the 20th IEEE Instrumentation Technology Conference (Cat. No. 03CH37412)* (Vol. 2, pp. 1288-1293). IEEE.

Bott, T.R., (2001). To foul or not to foul: That is the question. *Chemical Engineering Progress*, *97,* 30–37

Buckingham, E. (1914). On Physically Similar Systems; Illustrations of the Use of Dimensional Equations. *Physical Review*, *4(4),* 345-376.

Caponigro, V., Marini, F., Dorrepaal, R., Herrero-Langreo, A., Scannell, A., & Gowen, A. (2019). Raman and Fourier transform infrared hyperspectral imaging to study dairy residues on different surface. *Journal of Spectral Imaging*, *8(1),* a3.

Chandan, R. C., Kilara, A., & Shah, N. P. (2015). *Dairy Processing and Quality Assurance*, *Chicester, United Kingdom: John Wiley & Sons, Incorporated.*

Chaplin, L. G., & Lyster, R. L. (1988). Effect of temperature on the pH of skim milk. *Journal of Dairy Research*, *55*(2), 277-280.

Cheng, X., Liang, H., Ding, A., Qu, F., Shao, S., Liu, B., Wang, H., Wu, D., & Li, G. (2016). Effects of pre-ozonation on the ultrafiltration of different natural organic matter (NOM) fractions: Membrane fouling mitigation, prediction, and mechanism. *Journal of membrane science*, *505*, 15-25.

Considine, T., Patel, H. A., Anema, S. G., Singh, H., & Creamer, L. K. (2007). Interactions of milk proteins during heat and high hydrostatic pressure treatments—a review. *Innovative food science & emerging technologies*, *8*(1), 1-23.

Cortes, C., &Vapnik, V. (1995). Support-vector networks. *Machine Learning*, *20(3),* 273-297.

Crattelet, J., Ghnimi, S., Debreyne, P., Zaid, I., Boukabache, A., Esteve, D., Auret, L., & Fillaudeau, L. (2013). On-line local thermal pulse analysis sensor to monitor fouling and cleaning: Application to dairy product pasteurisation with an ohmic cell jet heater. *Journal of Food Engineering*, *119(1),* 72-83.

Dalmont, J. P. (2001). Acoustic impedance measurement, Part I: A review. *Journal of Sound and Vibration*, *243*(3), 427-439.

Dam Madsen, K. (1994). Vibration Sensor. *Sanitation of Food Processing Plants, Final Technical Report* (Mikkelsen, H.O., ed.), 72-86, Biotechnological Institute, Kolding, Denmark.

De Bonis, M. V., & Ruocco, G. (2009). Conjugate fluid flow and kinetics modeling for heat exchanger fouling simulation. *International Journal of Thermal Sciences*, *48*(10), 2006-2012.

Delaplace, G., Loubière, K., Ducept, F., & Jeantet, R. (2015). *Dimensional analysis of food processes*. Elsevier.

Díaz-Ovalle, C. O., González-Alatorre, G., & Alvarado, J. F. J. (2017). Analysis of the dynamic response of falling-film evaporators considering fouling. *Food and Bioproducts Processing*, *104*, 124-136

Ensminger, D., & Bond, L. J. (2011). *Ultrasonics: Fundamentals, Technologies, and Applications, Third Edition, CRC Press, Boca Raton.*

Epstein, N. (1988). General thermal fouling models. *Fouling Science and Technology*, 15-30. Springer, Dordrecht.

Fickak, A., Al-Raisi, A., & Chen, X. D. (2011). Effect of whey protein concentration on the fouling and cleaning of a heat transfer surface. *Journal of Food Engineering*, *104(3),* 323-331.

Flemming, H.C. (2003). Role and levels of real-time monitoring for successful anti-fouling strategies - An overview. *Water science and technology : a journal of the International Association on Water Pollution Research*, *47*, 1-8.

Foster, C. L., & Green, M. L. (1990). A model heat exchange apparatus for the investigation of fouling of stainless steel surfaces by milk II. Deposition of fouling material at 140 °C, its adhesion and depth profiling. *Journal of Dairy Research*, *57(3),* 339-348.

Fox, P. F. (1981). Heat-induced changes in milk preceding coagulation. *Journal of Dairy Science*, *64*(11), 2127-2137.

Fox, P. F., Uniacke-Lowe, T., McSweeney, P. L. H., & O'Mahony, J. A. (2015). Heat-induced changes in milk. *Dairy chemistry and biochemistry*, 345-375.

Fryer, P. J., & Belmar-Beiny, M. T. (1991). Fouling of heat exchangers in the food industry: a chemical engineering perspective. *Trends in Food Science & Technology*, *2*, 33-37.

Fysun, O., Anzmann, T., Gschwind, P., Rauschnabel, J., Kohlus, R., & Langowski, H.-C. (2019). Biofilm and dairy fouling detection in flexible tubing using low-field NMR. *European food research & technology*, *245(11),* 2579-2590.

Fysun, O., Khorshid, S., Rauschnabel, J., & Langowski, H.-C. (2020). Detection of dairy fouling by cyclic voltammetry and square wave voltammetry. *Food Science & Nutrition*, *8(7),* 3070-3080.

Gao, R., Shen, C., Wang, X., & Yao, Y. (2020). Experimental study on long-term fouling of enhanced tubes: Effect of water quality. *Science and Technology for the Built Environment*, *26(9),* 1191-1203.

Gaucheron, F. (2005). The minerals of milk. *Reproduction Nutrition Development*, *45*(4), 473-483.

Gaucheron, F. (2011). Milk salts: Distribution and analysis. In *Encyclopedia of dairy sciences* (2nd ed., pp. 908–916). Academic Press, Oxford, UK

Georgiadis, M. C., & Macchietto, S. (2000). Dynamic modelling and simulation of plate heat exchangers under milk fouling. *Chemical Engineering Science*, *55*, 1605–1619.

Gibbings, J. C. (2011). *Dimensional analysis*. Springer Science & Business Media.

Grijspeerdt, K., Hazarika, B., & Vucinic, D. (2003). Application of computational fluid dynamics to model the hydrodynamics of plate heat exchangers for milk processing. *Journal of food engineering*, *57(3),* 237-242.

Gu, Y., Bouvier, L., Tonda, A., & Delaplace, G. (2019). A mathematical model for the prediction of the whey protein fouling mass in a pilot scale plate heat exchanger. *Food control*. *106*, 106729.

Hasegawa, S., Miyoshi, T., Takagi, R., & Matsuyama, H. (2019). Fouling prediction method using TOC and EEM analysis. *Water science & technology, Water supply*, *19(2),* 610-617.

Hay, T. R., & Rose, J. L. (2003). Fouling detection in the food industry using ultrasonic guided waves. *Food control*, *14*(7), 481-488.

Hiddink, J., Lalande, M., Maas, A. J. R., & Stempher, A. (1986). Heat treatment of whipping cream. I. Fouling of the pasteurization equipment. *Milchwissenschaft-Milk Science International*, *41*, 542-546

Hill, J.P., Boland, M.J., & Smith, A.F. (1997). The effect of beta-lactoglobulin variants on milk powder manufacture and properties. In *Milk protein polymorphism, Palmerston North (New Zealand), Feb 1997*. International Dairy Federation.

Hoffmann, M. A., & van Mil, P. J. (1997). Heat-induced aggregation of β-lactoglobulin: role of the free thiol group and disulfide bonds. *Journal of Agricultural and Food Chemistry*, *45*(8), 2942-2948.

Holt, C. (1985). The milk salts: Their secretion, concentration, and physical chemistry. In P. F. Fox (Ed.), *Developments in dairy chemistry, volume 3, lactose and minor constituents* (pp. 143–181). London: Elsevier Applied Science.

Huppertz, T., & Nieuwenhuijse, H. (2022). Constituent fouling during heat treatment of milk: A review. *International Dairy Journal*, *126*, 105236.

Jones, A.D., Ward, N.J., Schreier, P.R., & Fryer, P.J. (1996). The use of a heat flux sensor in monitoring fouling. *EUR (Luxembourg)*, 230-241.

Jun, S., Puri, V. M., & Roberts, R. F. (2003). A dynamic model for thermal performance of plate heat exchangers. *Transactions of the ASAE*, *47(1),* 213–222.

Jun, S., & Puri, V. M. (2005). 3D milk fouling model of plate heat exchangers using computational fluid dynamics. In *2005 ASAE Annual Meeting* (p. 1). American Society of Agricultural and Biological Engineers.

Jun, S., & Puri, V. M. (2006). A 2D dynamic model for fouling performance of plate heat exchangers. *Journal of food engineering*, *75(3),* 364-374.

Kang, J., Kim, T., Tak, Y., Lee, J.-H., & Yoon, J. (2012). Cyclic voltammetry for monitoring bacterial attachment and biofilm formation. *Journal of Industrial and Engineering Chemistry*, *18(2),* 800-807.

Kern, D.Q., & Seaton R.E. (1959). A theoretical analysis of thermal surface fouling. *Br. Chem. Eng.*, *4*, 258-262.

Khaldi, M., Croguennec, T., André, C., Ronse, G., Jimenez, M., Bellayer, S., Blanpain-Avet, P., Bouvier, L., Six, T., Bornaz, S., Jeantet, R., & Delaplace, G. (2018). Effect of the calcium/protein molar ratio on β-lactoglobulin denaturation kinetics and fouling phenomena. *International Dairy Journal*, *78*, 1-10.

Khalid, N.I., Chan, K.W., Ab Aziz, N., Taip, F.S., & Anuar, M.S. (2013). Concentric tube-fouling rig for investigation of fouling deposit formation from pasteuriser of viscous food liquid. *Journal of Engineering Science and Technology*, *8*(1), 16-26.

Kushner, H. J., Yin, G. G., Kushner, H. J., & Yin, G. G. (1997). Applications to learning, state dependent noise, and queueing. *Stochastic Approximation Algorithms and Applications*, 25-46.

Lahoucine, C.O., & Khellaf, A., (2004). Periodic method: correction for thermocouple and simultaneous estimation of thermal conductivity and thermal diffusivity. *Review of Scientific Instruments, 75 (7),* 2356–2361.

Lalande, M., Tissier, J.-P., & Corrieu, G. (1984). Fouling of a plate heat exchanger used in ultra-high-temperature sterilization of milk. *Journal of Dairy Research*, *51(4),* 557-568.

Law, A. J., & Leaver, J. (2000). Effect of pH on the thermal denaturation of whey proteins in milk. *Journal of agricultural and food chemistry*, *48(3),* 672-679.

LeCun, Y., Bengio, Y., & Hinton, G. (2015). Deep learning. *Nature*, *521(7553),* 436-444.

Leenheer, J. A., & Croué, J.-P. (2003). Peer Reviewed: Characterizing Aquatic Dissolved Organic Matter. *Environmental science & technology*, *37(1),* 18A-26A.

Lohr, K. R., & Rose, J. L. (2003). Ultrasonic guided wave and acoustic impact methods for pipe fouling detection. *Journal of food engineering*, *56*(4), 315-324.

Li, W., & Webb, R. L. (2002). Fouling characteristics of internal helical-rib roughness tubes using low-velocity cooling tower water. *International Journal of Heat and Mass Transfer*, *45(8),* 1685-1691.

Li, W., Zhou, K., Manglik, R. M., Li, G.-Q., & Bergles, A. E. (2016). Investigation of CaCO3 fouling in plate heat exchangers. *Heat and Mass Transfer*, *52(11),* 2401-2414.

Li-Chan, E. C. Y. (1996). The applications of Raman spectroscopy in food science. *Trends in Food Science & Technology*, *7(11),* 361-370.

Mairal, A. P., Greenberg, A. R., Krantz, W. B., & Bond, L. J. (1999). Real-time measurement of inorganic fouling of RO desalination membranes using ultrasonic time-domain reflectometry. *Journal of membrane science*, *159(1),* 185-196.

Magens, O. M., Hofmans, J., & Wilson, D. I. (2017, June). A fouling micro-system for investigating fluoropolymer antifouling coatings in bovine milk pasteurisation. In *Proceeding of international conference on heat exchanger fouling and cleaning, Aranjuez (Madrid), Spain*.

Mahdi, Y., Mouheb, A., & Oufer, L. (2009). A dynamic model for milk fouling in a plate heat exchanger. *Applied mathematical modelling*, *33(2),* 648-662.

McDermott, D., & Doyle, J. (1980). Non-monotonic logic I. *Artificial Intelligence*, *13(1),* 41-72.

McMahon, D. J., Yousif, B. H., & Kalab, M. (1993). Effect of whey protein denaturation on structure of casein micelles and their rennetability after ultra-high temperature processing of milk with or without ultrafiltration. *International Dairy Journal*, *3*(3), 239-256.

Merheb, B., Nassar, G., Nongaillard, B., Delaplace, G., & Leuliet, J. C. (2007). Design and performance of a low-frequency non-intrusive acoustic technique for monitoring fouling in plate heat exchangers. *Journal of food engineering*, *82*(4), 518-527.

Mérian, T., & Goddard, J. M. (2012). Advances in Nonfouling Materials: Perspectives for the Food Industry. *Journal of Agricultural and Food Chemistry*, *60(12),* 2943-2957.

Milanovic, P., Jacimovic, B., & Genic, S. (2006). Experimental measurement of fouling resistance in the heat exchanger of a geothermal heating system. *Geothermics*, *35(1),* 79-86.

Mirceski, V., Komorsky-Lovric, S., & Lovric, M. (2007). *Square-wave voltammetry: theory and application*. Springer Science & Business Media.

Montavon, G., Samek, W., & Müller, K. R. (2018). Methods for interpreting and understanding deep neural networks. *Digital signal processing*, *73*, 1-15.

Morr, C. V., & Josephson, R. V. (1968). Effect of calcium, N-ethylmaleimide and casein upon heat-induced whey protein aggregation. *Journal of Dairy Science*, *51*(9), 1349-1355.

Mulvihill, D., & Donovan, M. (1987). Whey proteins and their thermal denaturation-a review. *Irish Journal of Food Science and Technology*, *11*(1), 43-75.

Muthukumaran, S., Jagadeesh, K., & Srividhya, V. (2016). On-line monitoring of biofilm forming pseudomonas sp on stainless steel electrodes by repetitive cyclic voltammetry. *International Journal of Biotech Trends and Technology*, *6*, 6–9.

Nonaka, M., Li-Chan, E., & Nakai, S. (1993). Raman spectroscopic study of thermally induced gelation of whey proteins. *Journal of Agricultural and Food Chemistry*, *41(8),* 1176-1181.

Nema, P. K., & Datta, A. K. (2005). A computer based solution to check the drop in milk outlet temperature due to fouling in a tubular heat exchanger. *Journal of food engineering*, *71*(2), 133-142.

Norton, T., & Sun, D.W. (2006). Computational fluid dynamics (CFD) – an effective and efficient design and analysis tool for the food industry: A review. *Trends in Food Science & Technology*, *17(11),* 600-620

Ojaniemi, U., Pättikangas, T., Jäsberg, A., Puhakka, E., & Koponen, A. (2022). Computational Fluid Dynamics Simulation of Fouling of Plate Heat Exchanger by Phosphate Calcium. *Heat Transfer Engineering*, *43*(15-16), 1396-1405.

On-Nom, N., Grandison, A. S., & Lewis, M. J. (2010). Measurement of ionic calcium, pH and soluble divalent cations in milk at high temperature. *Journal of Dairy Science, 93*, 515–523.

Pavia, D. L., Lampman, G. M., Kriz, G. S., & Vyvyan, J. A. (2014). *Introduction to spectroscopy*. Cengage learning.

Prakash, S., Datta, N., & Deeth, H. C. (2005). Methods of Detecting Fouling Caused by Heating of Milk. *Food Reviews International*, *21(3),* 267-293.

Rapp, B. E. (2017). Fluids. *Microfluidics: Modelling, mechanics and mathematics*, 243-263.

Ritter, R.B., 1983. Crystalline fouling studies. *Journal of Heat Transfer*, *105 (2),* 374–378.

Roefs, S. P. F. M., & De Kruif, K. G. (1994). A Model for the Denaturation and Aggregation of β-Lactoglobulin. *European Journal of Biochemistry*, *226(3),* 883-889.

Roscoe, S. G., Fuller, K. L., & Robitaille, G. (1993). An electrochemical study of the effect of temperature on the adsorption behavior of β-lactoglobulin. *Journal of Colloid and Interface Science*, *160*, 243–251.

Sahoo, P. K., Ansari, M. I. A., & Datta, A. K. (2003). A computer based iterative solution for accurate estimation of heat transfer coefficients in a helical tube heat exchanger. *Journal of Food Engineering*, *58(3),* 211-214.

Salaün, F., Mietton, B., & Gaucheron, F. (2005). Buffering capacity of dairy products. *International Dairy Journal*, *15*(2), 95-109.

Sava, N., Van der Plancken, I., Claeys, W., & Hendrickx, M. (2005). The kinetics of heat-induced structural changes of β-lactoglobulin. *Journal of Dairy Science*, *88*(5), 1646-1653.

Siegel, J. A., & Saukko, P. J. (2012). *Encyclopedia of forensic sciences*. Academic Press.

Simmons, M. J. H., Jayaraman, P., & Fryer, P. J. (2007). The effect of temperature and shear rate upon the aggregation of whey protein and its implications for milk fouling. *Journal of Food Engineering*, *79*(2), 517-528.

Stephani, R., de Sá Oliveira, K., de Almeida, C. E. R., Perrone, Í. T., de Carvalho, A. F., de Oliveira, L. F. C., & Almeida, M. R. (2017). Raman spectroscopy as a tool to identify modification of whey protein concentrate (WPC) during shelf life. *Food Packaging and Shelf Life*, *11*, 1-9.

Sundar, S., Rajagopal, M. C., Zhao, H., Kuntumalla, G., Meng, Y., Chang, H. C., Shao, C., Ferreira, P., Miljkovic, N., Sinha, S., & Salapaka, S. (2020). Fouling modeling and prediction

approach for heat exchangers using deep learning. *International journal of heat and mass transfer*, *159(C),* 120112.

Szirtes, T. (2007). *Applied dimensional analysis and modeling*. Butterworth-Heinemann.

Theodoridis, S. (2015). *Machine learning: a Bayesian and optimization perspective*. Academic press.

Thévenot, D. R., Toth, K., Durst, R. A., & Wilson, G. S. (2001). Electrochemical biosensors: recommended definitions and classification. *Analytical Letters*, *34*(5), 635-659.

Tolkach, A., & Kulozik, U. (2007). Reaction kinetic pathway of reversible and irreversible thermal denaturation beta-lactoglobulin. *Lait*., *87(4-5),* 301-315.

Van Boekel, M. A. J. S. (1998). Effect of heating on Maillard reactions in milk. *Food chemistry*, *62*(4), 403-414.

Vasbinder, A. J., & De Kruif, C. G. (2003). Casein–whey protein interactions in heated milk: the influence of pH. *International dairy journal*, *13*(8), 669-677.

Visser, J., & Jeurnink, T. J. M. (1997). Fouling of heat exchangers in the dairy industry. *Experimental Thermal and Fluid Science*, *14(4),* 407-424.

Vrouwenvelder, J. S., van Paassen, J. A. M., Wessels, L. P., van Dam, A. F., & Bakker, S. M. (2006). The Membrane Fouling Simulator: A practical tool for fouling prediction and control. *Journal of membrane science*, *281(1),* 316-324.

Wallhäußer, E., Hussein, W. B., Hussein, M. A., Hinrichs, J., & Becker, T. (2013). Detection of dairy fouling: Combining ultrasonic measurements and classification methods. *Engineering in life sciences*, *13(3),* 292-301.

Wang, M. (Ed.). (2015). *Industrial tomography: systems and applications*. Elsevier.

Wang, Q., & Ma, Y. (2020). Effect of temperature and pH on salts equilibria and calcium phosphate in bovine milk. *International Dairy Journal*, *110*, 104713.

Watkinson, A.P., & Martinez, O., (1975). Scaling of heat exchanger tubes by calcium carbonate. *Journal of Heat Transfer, 97(4),* 504–508.

Withers, P. M. (1996). Ultrasonic, acoustic, and optical techniques for the non-invasive detection of fouling in food processing equipment. *Trends in food science & technology*, *7*(9), 293-298.

Zubair, S. M., Sheikh, A. K., Younas, M., & Budair, M. O. (2000). A risk based heat exchanger analysis subject to fouling: Part I: Performance evaluation. *Energy*, *25(5),* 427-443.

Objectives

Evaporation is a thermal concentration process, where milk is heated under vacuum to temperatures in the range 55-70°C to remove water and concentrate skim milk to total solids typically in the range 48-50%, while minimising thermally induced changes in the resultant concentrated skim milk. This process of evaporation to 48-50% total solids is typically applied prior to spray drying in the production of skim milk powder and is also employed for concentration of skim milk to 40-42% total solids prior to transport between processing sites in the form of liquid concentrates. In spite of using moderate temperatures, the combination of high total solids and long tun times (typically 15-20 h) results in fouling being a key challenge during evaporation of skim milk. Fouling has significant operational, economic, and environmental consequences for the dairy industry, including increased cleaning chemical and water usage, increased energy consumption due to reduced heat transfer efficiency, deterioration in product quality due to insufficient heating and fouling deposit sedimentation, as well as increasing the risk of deterioration in microbial quality due to biofilm formation. Therefore, it is critically important that we develop a better understanding of fouling and the factors contributing to it, such that appropriate mitigation strategies can be researched, developed, and deployed.

Consequently, the overall objectives of this thesis were:

1. To investigate, and study systematically, the effect of pH on the heat stability and physicochemical properties of concentrated skim milk during thermal processing designed to simulate the prevailing conditions in an evaporator;
2. To evaluate the suitability and robustness of the methods used to analyse the physicochemical properties of concentrated skim milk before and after simulated evaporator thermal processing by upscaling heat treatment to a custom-built fouling rig, in the development of predictive indicators of fouling;
3. To examine the influence of pH on the occurrence of fouling of concentrated skim milk during heat treatment on a custom-built fouling rig by monitoring in-process changes, as well as analysis of the heat-induced changes in concentrated skim milk and cleaning-in-place chemicals, in order to characterize evaporator fouling

Chapter 2

The influence of pH on the heat stability and physicochemical properties of concentrated skim milk in relation to fouling

Tara R. Murphy, Eoin W. Finnegan, Tom F. O'Callaghan, James A. O'Mahony

School of Food and Nutritional Sciences, University College Cork, Cork, Ireland

The Dairy Processing & Technology Centre, University College Cork

Declaration

This chapter was written by author Tara R. Murphy (TRM) and reviewed by all co-authors. TRM co-designed the study and performed all of the experimental work.

Abstract

The objective of this study was to investigate the effect of pH on the heat stability and heat-induced changes to the fouling properties of concentrated skim milk. The heat coagulation time of the concentrated skim milk solutions (30%, w/w, total solids) was determined at 120 °C as a function of pH (pH range 6.0-6.7). These samples were heat-treated using a controlled-stress rheometer equipped with a starch-pasting cell geometry, and subsequently assessed in terms of their viscosity, particle size distribution, and sedimentation. As the pH of the samples decreased, an increase in both viscosity and particle size distribution coincided with an increase in sedimentation. Two pH points (pH 6.2 and pH 6.6) of the samples were chosen for upscaling the analysis to a fouling rig to determine if the heat-induced changes identified at small scale would be replicable and to identify the mechanisms in the fouling of concentrated skim milk. After recirculation on the fouling rig, the samples were recovered for analysis of particle size and dry sediment. Cleaning in place solutions applied to the fouling rig after recirculation, and the recirculated skim milk samples were analysed for total solids, protein, and ash content. Recirculation of the sample at pH 6.2 on the fouling rig resulted in severe fouling, however no fouling was observed at pH 6.6. Compositional analysis of the concentrated skim milk sample at pH 6.2 after recirculation on the fouling rig showed a reduction in protein and ash content compared to the starting material. These results, accompanied by compositional analysis of CIP solutions, demonstrated that the foulant deposit formed was mainly comprised of aggregated protein, with some calcium phosphate binding promoted by the low pH and high recirculation temperature. Analysis of the low pH skim milk solution after recirculation for particle size and sedimentation showed results consistent with the initial small-scale heat treatment analysis. These findings provide new insight into the impact of pH on fouling during thermal treatment of concentrated skim milk, using a combination of analytical approaches and tools to allow for a deeper understanding of concentrate behaviour, helping to reduce its occurrence in the future

2.1. Introduction

In the dairy industry, evaporation is used to concentrate skim milk prior to drying in the production of skim milk powder (SMP) (Wiegand, 1971). Evaporation is a thermal process, whereby the milk is heated under vacuum to 55-70°C to remove water at a reduced boiling point, typically targeting a total solids content of 48-50% before spray-drying to a powder (96-97% total solids content) (Bylund, 2015). Fouling of thermal processing equipment during production of dairy products and ingredients is a challenge for the dairy industry, with evaporator fouling being an area of particular focus. Fouling during thermal processing is defined as the build-up of foulant mass deposit in different parts of the thermal processing equipment, such as in pipes, on the heat exchange surface, and in any other fittings in the apparatus (Milanovic *et al.*, 2006). The formation of both dairy foulant (in product) and fouling deposits (on surfaces) is a complex process that involves both aggregation of protein and formation of calcium phosphate in the bulk (i.e., the inner matter) of the fluid (Mahdi *et al.*, 2009). Georgiadis & Macchietto (2000) proposed that the protein reaction takes place in the bulk and at the thermal boundary layer of milk; a first order reaction causes native protein to unfold, followed by a second order reaction causing the unfolded protein to aggregate, with predominantly the aggregated protein forming deposits on heat transfer surfaces. This study also showed that the deposition rate is proportional to the amount of aggregated protein in the thermal boundary layer; the thicker the deposit, the greater the difference in temperature between the heating medium and the product temperature (ΔT). Another important aspect of the dairy fouling process is mineral deposition as there is an inverse relationship between calcium phosphate solubility and temperature that results in further fouling deposition. As calcium phosphate becomes less soluble in milk with increasing temperature, it precipitates out of solution and can produce deposits in the form of crystals on the heat transfer surface (Visser & Jeurnink, 1997). Calcium phosphate can deposit onto the surface of the already deposited beta-lactoglobulin (β-Lg) molecules to further stabilize the structure, creating a strongly adhered foulant layer, as well as mediating protein-protein interactions through electrostatic bridging caused by charge neutralisation (Dalgleish & Law, 1989).

Fouling has significant economic, operational, and environmental consequences for the dairy industry. The formation of deposits can cause challenges during production by increasing the overall thermal resistance, resulting in a decline in the heat performance of the equipment. This can lead to obstructions to fluid flow, increased pressure drop, and reduced heat transfer coefficient (Grijspeerdt *et al.*, 2003), which causes increased total operating costs due to more

frequent cleaning required and increased energy consumption. The additional cleaning in place protocols required to remove fouling deposits are time consuming leading to increased downtimes, as well as causing major environmental impact due to the amount of chemicals, water, and heat needed (Hagsten *et al.,* 2016). There is also a possibility of deterioration in product quality, as the required product temperature may not be achieved (Mahdi, *et al.*, 2009), or erosion of the fouling layer may deposit into the bulk fluid causing product sedimentation (Saget *et al.,* 2021). Deterioration in microbial quality may also occur due to biofilm formation (Mérian & Goddard, 2012), as the bacteria in milk, which includes spoilage and pathogenic microorganisms, can adhere to the foulant deposited on the stainless steel surfaces, and migrate into the product (Marchand *et al.,* 2012).

With these operational and environmental costs in mind, it would be valuable for the dairy industry to have the ability to measure or predict the presence, type, and/or intensity of fouling that occurs in a thermal process when designing, improving, or adapting production processes in order to avoid unnecessary product or capital loss (Wallhäußer *et al*., 2013). However, fouling is a complicated process that depends on several difficult-to-measure parameters, meaning it is challenging to achieve an accurate quantification of overall fouling resistance (Bott, 2001). Therefore, the aim of this study was to investigate the influence of pH on the heat stability and heat-induced changes in concentrated skim milk to determine the suitability and inter-relationships between potential measures and/or indicators of fouling. Initially a small-scale heat treatment of concentrated skim milk at 30% total solids was conducted over a pH range of pH 6.0 to 6.7. Two pH points (pH 6.2 and pH 6.6) of the concentrated skim milk were chosen for upscaling the analysis to a fouling rig to determine if the heat-induced changes identified at small scale would be replicable and to identify the mechanisms in the fouling of concentrated skim milk. This study categorises fouling into two types: ‘adhered fouling’ and ‘non-adhered fouling’ (Figure 2.1), with adhered fouling referring to a build-up of fouling deposit on thermal equipment, and non-adhered fouling referring to any changes in product that are caused either by physicochemical reactions related to fouling, or sedimentation of the fouling layer into the product.

2.2. Materials and Methods

2.2.1. Materials

Medium-heat skim milk powder (SMP) was provided by a local Irish dairy company. The total protein, fat, ash, and carbohydrate of the SMP were 34.29, 0.8, 8.00 and 56.91% (w/w) respectively, as provided by the manufacturer. All chemicals and reagents, unless otherwise stated, were sourced from Sigma-Aldrich (Wicklow, Ireland) and were of analytical grade.

2.2.2. Preparation of high total-solids skim milk solutions

Preliminary rehydration trials were carried out to determine the highest feasible total solids (TS) content that could be attained when rehydrating skim milk powder. Initial rehydration trials using magnetic stirring at room temperature were carried out at 20, 25, 30, 35 and 40% TS. It was found that at a TS content of 30%, severe foaming and sedimentation indicated that the powder was not fully solubilised after stirring at 4°C overnight, and at a TS content >35% the skim milk solution gelled when stirring at 4°C overnight. In the next stage of preliminary trials, rehydration was carried out at 30, 31, 32, 33 and 34% TS using overhead stirring in a waterbath at 50°C. Foaming and sedimentation was observed in the samples at 33 and 34% TS after overnight stirring at 4°C. The samples between 30-33% total solids were analysed for particle size distribution using a laser light diffraction unit (Mastersizer 3000 S, Malvern Instruments Ltd., Worcestershire, UK) to determine if any insolubilized powder particles were present in the solution. Only the sample at 30% total solids was fully solubilised and was therefore chosen as the target TS for the study. It was critical for the study that the total solids content chosen was both comparable to the skim milk evaporation process and feasible to rehydrate to a fully solubilised solution in a replicable manner.

Reconstituted skim milk was prepared by adding medium-heat SMP to ultrapure water over 1 h at 50 ºC to attain 30% (w/w) TS (and 9% (w/w) TS for Section 2.2.3) while stirring using an overhead stirrer (Eurostar 60 control, IKA, Staufen, Germany) with a spiral mixing element (Visco Jet 3x spiral mixing element d = 80 mm, Küssaberg, Germany). During rehydration the stirring speed was gradually increased from 100 to 250 rpm. The solutions were stirred at 50°C for a further 3 h at 200 rpm, after which the solutions were cooled to 20 ºC while magnetically stirring during pH adjustment. The pH of the skim milk solutions were measured using a standard pH meter at 20 °C (Metler Toledo, FiveEasy pH / mV bench meter, F20,

Switzerland).The pH of the skim milk solutions, at 30% (w/w) TS, were adjusted to pH 6.0, 6.1, 6.2, 6.3, 6.4, 6.5, 6.6 and 6.7 using 1 N NaOH and HCl as appropriate. The skim milk solutions were magnetically stirred for a further 2 h, after which pH was readjusted to the target pH, if required. The skim milk solutions were then stored at 4°C overnight, with low speed magnetic stirring, to facilitate complete rehydration. After overnight rehydration, the samples were equilibrated to 22ºC for 2 h, after which the pH was checked and re-adjusted to the target pH, as required.

2.2.3. Heat coagulation time as a function of pH

Heat coagulation time (HCT) of skim milk solutions at 9 and 30% (w/w) TS, was determined at 120 °C as a function of pH in the range 6.0 – 6.7 using the method of Davies and White (1966). Samples (2 mL) were added to heat-resistant glass tubes and stoppered using a rubber bung, placed in a steel rack, and immersed in a silicone oil bath (Hettich ESP oilbaths; Hettich Benelux BV). The HCT was recorded as the time elapsed between immersing the sample in the oil bath and the visible detection of aggregates within the sample.

2.2.4. Viscosity during heat treatment

The skim milk solutions (30%, w/w, TS; pH 6.0-6.7) were heat treated using an AR-G2 controlled-stress rheometer (TA Instruments, Crawley, UK) equipped with a starch pasting cell (SPC) geometry. Samples (28 g) were subjected to a temperature profile, at a shear rate of 15 s^{-1}, as follows: initial temperature (25 ºC) was held for 7 min, then increased at a rate of 10 ºC min^{-1} to reach the target temperature of 90 ºC; samples were then held at 90 ºC for 3 min and cooled to 25 ºC at a rate of 10 ºC min^{-1}, before holding at 25 ºC for 10 min.

2.2.5. Particle size distribution

Particle size distribution (PSD) of the skim milk solutions (after heat treatment, as detailed in Section 2.2.4.) was measured using a laser light diffraction unit (Mastersizer 3000 S, Malvern Instruments Ltd., Worcestershire, UK) equipped with a 300 RF (reverse Fourier) lens and He–Ne laser (λ of 633 nm). The samples were introduced to the dispersing unit using ultrapure water as dispersant to reach an obscuration of 10% (± 1%). Analysis of PSD was performed using the generalised polydisperse model, with particle refractive index of 1.46,

absorption of 0.1 and dispersant refractive index of 1.33. Non-heated samples of the skim milk solutions were used as controls. The skim milk solution at pH 6.0 was not analysed as extensive aggregation made the sample unsuitable for analysis using this method.

2.2.6. Dry Sediment

Sediment was measured following a centrifugation method of Chen *et al.* (2012), with minor modifications to adapt the method for a high total solids material. After heat treatment, as detailed in Section 2.2.4., the skim milk solutions were well shaken, and 20 g was accurately weighed into a calibrated tube and centrifuged (Sorvall RC5C Plus, Massachusetts, United States) at 12,000 g for 1 h. After the supernatant was removed, the sediment was oven-dried at 105°C until a constant weight was obtained, to determine its percentage dry weight. The moisture content (%w/w) of the sediment was calculated by the difference in weight before and after oven drying the sediment. Non-heated samples of the skim milk solutions were used as controls.

Protein and ash content (%,w/w) of the skim milk solutions after heat treatment, and the supernatant formed during the dry sediment method were determined using the Kjeldahl method with a nitrogen-to-protein conversion factor of 6.38 (IDF, 2001), and by dry ashing in a muffle furnace (Nabertherm GmbH, Lilienthal, Germany) at 650 ºC until a white ash was obtained (IDF, 2008). The protein and ash content of the sediment which was calculated as follows:

$$\textit{Skim milk solution crude protein} - \textit{Supernatant crude protein} = \textit{Sediment crude protein}$$

$$\textit{Skim milk solution ash} - \textit{Supernatant ash} = \textit{Sediment ash}$$

2.2.8. Fouling

Fouling behaviour of the skim milk solutions (4 L) at pH 6.2 and pH 6.6 was determined using a custom-built fouling rig, as per the method developed by Hebishy *et al.* (2019), with modifications detailed in Appendix 1. The fouling rig used in this study was a stainless steel, shell and tube heat exchanger of length 90 cm and internal diameter 5 cm (Liam A. Barry Ltd., Cork, Ireland), connected to a circulating waterbath (Grant, LT ecocool™100, Cambridge, UK) which controlled temperature of the water used as the heating medium. Two electronic pressure transducers (PR-33X, Keller-druck, Dorchester, UK), one located immediately before

and one immediately after the heat exchanger were used to measure temperature and pressure in-line. The unit had a stainless steel feed vessel (capacity 4 L), connected directly to a positive displacement, progressive cavity pump (Torqueflow, Sydex, UK); the liquid flow rate through the heat exchanger was controlled by means of a variable speed drive. The pressure on the recirculating samples was set using a manual diaphragm throttling valve, with pressure recorded using an analogue pressure gauge (1107J486, WIKA, Los Angeles, CA, USA). The initial back pressure was set at 1 bar using the throttling valve and was not adjusted during the runs. Temperature of the samples was also measured using a thermocouple mounted to the feed vessel (Digitron 2024T Digital Thermometer Pt100, Port Talbot, UK). The fouling system was operated at a laminar flow rate (25 Hz) in batch recirculation mode. The samples were supplied at an initial temperature of 25 ºC, and the fouling experiments were conducted at 90 ºC (temperature of the heating medium) to simulate thermal processing and preheating of spray dryer liquid concentrate feeds during ingredient manufacture and to enable sufficient denaturation and deposit build-up on the heat exchanger (Jimenez *et al*., 2013; Khalid *et al.,* 2013). The experiment was stopped after 2 h of recirculation, after which, the samples were recovered for analysis of particle size (as detailed in Section 2.2.5) and dry sediment (as detailed in Section 2.2.6). Results are the mean of triplicate measurements from one independent trial.

The system was cleaned in place (CIP) using a standardised CIP protocol. The system was first rinsed using deionised water (4 L) for 10 min, after which a caustic wash was performed using 4 L of 1% (v/v) NaOH solution containing sodium hypochlorite (5%) (Ansep CIP, Ecolab, Co. Meath, Ireland) at 64 ºC for 30 min to dissolve fat, protein, and carbohydrate deposits. After the caustic CIP step, the system was rinsed for 10 min with deionised water (4 L) to remove any residues of caustic. An acid wash was then performed using 4 L of 1% (v/v) acid solution containing nitric acid (>30%) and orthophosphoric acid (<5%) (Horolith V, Ecolab, Co. Meath, Ireland) at 46 ºC for 30 min to dissolve any remaining carbohydrate and mineral deposits. After the acid wash, the system was rinsed for 10 min with deionised water (4 L) to remove any residues of acid.

Samples of the CIP solutions were analysed for total solids (%, w/w), protein (%,w/w), and ash content (%,w/w). Total solids content was determined by oven drying at 104°C until a constant weight was obtained (IDF, 2010). Total nitrogen was determined using the Kjeldahl method (IDF, 2001) and converted to protein using a conversion factor of 6.38. Ash content was determined by dry ashing in a muffle furnace (Nabertherm GmbH, Lilienthal, Germany)

at 650 ºC until a white ash was obtained (IDF, 2008). Skim milk solutions after recirculation on the fouling rig were analysed for total solids, protein, and ash (using the above methods). Results are the means of data from one independent trial, with triplicate measurements carried out for each sample.

2.2.9 Statistical analysis

All experimental analyses were conducted in duplicate, with samples produced from three independent trials for each pH, unless otherwise stated. Results are expressed as mean ± standard deviation. Analysis of variance (ANOVA; Tukey's HSD test) was performed using R i386 version 4.0.2 (R Foundation for Statistical Computing, Vienna, Austria) to identify statistically significant differences between mean values for different samples. The level of significance was determined at $p < 0.05$ to determine whether statistically significant differences existed between the mean values.

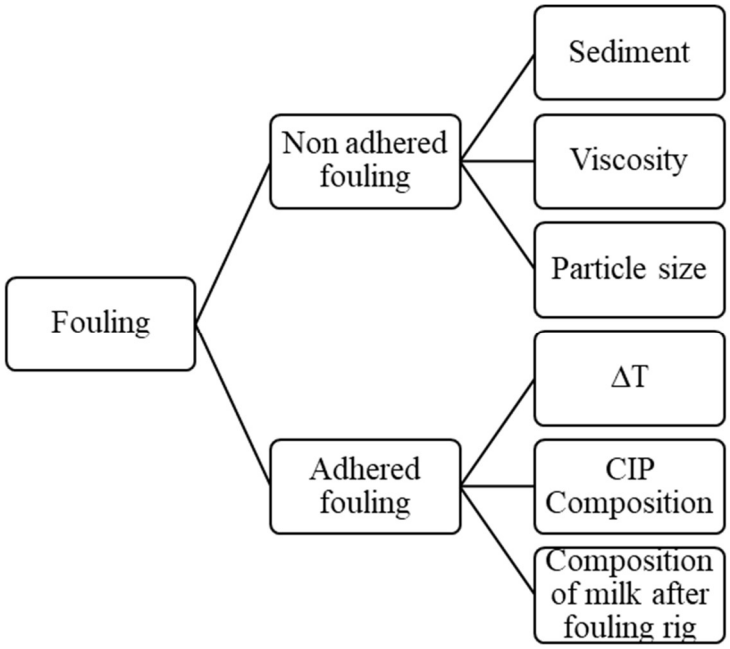

***Figure 2.2.**: Summary of fouling analysis methods. This study categorises fouling into two types: 'adhered fouling' and 'non adhered fouling'.*

2.3. Results and discussion

2.3.1. Heat Stability

To assess the effects of total solids (TS) concentration on the heat stability of the samples (at 9 and 30% (w/w) TS), the heat coagulation time (HCT) was determined at 120 °C as a function of pH in the range 6.0-6.7 (Figure 2.2). The wide pH range was essential for this study, as in-house preliminary trials (data not shown) demonstrated that during evaporation, as total solids increased, the pH decreased. Reconstituted skim milk at 20% (w/w) TS was concentrated using a rotary evaporator at 50 °C, and as the total solids increased from 20 to 30% (w/w) TS, the pH decreased from 6.3 to 6.1. This coincides with findings in a study by Anema (2009), where a linear decrease in pH was observed when heating a 28.8% TS skim milk solution from 20-80°C. As evaporation increases the dry matter content of milk, the decrease in pH can be attributed to the resultant increase in ionic components, precipitation of calcium phosphate and release of hydrogen ions from the casein micelle (Sutariya *et al.,* 2017).

In the present study, at 9% (w/w) TS, the maximum HCT was observed at pH 6.6, and as the samples were acidified, the HCT decreased. The samples had significantly higher ($p < 0.05$) HCTs between pH 6.4-6.7, compared to pH 6.0-6.3. In addition, between pH 6.4-6.7 the HCTs differ significantly ($p < 0.05$) varying from 20.0 to 42.7 min. The heat stability of milk falls into two main profiles: Type A and Type B (Rose 1961a, 1961b). Type A milk shows a maximum in HCT usually at the natural pH of milk at pH 6.6-6.8 and a local minimum at pH 6.9-7.0. Type B milk shows an increase in HCT with increasing pH. The control sample of 9% TS skim milk solution followed the Type A profile at 120°C, which is the most dominant profile found in standard skim milk (Fox and McSweeney, 2003). The higher heat stability observed in the samples between pH 6.4 and 6.7 is attributable to the stability of the casein micelles as the pH is within the region of the native pH of milk, making them less prone to aggregation due to denatured whey proteins adsorbed to the micelle surface, forming a less calcium sensitive steric barrier. The low heat stability of the samples between pH 6 and 6.3 can be attributed to 'salt-induced' coagulation. At low pH, the colloidal stability of casein micelles is lowered by a decrease in surface charge of casein micelles, a reduced electrostatic repulsion, and a collapse of the kappa casein layer due to charge neutralisation. This results in an increased tendency towards aggregation (van Boekel *et al*. 1989). An increase in calcium activity and ionic strength by the dissolution of colloidal calcium phosphate (CCP) also contributes to an increase in calcium-mediated bridging between casein micelles (Nieuwenhuijse *et al*. 1991).

For the skim milk solution at 30% (w/w) TS, the maximum HCT was observed at pH 6.5, and as the samples were acidified, the HCT decreased, but not as severely as the HCT decrease observed on acidification at 9% (w/w) TS. The samples at 30% (w/w) TS had significantly higher ($p < 0.05$) HCTs between pH 6.4-6.7, compared to pH 6.0-6.3. In addition, between pH 6.4-6.7 the HCTs differ significantly ($p < 0.05$) in a small range, varying from 7.78 to 8.86 min, which was much lower than the HCTs observed at 9% (w/w) TS in the same pH range. The HCT at 30% (w/w) TS was slightly higher between pH 6.0 and 6.3 compared to 9% (w/w) TS, and the HCT of the 30% (w/w) TS samples at pH 6.2 and 6.3 were significantly higher ($p < 0.05$) than the samples at pH 6.0 and 6.1, which was not observed at 9% (w/w) TS where there was no significant differences ($p > 0.05$) in this pH range.

The explanation for the difference in HCT between low pH (6.0-6.3) and high pH (6.4-6.7) samples at 30% (w/w) TS is the same as the reasoning above for 9% (w/w) TS. However, there have been several studies exploring why the heat stability of concentrated skim milk is lower than that of unconcentrated skim milk, as heat induced coagulation is a complex process with at least 2 stages (destabilisation and aggregation) which is affected by multiple environmental conditions that mutually influence each other (O'Connell & Fox, 2003). A study by Dumpler (2018b) showed the dependency of HCT on pH for unconcentrated milk and concentrated milk up to a TS content of 35%. HCT decreased significantly ($p < 0.05$) with increasing total solids content, and the increase in pH by NaOH addition to improve heat stability of concentrated skim milk became less effective with increasing TS content. This could provide an explanation for the lower HCT observed between pH 6.4 and 6.7 for 30% (w/w) TS compared to 9% (w/w) TS. Other factors that have been shown to affect the heat stability of concentrated skim milk include an increase in the concentration of soluble calcium (Anema, 2009; Faka *et al.,* 2009), an increase in ionic strength proportional to volume reduction (Augustin & Clarke, 1990), and an increase in protein content (Morrissey & O'Mahony, 1976). It has also been shown by FTIR analysis that protein in milk undergo imperative structural changes during concentration that make them more prone to destabilisation reactions during heating (Markoska *et al.,* 2019). All of these factors contribute to the increased susceptibility of concentrated skim milk to aggregation, and therefore a lower heat stability than unconcentrated skim milk.

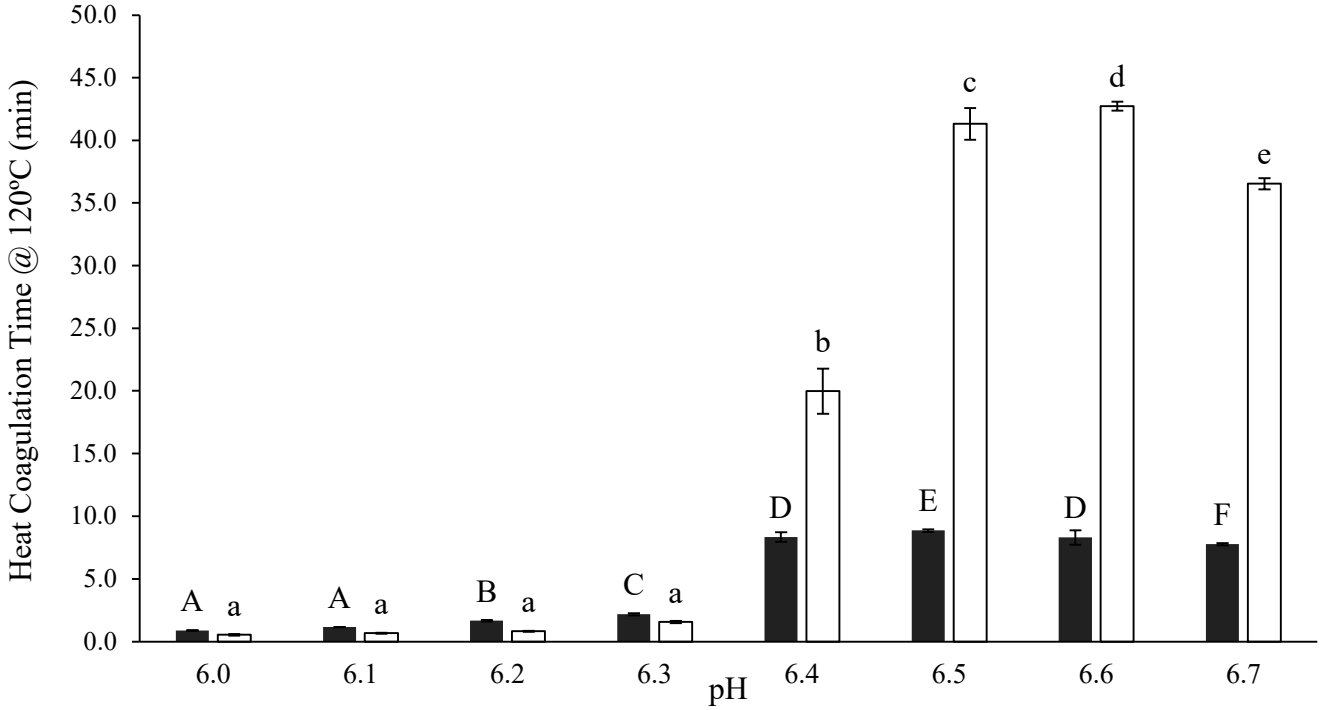

Figure 2.2.*: Heat coagulation time (HCT) at 120 ºC as a function of pH. Data shown is for concentrated reconstituted skim milk at 30% total solids (TS) (■). HCT of reconstituted skim milk at 9% TS (□) was measured as a control. Results are the means of data from three independent trials. Error bars represent standard deviation. Mean values with different superscript letters within each %TS are significantly different ($p < 0.05$).*

2.3.2. Viscosity development on heating

The viscosity of each skim milk solution was measured continuously during lab-scale high temperature short time (HTST) processing (Figure 2.3). At the initial temperature of 25 ºC, there were no significant differences ($p > 0.05$) in viscosity between the samples, with viscosity ranging from 31.4 to 33.3 mPa.s (Table 2.1). Upon heating, as the temperature increased, the viscosity of all samples decreased slightly (Figure 2.3). This slight decrease in viscosity on heating has been previously observed in other concentrated dairy systems and can be attributed to a decrease in the hydrodynamic volume of the protein before physicochemical and conformational changes of the protein occur, such as protein unfolding, protein aggregation and hydrophobic interactions between proteins (Considine *et al.,* 2007; Kasinos *et al.,* 2014). Upon holding at 90 ºC, the viscosity increased, with no significant difference ($p > 0.05$) between the samples in the pH range 6.3-6.7, while the viscosities of the samples at pH 6.0, 6.1 and 6.2 were considerably higher and significantly different ($p < 0.05$) from each other at 148, 74.4, and 30.8 mPa.s respectively (Table 2.1). On cooling to 25 ºC, there was a

considerable increase in viscosity of all samples. There was no significant difference in peak viscosities on cooling between pH 6.3 and 6.7, while between pH 6.0 and 6.2 the peak viscosities on cooling were much higher and had significant differences (Table 2.1).

During holding and cooling, the samples with pH in the range 6.2-6.7 displayed a gradual increase in viscosity that peaked and plateaued, whereas at pH 6.0 and 6.1, a different viscosity profile was observed with a peak followed by a sharp decrease in viscosity during both holding and cooling (Figure 2.3), indicating a two-stage aggregation process occurring at low pH where protein structure unfolding (with resultant exposure of reactive groups) would precede protein-protein association to form larger protein aggregates (Schmidt, 1981). Following HTST treatment, it was observed that the viscosity was higher than the initial viscosity prior to heating for the samples with pH 6.0-6.5, implying that heating to 90 ºC irreversibly impacted on the viscosity of the samples as the protein molecules unfold and aggregate. The final viscosities of the samples at pH 6.6 and 6.7 returned to the initial value, indicating that protein aggregation did not occur, or any association was reversible.

As discussed in Section 2.3.1, evaporation of milk results in a decrease in pH due to increased concentration ionic components, formation/precipitation of calcium phosphate and release of hydrogen ions (Sutariya *et al.*, 2017), which in turn increases the degree of protein denaturation and aggregation. In a study by Anema *et al.* (2004) showed decreasing the pH during heat treatment of skim milk resulted in a greater increase in viscosity, along with increased casein micelle size. The results from the current study show that as the pH of the samples decreased, the viscosity on heating increased. These increases in viscosity could be due to an increased level in protein denaturation. When milk is heated, conformational changes in the whey protein's tertiary structure occur causing the protein to unfold and denature, which exposes the reactive thiol groups that interact with each other to form disulphide bonds, allowing them to associate with κ-casein, hydrophobic regions of the casein micelle, and other whey proteins. These interactions result in protein aggregation, which causes an increase in the volume fraction and voluminosity of the casein micelles. This increase in volume fraction and casein micelle voluminosity, as well as the increased repulsion between micelles cause the increase in viscosity (Jeurnink & De Kruif, 1993; Ho *et al.,* 2018). Although some of the literature referenced here was not based on concentrated skim milk, it was suggested by Anema (2000) that the effect of skim milk concentration on protein denaturation and viscosity becomes less apparent between temperatures of 75 to 100 ºC due to a shift of the rate limiting factor from denaturation at < 90 °C to aggregation at > 90 °C. Therefore, it can be concluded that the

viscosity development of concentrated skim milk on heating follows the same reaction kinetics as unconcentrated skim milk.

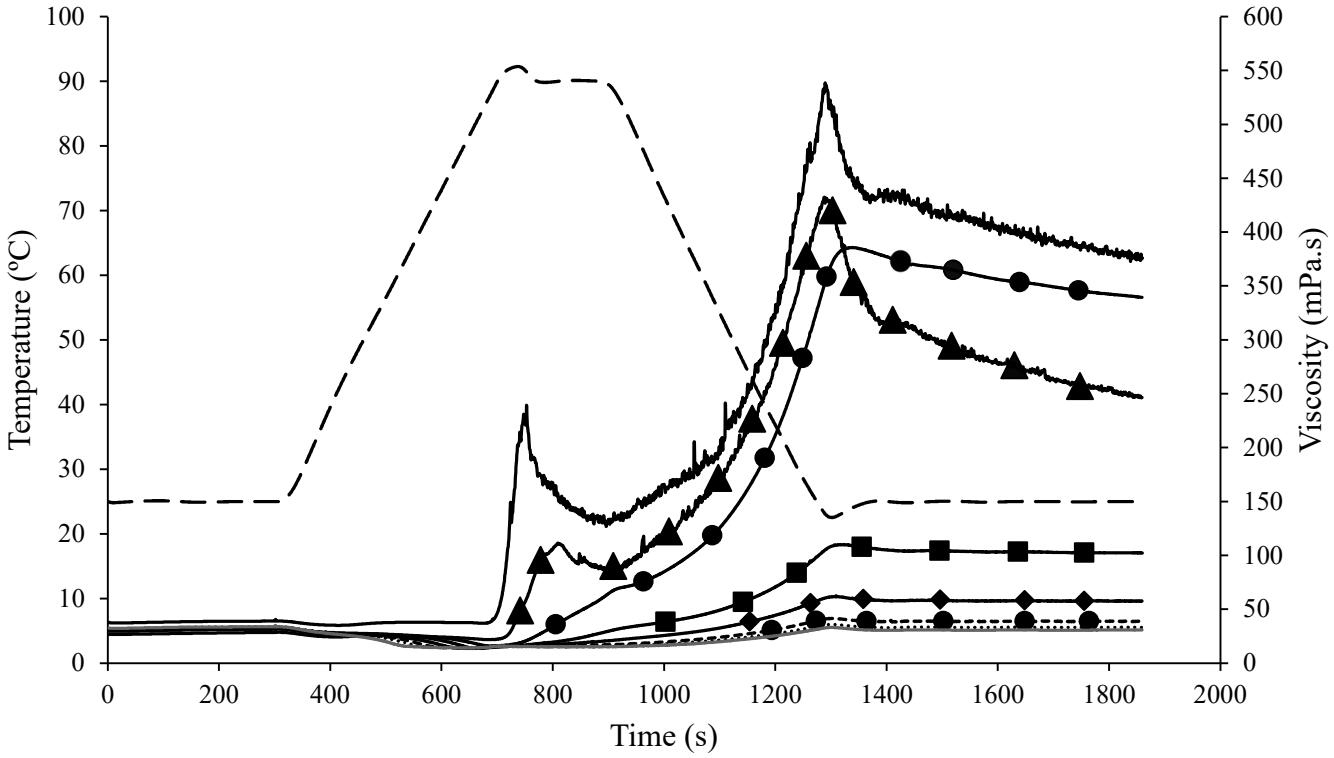

***Figure 2.3.**: Temperature (dashed line) and viscosity during lab-scale high-temperature short-time heating to 90°C of concentrated reconstituted skim milk solutions (30% w/w, total solids). Viscosity profiles shown are the solutions at following pH values: pH 6.0 (solid line); pH 6.1 (▲); pH 6.2 (●); pH 6.3 (■); pH 6.4 (♦); pH 6.5 (- -●- -); pH 6.6 (dotted line); pH 6.7 (grey line). Results are the means of data from three independent trials*

***Table 2.1.**: Viscosity of concentrated skim milk solutions (30% w/w, total solids, pH 6.0-6.7) at different stages during lab-scale high-temperature short-time treatment (HTST) and the area under the curve during the holding and cooling stages during HTST. Values within a column not sharing a common superscript letter differ significantly ($p < 0.05$).*

Sample (pH)	Viscosity at 25°C before heating	Viscosity at 90°C	Peak viscosity on holding	Viscosity at 25°C after cooling	Peak viscosity on cooling	Final Viscosity
	(mPa.s)					
6.0	31.4 ± 1.68^{a}	148 ± 63.6^{a}	339 ± 52.2^{a}	417 ± 107.6^{a}	495 ± 46.9^{a}	376 ± 120.2^{a}
6.1	31.7 ± 1.32^{a}	74.4 ± 34.9^{b}	133 ± 5.74^{b}	299 ± 51.7^{b}	386 ± 13.9^{b}	246 ± 22.1^{b}
6.2	31.2 ± 3.00^{a}	30.8 ± 13.2^{c}	54.6 ± 7.58^{c}	359 ± 74.4^{ab}	303 ± 79.4^{c}	340 ± 70.8^{ab}
6.3	32.3 ± 1.60^{a}	19.1 ± 3.66^{cd}	26.1 ± 4.59^{cd}	104 ± 27.4^{c}	92.9 ± 23.1^{d}	102 ± 29.2^{c}
6.4	30.7 ± 1.38^{a}	17.2 ± 1.66^{cd}	19.8 ± 2.10^{cd}	58.3 ± 12.2^{c}	55.0 ± 12.1^{d}	57.8 ± 13.0^{c}
6.5	32.0 ± 1.98^{a}	16.1 ± 0.68^{d}	17.4 ± 0.67^{d}	39.1 ± 3.35^{c}	37.8 ± 3.25^{d}	38.9 ± 3.33^{c}
6.6	33.0 ± 2.14^{a}	15.7 ± 0.48^{d}	16.5 ± 0.45^{d}	33.6 ± 1.66^{c}	32.8 ± 1.59^{d}	33.4 ± 1.60^{c}
6.7	33.3 ± 2.79^{a}	15.4 ± 0.42^{d}	16.6 ± 0.45^{d}	31.0 ± 1.31^{c}	30.4 ± 1.26^{d}	30.8 ± 1.24^{c}

2.3.3. Particle size distribution

Particle size analysis was conducted to assess the extent of aggregation taking place during heat treatment as influenced by pH. The unheated control and the heated samples with pH between 6.5 and 6.7 all displayed monomodal particle size distributions (PSD's), with one peak identified between 0.01 and 1 μm (Figure 2.4). At pH 6.4, an additional shoulder is observed between 1 and 10 μm, indicating a very low level of protein denaturation and aggregation (Figure 2.4). The heated samples at pH 6.1 also displayed a monomodal particle size distribution of large particles (~10 – 1000 μM) indicative of extensive protein aggregation. Both heated samples at pH 6.2 and 6.3 were poly-dispersed, with pH 6.2 displaying one large peak between 10 and 100 μm, and pH 6.3 displaying one large peak between 0.01-1 μm, followed by two smaller peaks between 1 and 10 μm, and 100-1000 μm. The large standard deviations observed in the particle size distributions for pH 6.1 and 6.3 can be attributed to the partial protein aggregation that can cause variability in results. These results show that as the pH of concentrated skim is decreased, the degree of protein denaturation and aggregation increases (Anema & Li, 2003).

There was no significant difference ($p > 0.05$) in volume mean diameter (D [4,3]) for the unheated control and the heated samples with pH between 6.4 and 6.7 (Table 2.2). The heated samples at pH 6.2 and 6.3 showed significantly higher ($p < 0.05$) values for the D[4,3] at 35.9 and 21.5 μm respectively, while D[4,3] of the heated skim milk solution at pH 6.1 was significantly higher ($p < 0.05$) than all samples at 373 μm due to the dominance of very large, aggregated particles present (Table 2.2). These results are in agreement with a study by Anema *et al.* (2004) that showed an increase in particle size of heated skim milk with a decrease in pH. It was also observed that the span of the heated skim milk solution at pH 6.3 was significantly different ($p < 0.05$) from all other samples, as it displayed the most polydisperse particle size distribution. It can be concluded there is a pH-dependent increase in particle size of concentrated skim milk on heating. At low pH (i.e., between pH 6.1 and 6.3), heat-induced whey protein association with casein micelles occurs, resulting in an increase in casein micelle size (Beaulieu *et al.,* 1999), which is reflected in the results of the present study.

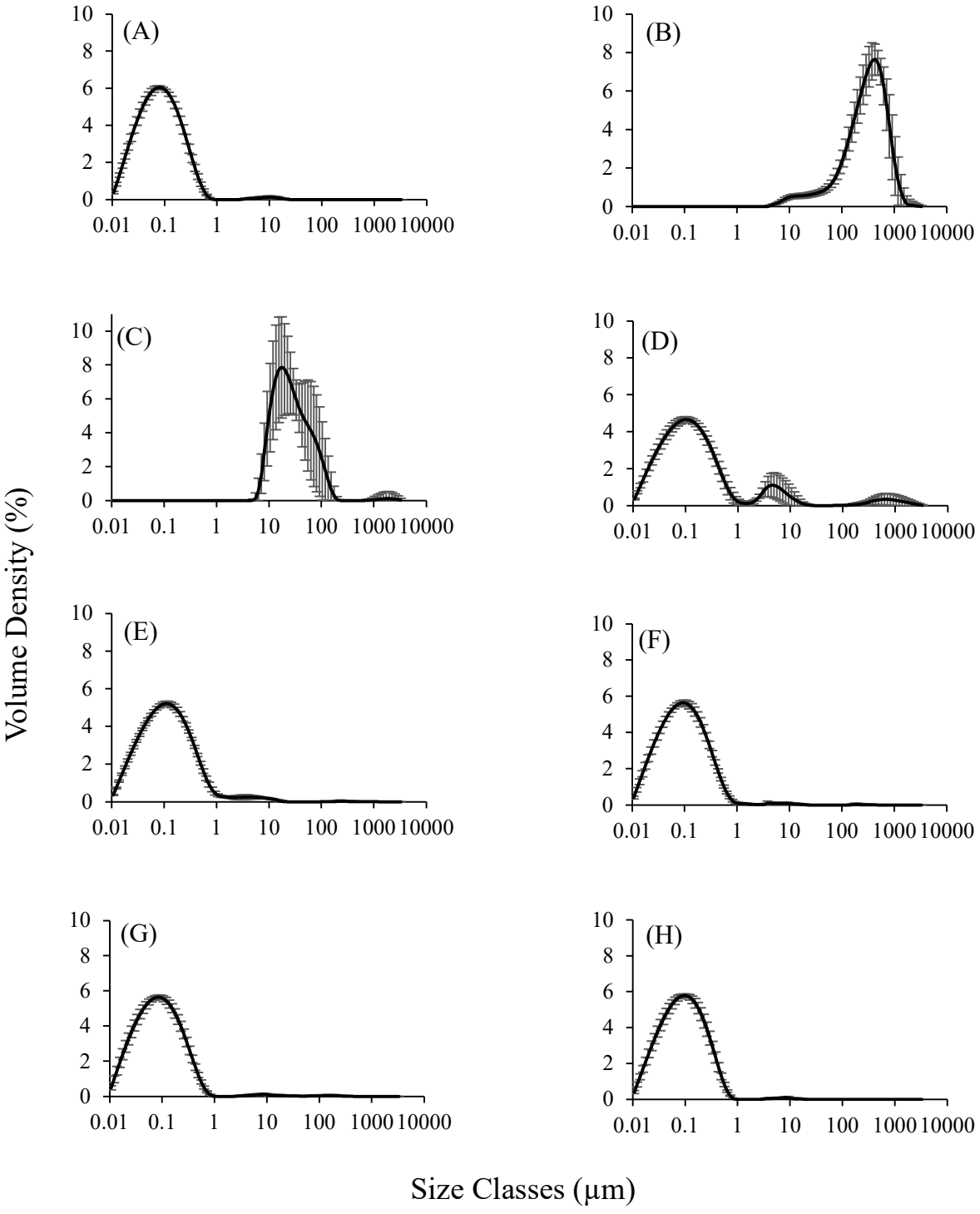

***Figure 2.4.**: Particle size distribution of concentrated skim milk solutions (30% w/w, total solids) after lab-scale high-temperature short-time heating to 90°C at pH 6.1 (B), pH 6.2 (C), pH 6.3 (D), pH 6.4 (E), pH 6.5 (F), pH 6.6 (G) and pH 6.7 (H). The unheated control (A) was not subjected to any heat treatment. Results are the means of data from three independent trials.*

***Table 2.2.**: Particle size distribution parameters (µm) for concentrated skim milk solutions (30% w/w, total solids) after lab-scale high-temperature short-time heating. The unheated control was not subjected to any heat treatment. Samples analysed after heating are abbreviated to 'AH'.*

Sample	D [3,2]	D [4,3]	Dv (10)	Dv (50)	Dv (90)	Span
	(µm)					
Unheated Control	0.05 ± 0.00[a]	0.20 ± 0.07[a]	0.02 ± 0.00[a]	0.08 ± 0.00[a]	0.26 ± 0.02[a]	3.03 ± 0.08[a]
pH 6.1 AH	115 ± 16.9[b]	373 ± 62.5[b]	66.7 ± 15.9[b]	321 ± 46.8[b]	758 ± 86.4[b]	2.18 ± 0.26[a]
pH 6.2 AH	22.6 ± 7.18[c]	35.9 ± 14.4[c]	11.5 ± 2.35[c]	19.6 ± 2.41[c]	51.8 ± 7.89[c]	2.20 ± 0.70[a]
pH 6.3 AH	0.07 ± 0.01[a]	21.5 ± 9.37[d]	0.03 ± 0.00[a]	0.12 ± 0.01[a]	2.57 ± 1.09[d]	37.9 ± 11.8[b]
pH 6.4 AH	0.07 ± 0.00[a]	0.35 ± 0.06[a]	0.03 ± 0.00[a]	0.11 ± 0.00[a]	0.46 ± 0.04[a]	4.06 ± 0.32[a]
pH 6.5 AH	0.06 ± 0.00[a]	0.20 ± 0.06[a]	0.02 ± 0.00[a]	0.09 ± 0.00[a]	0.32 ± 0.02[a]	3.36 ± 0.24[a]
pH 6.6 AH	0.05 ± 0.00[a]	0.15 ± 0.01[a]	0.02 ± 0.00[a]	0.08 ± 0.01[a]	0.30 ± 0.03[a]	3.34 ± 0.20[a]
pH 6.7 AH	0.06 ± 0.00[a]	0.17 ± 0.03[a]	0.02 ± 0.00[a]	0.09 ± 0.00[a]	0.30 ± 0.01[a]	3.08 ± 0.12[a]

Results are the means of data from three independent trials. Mean values within a column not sharing a common superscript letter differ significantly ($p < 0.05$).
D[4,3] = volume-weighted mean particle diameter.
D[3,2] = surface-weighted mean particle diameter.
Dv(10) = particle size below which 10% of sample volume is found.
Dv(50) = particle size below which 50% of sample volume is found.
Dv(90) = particle size below which 90% of sample volume is found

2.3.4. Sediment formation

Sediment formation during heating of concentrated skim milk is related to poor heat stability (Chen *et al.*, 2012), and is formed by casein micelle aggregation (Chen & O'Mahony, 2016). On-Nom *et al.,* (2012) found that the dry weight of sediments formed in samples of reconstituted milk heated and dialysed at 115°C for 30 min consisted of 50-60% protein, with all the major whey protein and casein fractions being identified in the sediment. Calcium ions have also been shown to be a predominant factor influencing sediment formation in a study by Lewis *et al.,* (2011), where milk with calcium chloride additions were ultra-heat treated and analysed for sediment formation.

In this study, sediment is used as a measure of fouling as sedimentation of the foulant into the product is a common occurrence during thermal processing in the dairy industry (Swartzel, 1983). The sediment formation in the unheated control is significantly different ($p < 0.05$) from the heated samples with pH between 6.0 and 6.3, whereas samples between pH 6.4 and 6.7 do not differ significantly ($p > 0.05$) from the unheated control (Figure 2.5). The largest amount of sediment was formed at pH 6.2, followed by pH 6.0 and 6.1, with sediment values of 49.3, 41.7 and 37.9% respectively. These results coincide with findings by On-Nom *et al.* (2012), where no significant sediment was formed in heated samples of reconstituted skim milk if the pH was maintained above 6.3. The large amount of sediment formation in the low pH range is likely as a result ofthe increased particle size due to protein aggregation. A similar method for determining sediment was used in a study by Havea (2006), in which milk protein concentrate was separated into two parts: the supernatant which consisted of the soluble protein, and the sediment which consisted of the insoluble protein. The aggregated proteins were defined as the insoluble protein that formed the sediment.

The sediment's protein, ash, and moisture levels, represented as a percentage of the total sediment formed, offer insights into the varying composition of concentrated skim milk sediment at different pH levels (Figure 2.5). Protein and moisture were found to be the primary components in all formed sediments. The control sample, which was not heated, had a minimal percentage of moisture in the sediment due to its compact and firm nature, causing any moisture to be easily expelled during centrifugation. As the pH of the concentrated milk decreased, the sediment's protein and moisture content increased. The sediments formed at between pH 6.0-6.3 exhibited a higher percentage of protein, which can be attributed to extensive protein aggregation occurring at low pH as the micelles lose stability. This observation aligns with previous hypotheses suggesting that aggregated protein primarily constitutes the sediment

(Chen & O'Mahony, 2016; On-Nom et al., 2012). The sediments formed at pH 6.2 and 6.3 displayed a high percentage of moisture due to the presence of large protein aggregates, resulting in a soft and porous structure. These large aggregates hindered the sediment from compacting as firmly as the unheated control during centrifugation, leading to a significant amount of trapped moisture in the sediment. The sediments formed by the samples between pH 6.0-6.3 contained the highest amount of ash, while all other samples had ash levels comparable to the unheated control. This outcome was expected since the low pH of the sample promotes calcium activity through the dissolution of the CCP (Nieuwenhuijse et al., 1991), indicating that the substantial sediments formed between pH 6.0-6.3 were likely due to calcium-mediated bridging between casein micelles and denatured whey proteins associated with κ-casein. Overall, these findings align with prior research on sediment formation in both unconcentrated and concentrated milk upon heating (Chen & O'Mahony, 2016; Havea, 2006; Lewis et al., 2011; On-Nom et al., 2012). These studies have consistently demonstrated that as the pH of the product decreases, the quantity of sediment formed increases. Furthermore, it has been established that the sediment primarily comprises aggregated protein, with minerals being the secondary component.

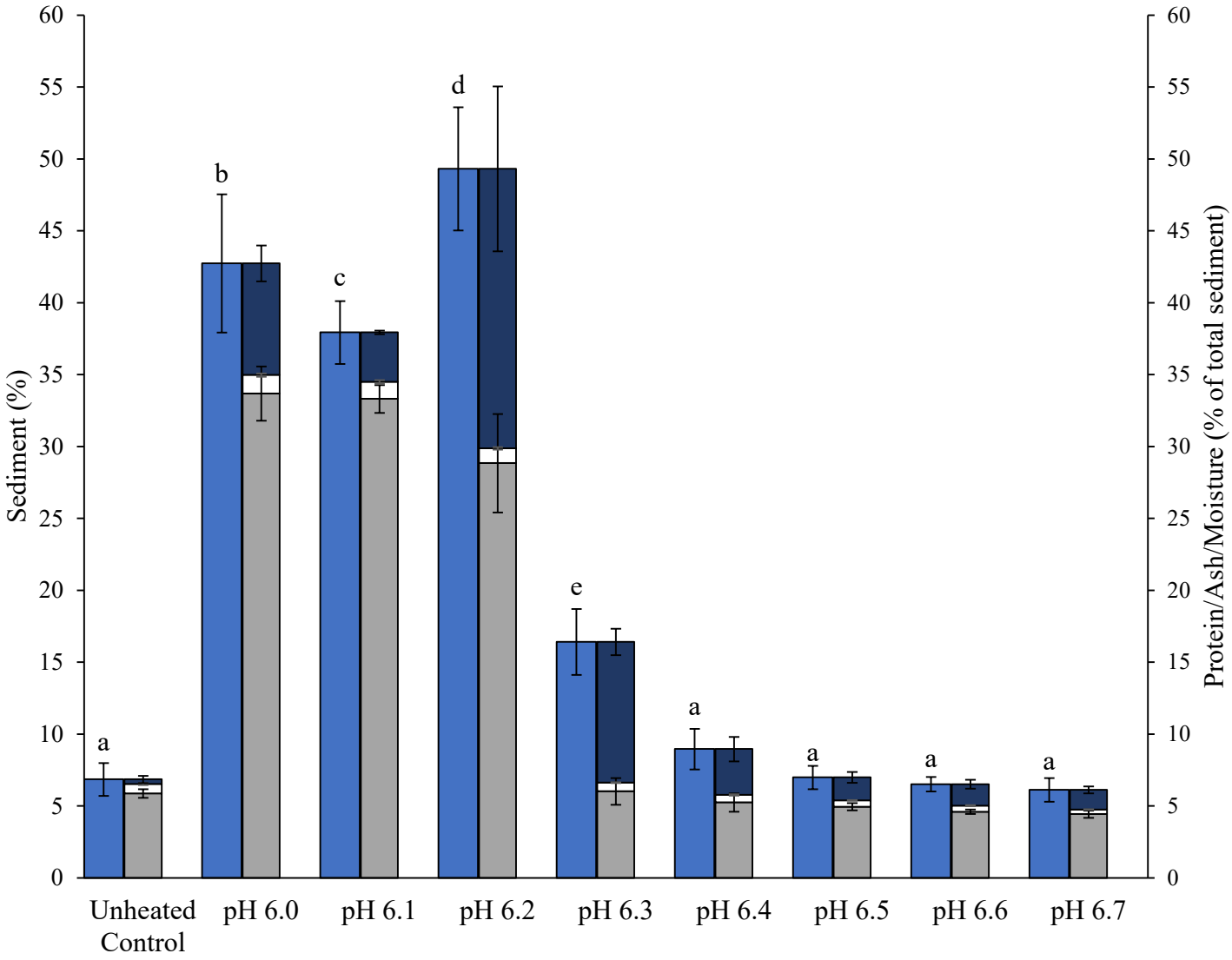

***Figure 2.5.**: The relationship between pH and sediment (■) formation (%)following lab-scale high-temperature short-time heating to 90°C of concentrated skim milk solutions (30% w/w, total solids). The protein (■), ash (□) and moisture (■) content of the sediments is expressed as a percentage of the total sediment formed for each sample. The unheated control was not subjected to any heat treatment. Results are the means of data from three independent trials. Mean values with different superscript letters are significantly different ($p < 0.05$).*

2.3.5. Fouling analysis

2.3.5.1. Fouling behaviour of concentrated skim milk

Concentrated skim milk solutions at pH 6.2 and 6.6 were chosen for fouling analysis based on the results from Section 2.3.1-2.3.4, as they represent the two distinct effects of pH on heat-induced changes in concentrated skim milk i.e., pH 6.2 coincides with results indicative of protein aggregation, whereas pH 6.6 represents results with little heat induced changes. The temperatures of the samples at pH 6.2 and pH 6.6 on recirculation through the fouling rig at 90 ºC are shown in Figure 2.6. For both samples, an initial heat-up time was observed from 0-40 min with a rapid increase in temperature, followed by a gradual temperature change from 40-90 min. The temperature of the sample at pH 6.2 increased with circulation through the fouling rig to reach 79.5 ºC after 40 min, whereas the sample at pH 6.6 increased to 81.1°C after 40 min. As recirculation continued, the temperature of the sample at pH 6.2 decreased to a final value of 75.4 ºC by the end of the run. This temperature reduction was due to the build-up of fouling deposits in the heat exchanger, as seen in the image in Figure 2.6. In contrast, the sample at pH 6.6 had a gradual increase in temperature (from 81.3 to 86.8 ºC) after the initial heat-up time, indicating that concentrated skim milk at pH 6.6 does not foul the heat exchanger.

The foulant formed at pH 6.2 was characteristic of 'type-A deposit', distinguished by Burton (1968), which is a soft, curd-like material that forms at temperatures between 70-110 ºC. A similar deposit was formed in a fouling study by Jeurnink *et al.* (1996), and it was determined that the deposit consisted mainly of whey proteins, followed by minerals and caseins; the authors also reported that lowering the pH of milk results in severe fouling caused by casein micelles. Therefore, it can be hypothesised that the foulant formed in this current study can be attributed to mutual interactions of casein micelles due to aggregation facilitated by denatured whey proteins and solubilised calcium phosphate salts (Smits & van Brouwershaven, 1980). This reaction, partnered with heat-induced disulphide bonds between whey proteins and κ-caseins, results in a significant degree of protein aggregation that can contribute to fouling (Lowe *et al.,* 2004). No adhered foulant was formed by the sample at pH 6.6, further supporting the hypothesis that the build-up of foulant is due to association of denatured whey proteins and casein micelles; as the pH approached the native pH of milk, the micelle surface charge will increase reducing the tendency of the denatured whey proteins and casein micelles to associate (Anema & Li, 2003).

As the build-up of fouling reduces the heat transfer efficiency of thermal equipment, the temperature of the heating medium must increase in order to maintain product temperature for

product quality and safety. Therefore, this temperature increase can be used as an indirect measure of fouling (Prakash *et al.,* 2005). This concept was implemented and adapted by Hill *et al.* (1997) when investigating the impact of different genetic variants of β-lg on fouling in ultra-high temperature (UHT) milk. The temperature difference (ΔT) between the heating medium and the treated milk leaving the system was monitored with an increase in this temperature difference indicating fouling deposit build-up. In this current study, the ΔT was measured differently, with the heating medium remaining a constant temperature and the product temperature changing, as maintaining product temperature was not a concern for this study. There was a considerable difference in ΔT between the samples at pH 6.2 and 6.6; after 2 h of recirculation at pH 6.2 the ΔT was 14.6 ºC, whereas at pH 6.6 the ΔT was 3.2 ºC. This higher ΔT at pH 6.2 can be attributed to the build-up of the fouling deposit in the heat exchanger, impeding the heat transfer. The ΔT of the sample at pH 6.6 remained stable after the initial heat up time, as no adhered foulant built up in the heat exchanger. An 'acceptable' ΔT, i.e., indicative of no fouling, is process and product specific, and for the fouling rig used in this study, it was determined through several preliminary trials that a ΔT that indicates no fouling is between 2-8°C. In conclusion, these results demonstrate that the pH level of concentrated skim milk has a major impact on the occurrence of fouling.

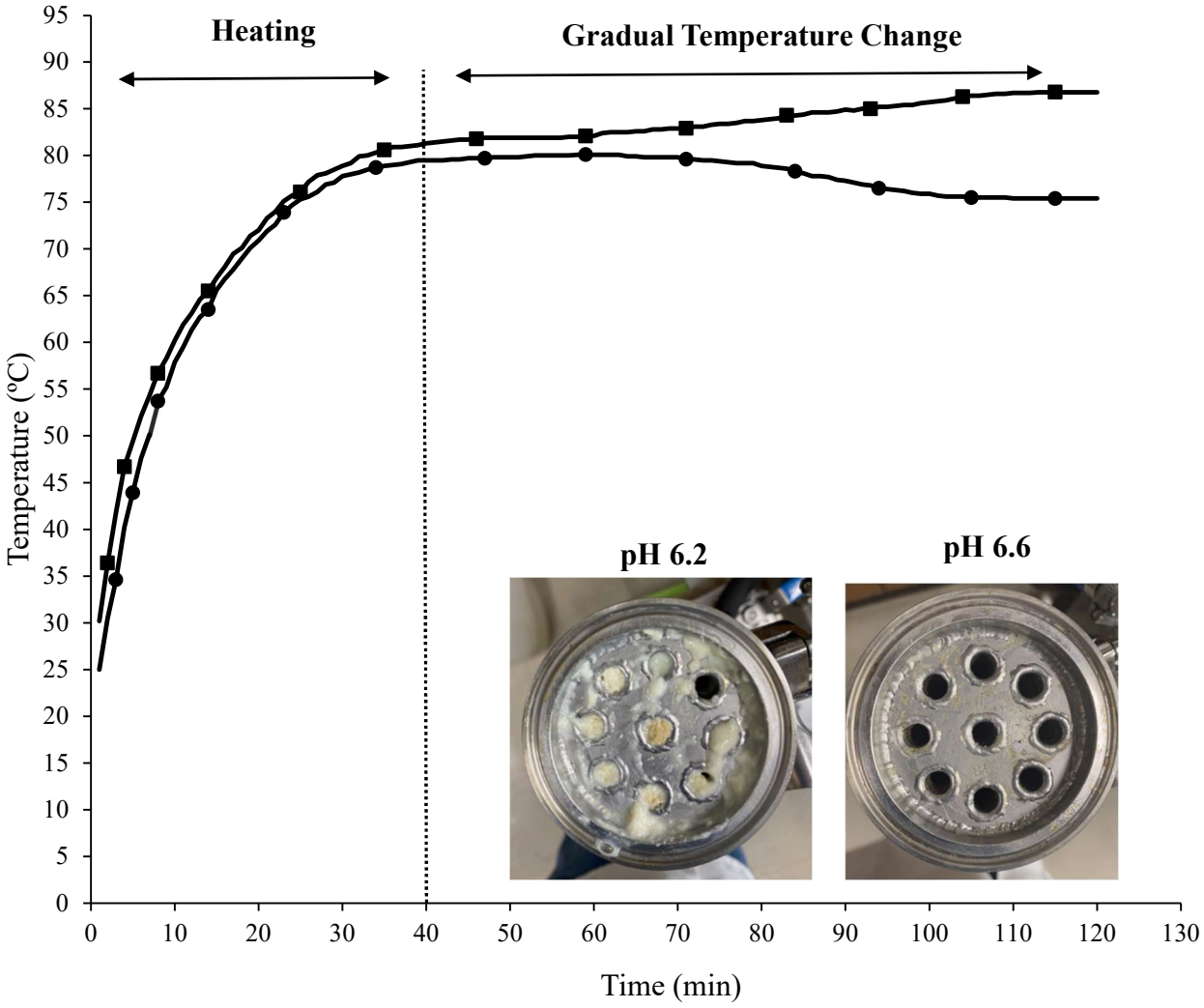

Figure 2.6.*:* Temperature as a function of time for concentrated skim milk solutions (30% w/w, total solids) at pH 6.2 (●) and pH 6.6 (■) measured using a thermocouple mounted to the feed vessel. Inserted photographs show the surface of the tube outlet of the heat exchanger for the sample at pH 6.2 and pH 6.6 after 2 h of running at 90 ºC.

2.3.5.2. Particle size distribution following fouling rig

The unheated control and the recirculated sample at pH 6.6 displayed monomodal particle size distributions, with one peak identified between 0.01 and 1 μm (Figure 2.7). On heating at pH 6.6, an additional shoulder is observed between 1 and 10 μm, indicating a very low level of protein denaturation and aggregation due to the severe time and temperature conditions of the fouling experiment (Figure 2.7). The recirculated skim milk solution at pH 6.2 also displayed a monomodal particle size distribution of large particles (~10-100 μm), indicative of protein aggregation (Figure 2.7). There was no considerable difference in volume mean diameter (D [4,3]) for the unheated control (0.20 μm) and the recirculated skim milk solution at pH 6.6 (0.15 μm), whereas the recirculated skim milk solution at pH 6.2 showed a much higher value for the D [4,3] at 54.0 μm (Table 2.3), indicating that the formation of protein aggregates via intermolecular disulphide bridges resulted in an increase in particle size diameter, as also previously reported (Donato & Guyomarc'h, 2009). These results are comparable to the particle size analysis in Section 2.3.3, which showed large particle size indicative of protein aggregation for the heated concentrated skim milk solution at pH 6.2, whereas at pH 6.6 a considerably lower particle size was observed due to reduced protein aggregation. These results support the above hypothesis (Section 2.3.5.1) that the fouling caused by concentrated skim milk could be related to the increase in particle size due to protein aggregation, showing that this phenomenon is the same in both lab-scale and large scale systems. This highlights the relevance, robustness, and scalability of lab-scale methods for measurement of fouling characteristics at a larger scale, as understanding the mechanisms causing fouling is key in the development of strategies for reducing the occurrence of fouling.

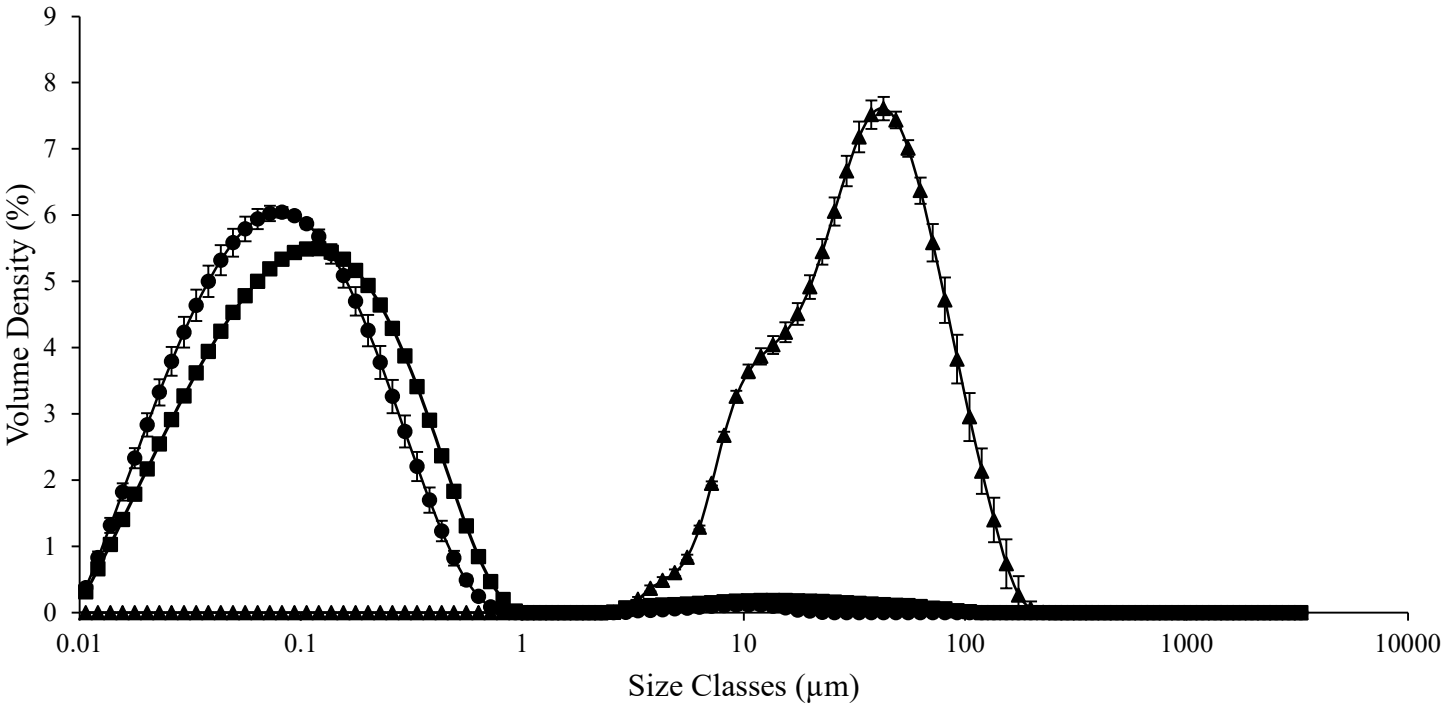

***Figure 2.7.**: Particle size distribution of concentrated skim milk solutions (30% w/w, total solids) without heat treament (●), and after 2 h of running on the fouling rig at 90 ºC at pH 6.2 (▲) and pH 6.6 (■). Results are the means of data from one independent trial.*

***Table 2.3.**: Particle size distribution parameters (µm) for concentrated skim milk solutions (30% w/w, total solids) after 2 h of running on the fouling rig at 90 ºC. The unheated control was not subjected to any heat treatment. Samples analysed after heating are abbreviated to 'AH'.*

Sample	D [3,2]	D [4,3]	Dv (10)	Dv (50)	Dv (90)	Span
	(µm)					
Unheated Control	0.05 ± 0.00	0.20 ± 0.07	0.02 ± 0.00	0.08 ± 0.00	0.26 ± 0.01	3.01 ± 0.09
pH 6.2 AH	33.1 ± 2.84	54.0 ± 7.83	11.6 ± 1.64	44.4 ± 6.59	108 ± 14.7	1.97 ± 0.10
pH 6.6 AH	0.06 ± 0.00	0.15 ± 0.01	0.02 ± 0.00	0.08 ± 0.01	0.30 ± 0.03	3.42 ± 0.23

Results are the means of data from one independent trials.

D[4,3] = volume-weighted mean particle diameter.
D[3,2] = surface-weighted mean particle diameter.
Dv(10) = particle size below which 10% of sample volume is found.
Dv(50) = particle size below which 50% of sample volume is found.
Dv(90) = particle size below which 90% of sample volume is found.

2.3.5.3. Sediment formation following fouling

In Section 2.3.4, the sediment test was used to demonstrate its applicability as a simple measurement of heat stability. In this section, the sediment test is being used for this purpose, as well as a measure of the extent of fouling, as transfer of fouling deposit into evaporated milk products is a common issue in the dairy industry as the excessive sediment formation reduces product quality (Dumpler & Kulozik, 2016; Kasinos *et al.,* 2014; Swartzel, 1983). The sediment formation in the recirculated skim milk solution at pH 6.6 and the unheated control differed slightly, at 13.3 and 6.86% respectively (Figure 2.8). The recirculated skim milk solution at pH 6.2 formed the largest amount of sediment at 47.2%. The large amount of sediment formation at low pH can be attributed to the fouling that was shown to occur at pH 6.2 in Section 2.3.5.1, as flecking and transfer of the fouling deposit into the recirculating concentrated skim milk solution was likely to have occurred. The composition of the sediments was found to be mainly protein and moisture, with a considerable amount of ash constituting the sediment formed at pH 6.2. As observed in the results in Section 2.3.4, the higher percentage protein present in the sediment formed at pH 6.2 can be attributed to extensive protein aggregation that occurs at low pH as the micelles become destabilised (On-Nom *et al.*, 2012), with an accompanied high percentage moisture attributed to the presence of large protein aggregates resulting in a soft and porous structure that traps moisture in the sediment. These results are comparable to the sediment test in Section 2.3.4, with very similar amounts of sediment with comparable protein, ash and moisture contents formed at pH 6.2 and 6.6 after small-scale heat treatment and recirculation on the fouling rig. This shows the usefulness of the sediment test as a simple measurement of the extent of non-adhered fouling material (Figure 2.1), as a relationship has been established between the occurrence of fouling and the formation of sediment in the material that causes fouling i.e., the concentrated skim milk.

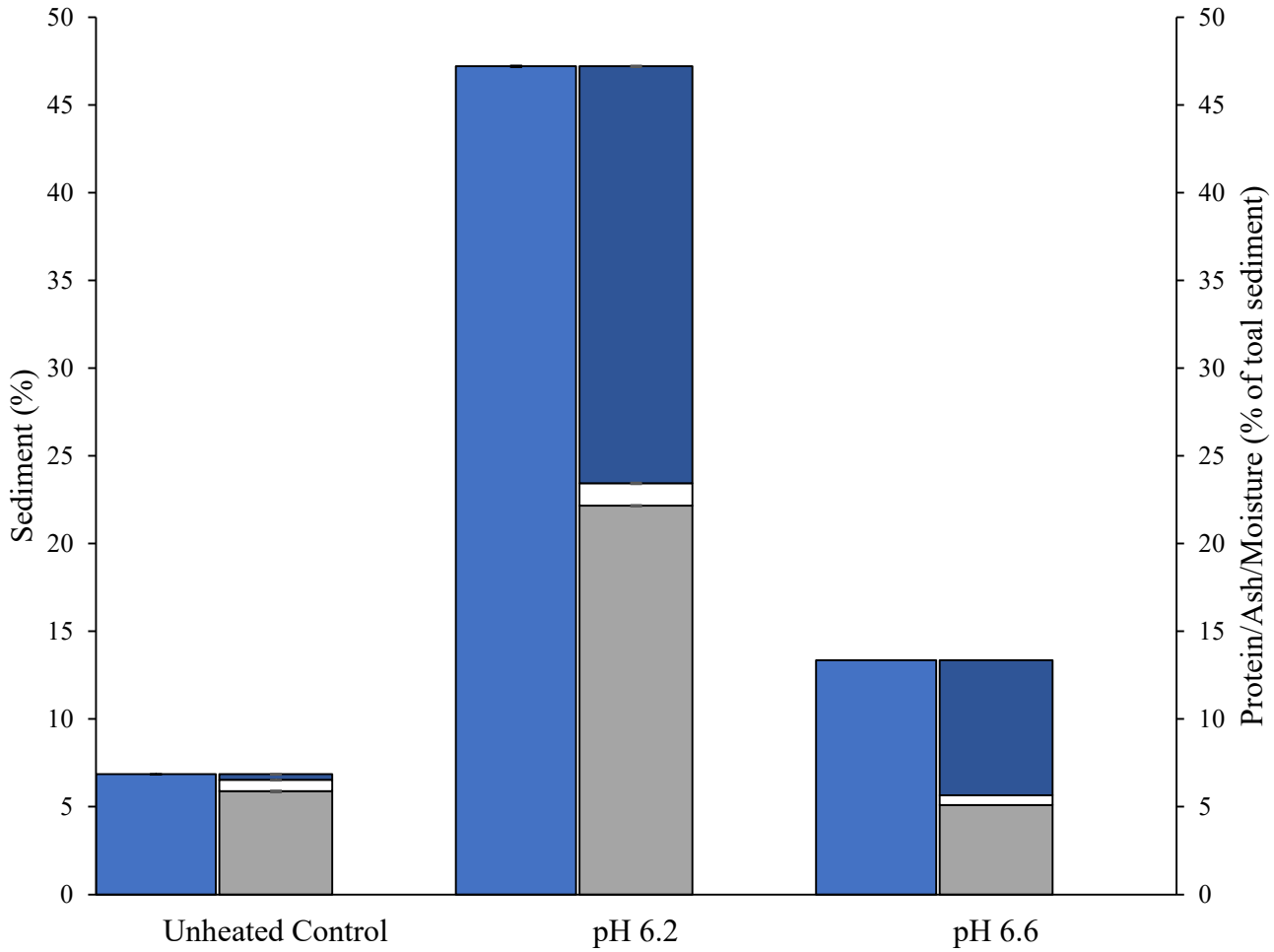

Figure 2.8.: *.The relationship between pH and sediment (■) formation (%) following running concentrated skim milk solutions (30% w/w, total solids) on the fouling rig at 90°C for 2 h. The protein (■), ash (□) and moisture (■) content of the sediments is expressed as a percentage of the total sediment formed for each sample. The unheated control was not subjected to any heat treatment. Results are the means of data from one independent trial.*

2.3.5.3 Composition of the concentrated skim milk solutions following fouling rig recirculation

To determine what components of the concentrated skim milk solutions contributed to fouling, measurement of the total solids, protein, and ash content of the samples before and after recirculation on the fouling rig was performed (Table 2.4). The total solids, protein and ash content of the starting material was 30.0, 9.46, and 2.70% respectively. The total solids content was lower after recirculating the samples at pH 6.2 and 6.6, reducing to 24.3 and 25.0% respectively. After recirculating the sample at pH 6.2, the protein content decreased to 7.56% whereas a less extensive change in protein content was observed after recirculating the skim milk solution at pH 6.6, with the protein content reducing to 8.34%. The ash content was lower after recirculating the samples at pH 6.2 and 6.6, reducing to 1.78 and 1.74% respectively. This indicates that minerals were less of a contributing factor to fouling caused by concentrated skim milk, as both the fouled and unfouled samples had similar ash contents after recirculation, further supporting that the fouling deposit was caused mainly by aggregated proteins, i.e., 'type A fouling'. This is to be expected, as mineral fouling ('type B fouling') usually takes place at temperatures >110 ºC (Lund & Bixby, 1975); however small amounts of solubilised calcium phosphate from the casein micelle can facilitate protein-protein interactions, and thus the drop in ash content between the starting material and the samples drained from the fouling rig could be attributed to this (Singh & Creamer, 1991) . In previous studies where the composition of fouling deposits were analysed, it was found that whey proteins account for more than 50% of the fouling deposits in type A fouling, with the β-lg being the dominant protein due to its high heat sensitivity (Lalande *et al.*, 1985; Gotham *et al.*, 1992).

2.3.5.4 Composition of the recovered CIP solutions

The recovered CIP solutions obtained after applying the CIP protocols were analysed for total solids, protein, and ash content to further investigate the components of concentrated skim milk contributing to fouling (Table 2.4). The total solids, protein and ash content of the water rinses did not differ considerably between the different recirculation experiments; however, substantial differences were observed between the samples of the caustic and acid washes. After recirculation of the sample at pH 6.2, the subsequent caustic solution had a protein content of 0.82% after the CIP regime, whereas after recirculation of the skim milk solution at pH 6.6 the caustic solution had a protein content of 0.25% after the CIP regime. The results show that considerably more protein adhered to the stainless-steel surfaces within the fouling rig at pH 6.2, further confirming that heat induced protein denaturation contributes to fouling and that the reactions are promoted at low pH. In the acid washes, an ash content of 1.06% was observed after the CIP regime for the recirculation of the skim milk solution at pH 6.2, whereas after recirculation of the skim milk solution at pH 6.6 the acid wash had an ash content of 0.29% after the CIP regime. These results further support the hypothesis in Section 2.3.5.5 that solubilised calcium phosphate is involved in the formation of fouling deposits caused by concentrated skim milk at low pH. As the natural pH of milk (pH 6.7) decreases towards its iso-electric point, the net charge of the casein micelle decreases. This causes progressive protonation of organic and inorganic phosphate present in the casein micelles resulting in dissolution of the CCP (Dalgleish & Law, 1989; Marchin *et al*., 2007).

***Table 2.4.**: Protein, ash, and total solids content (% w/w) of concentrated skim milk solutions (30% w/w, total solids) at pH 6.2 and pH 6.6 after running on the fouling rig at 90°C for 2 h. Unheated control was not subjected to any heat treatment. Samples analysed after heating are abbreviated to 'AH'. Composition of the cleaning solutions recovered after applying a cleaning in place (CIP) protocol to the fouling rig after recirculation is also shown. Results are the means of data from one independent trial.*

	Skim Milk Solutions			**CIP after fouling rig at pH 6.2**			**CIP after fouling rig at pH 6.6**		
Composition (%w/w)	Unheated Control	pH 6.2 AH	pH 6.6 AH	Water Rinse	Caustic Wash	Acid Wash	Water Rinse	Caustic Wash	Acid Wash
Protein	9.46 ± 0.34	7.56 ± 0.02	8.34 ± 0.02	1.08 ± 0.06	0.82 ± 0.00	0.00 ± 0.00	1.07 ± 0.06	0.25 ± 0.02	0.00 ± 0.00
Ash	2.70 ± 0.02	1.74 ± 0.00	1.78 ± 0.03	0.30 ± 0.02	0.00 ± 0.00	1.06 ± 0.04	0.22 ± 0.01	0.00 ± 0.00	0.29 ± 0.04
Total Solids	30.0 ± 0.02	24.3 ± 0.06	25.0 ± 0.48	1.60 ± 0.01	3.45 ± 0.24	3.05 ± 0.22	1.16 ± 0.00	1.12 ± 0.02	0.50 ± 0.07

2.4. Conclusion

This study demonstrated the complex interrelationships between heat stability, viscosity, particle size, sedimentation and ultimately fouling of concentrated skim milk during thermal processing. As the pH of the concentrated skim milk solutions decreased, heat stability decreased, viscosity development on heating increased, particle size after heating increased, and formation of sediment in solution after heating increased. Recirculating a low pH sample (pH 6.2) on a custom-built fouling rig resulted in severe fouling, which was visually apparent and also confirmed by a high ΔT. Analysis of the composition of the low pH skim milk solution after recirculation on the fouling rig showed a reduction in protein and ash content compared to the starting material. These results, accompanied by compositional analysis of CIP solutions, demonstrate that the fouling deposit formed was mainly comprised of aggregated protein, with some calcium phosphate binding promoted by the low pH and high recirculation temperature. Analysis of the low pH skim milk solution after recirculation for particle size and sedimentation showed results consistent with the earlier small-scale heat treatment analysis, supporting that the formation of protein aggregates and sediment could be related to fouling. The combination of analytical approaches and tools allows for a deeper understanding of fouling, helping to reduce its occurrence in the future. This study showed that the custom-fabricated fouling rig is a powerful tool to investigate the fouling and cleaning behaviour of dairy heat exchangers. Its modular design facilitated the generation of deposits under high temperature short time conditions for compositional characterisation and evaluation of cleaning in place solutions. The fouling rig could be used in the future to study potential process modifications to reduce the occurrence of fouling.

2.5. Acknowledgements

The authors would like to acknowledge the Dairy Processing Technology Centre (DPTC), an Enterprise Ireland initiative, for financial support of this work (Grant Number TC/2020/0028).

2.6 References

Anema, S.G. (2000). Effect of milk concentration on the irreversible thermal denaturation and disulfide aggregation of β-lactoglobulin. *Journal of Agricultural and Food Chemistry*, *48*(9), 4168-4175.

Anema, S.G. (2009). Effect of milk solids concentration on the pH, soluble calcium, and soluble phosphate levels of milk during heating. *Dairy Science and Technology*, *89*(5), 501-510.

Anema, S.G. and Li, Y. (2003). Effect of pH on the association of denatured whey proteins with casein micelles in heated reconstituted skim milk. *Journal of Agricultural and Food Chemistry*, *51*(6), 1640-1646.

Anema, S.G., Lowe, E.K. and Li, Y. (2004). Effect of pH on the viscosity of heated reconstituted skim milk. *International Dairy Journal*, *14*(6), 541-548.

Augustin, M.A. and Clarke, P.T. (1990). Effects of added salts on the heat stability of recombined concentrated milk. *Journal of Dairy Research*, *57*(2), 213-226.

Beaulieu, M., Pouliot, Y. and Pouliot, M., (1999). Thermal aggregation of whey proteins in model solutions as affected by casein/whey protein ratios. *Journal of Food Science*, *64*(5), 776-780.

Burton, H., (1968). Section G. Deposits from whole milk in heat treatment plant—a review and discussion. *Journal of Dairy Research*, *35*(2), 317-330.

Bylund, G. (2015). *Dairy processing handbook.* Tetra Pak Processing Systems AB.

Chen, B. Y., Grandison, A. S. and Lewis, M. J. (2012). Comparison of heat stability of goat milk subjected to ultra-high temperature and in-container sterilization. *Journal of Dairy Science*, 95(3), 1057-1063.

Chen, B., & O'Mahony, J.A. (2016). Impact of glucose polymer chain length on heat and physical stability of milk protein-carbohydrate nutritional beverages. *Food chemistry*, *211*, 474-482.

Considine, T., Patel, H. A., Anema, S. G., Singh, H., & Creamer, L. K. (2007). Interactions of milk proteins during heat and high hydrostatic pressure treatments—a review. *Innovative food science & emerging technologies*, *8*(1), 1-23.

Dalgleish, D.G. and Law, A.J. (1989). pH-induced dissociation of bovine casein micelles. II. Mineral solubilization and its relation to casein release. *Journal of Dairy Research*, *56*(5), 727-735.

Davies, D. T., & White, J. C. D. (1966). The stability of milk protein to heat: I. Subjective measurement of heat stability of milk. *Journal of Dairy Research*, 33, 67-81.

Donato, L. and Guyomarc'h, F. (2009). Formation and properties of the whey protein/kappa-casein complexes in heated skim milk–A review. *Dairy Science and Technology*, *89*(1), 3-29.

Dumpler, J. (2018a). General introduction. *Heat Stability of Concentrated Milk Systems: Kinetics of the Dissociation and Aggregation in High Heated Concentrated Milk Systems* (pp. 1-43). Springer.

Dumpler, J. (2018b). Heat stability of concentrated skim milk on lab scale. *Heat Stability of Concentrated Milk Systems: Kinetics of the Dissociation and Aggregation in High Heated Concentrated Milk Systems*. (pp. 47-61). Springer.

Dumpler, J., & Kulozik, U. (2016). Heat-induced coagulation of concentrated skim milk heated by direct steam injection. *International Dairy Journal*, *59*, 62-71.

Faka, M., Lewis, M. J., Grandison, A. S. and Deeth, H. (2009). The effect of free Ca2+ on the heat stability and other characteristics of low-heat skim milk powder. *International Dairy Journal*, 19(6), 386-392.

Foster, C. L. and Green, M. L. (1990). A model heat exchange apparatus for the investigation of fouling of stainless steel surfaces by milk II. Deposition of fouling material at 140 °C, its adhesion and depth profiling. *Journal of Dairy Research*. 57(3), 339-348.

Fox, P. F. & McSweeney, P. L. H. (2003). *Advanced Dairy Chemistry—1 Proteins, 3rd edition.* Plenum Press, New York.

Georgiadis, M. C., & Macchietto, S. (2000). Dynamic modelling and simulation of plate heat exchangers under milk fouling. *Chemical Engineering Science*, 55, 1605–1619.

Grijspeerdt, K., Hazarika, B. and Vucinic, D. (2003). Application of computational fluid dynamics to model the hydrodynamics of plate heat exchangers for milk processing. *Journal of food engineering*. 57(3), 237-242.

Hagsten, C., Altskär, A., Gustafsson, S., Lorén, N., Hamberg, L., Innings, F., Paulsson, M. and Nylander, T. (2016). Composition and structure of high temperature dairy fouling. *Food Structure*, *7*, 13-20.

Havea, P. (2006). Protein interactions in milk protein concentrate powders. *International Dairy Journal*, *16*(5), 415-422.

Hebishy, E., Joubran, Y., Murphy, E. and O'Mahony, J.A. (2019). Influence of calcium-binding salts on heat stability and fouling of whey protein isolate dispersions. *International Dairy Journal*, *91*, 71-81.

Hill, J.P., Boland, M.J. and Smith, A.F. (1997). The effect of beta-lactoglobulin variants on milk powder manufacture and properties. In *Milk protein polymorphism, Palmerston North (New Zealand), Feb 1997*. International Dairy Federation.

Ho, Q. T., Murphy, K. M., Drapala, K. P., O'Callaghan, T. F., Fenelon, M. A., O'Mahony, J. A., & McCarthy, N. A. (2018). Effect of pH and heat treatment on viscosity and heat coagulation properties of milk protein concentrate. *International Dairy Journal*, *85*, 219-224.

Huppertz, T. and Nieuwenhuijse, H. (2022). Constituent fouling during heat treatment of milk: A review. *International Dairy Journal*. 126, 105236.

International Dairy Federation (IDF) (2001). Milk. Determination of nitrogen content, ISO 8968-5. IDF standard 020-5:2001.

International Dairy Federation (IDF) (2010). Milk, cream, and evaporated milk – Determination of total solids content, ISO 6731. IDF standard 21:2010.

Jeurnink, T. J. M. and De Kruif, K. G. (1993). Changes in milk on heating: viscosity measurements. *Journal of Dairy Research*, *60(2),* 139–150.

Jeurnink, T.J., Walstra, P. and De Kruif, C.G. (1996). Mechanisms of fouling in dairy processing. *Netherlands Milk and Dairy Journal*, *50*, 407-426.

Jimenez, M., Delaplace, G., Nuns, N., Bellayer, S., Deresmes, D., Ronse, G., Alogaili, G., Collinet-Fressancourt, M. and Traisnel, M. (2013). Toward the understanding of the interfacial dairy fouling deposition and growth mechanisms at a stainless steel surface: a multiscale approach. *Journal of colloid and interface science*, *404*, 192-200.

Kasinos, M., Le, T. T., & Van der Meeren, P. (2014). Improved heat stability of recombined evaporated milk emulsions upon addition of phospholipid enriched dairy by-products. *Food Hydrocolloids*, *34*, 112-118.

Kastanas, P., Lewis, M. J., & Grandison, A. S. (1995). Design and development of a miniature UHT plant for fouling studies and its evaluation using milk adjusted to different pH values, goat's milk and milk permeate. *Food and bioproducts processing: transactions of the Institution of Chemical Engineers, Part C*.

Khaldi, M., Croguennec, T., André, C., Ronse, G., Jimenez, M., Bellayer, S., Blanpain-Avet, P., Bouvier, L., Six, T., Bornaz, S., Jeantet, R. and Delaplace, G. (2018). Effect of the calcium/protein molar ratio on β-lactoglobulin denaturation kinetics and fouling phenomena. *International Dairy Journal*. 78, 1-10.

Lalande, M., Tissier, J.-P. and Corrieu, G. (1984). Fouling of a plate heat exchanger used in ultra-high-temperature sterilization of milk. *Journal of Dairy Research*. 51(4), 557-568.

Lalande, M. and Tissier, J.P. (1985). Fouling of heat transfer surfaces related to β-lactoglobulin denaturation during heat processing of milk. *Biotechnology progress*, *1*(2), 131-139.

Lewis, M., Grandison, A., Lin, M., & Tsioulpas, A. (2011). Ionic calcium and pH as predictors of stability of milk to UHT processing. *Milchwissenschaft*, *66*(2), 197-200.

Lowe, E. K., Anema, S. G., Bienvenue, A., Boland, M. J., Creamer, L. K., & Jiménez-Flores, R. (2004). Heat-induced redistribution of disulfide bonds in milk proteins. 2. Disulfide bonding patterns between bovine β-lactoglobulin and κ-casein. *Journal of Agricultural and Food Chemistry*, *52*(25), 7669-7680.

Mahdi, Y., Mouheb, A. and Oufer, L. (2009). A dynamic model for milk fouling in a plate heat exchanger. *Applied mathematical modelling*. 33(2), 648-662.

Marchand, S., De Block, J., De Jonghe, V., Coorevits, A., Heyndrickx, M., & Herman, L. (2012). Biofilm formation in milk production and processing environments; influence on milk quality and safety. *Comprehensive Reviews in Food Science and Food Safety*, *11*(2), 133-147.

Marchin, S., Putaux, J.L., Pignon, F. and Léonil, J. (2007). Effects of the environmental factors on the casein micelle structure studied by cryo transmission electron microscopy and small-angle x-ray scattering/ultrasmall-angle x-ray scattering. *The Journal of chemical physics*, *126*(4), 01B617.

Markoska, T., Huppertz, T., Grewal, M. K., & Vasiljevic, T. (2019). FTIR analysis of physiochemical changes in raw skim milk upon concentration. *LWT*, *102*, 64-70.

Mérian, T. and Goddard, J. M. (2012). Advances in Nonfouling Materials: Perspectives for the Food Industry. *Journal of Agricultural and Food Chemistry*, *60(12),* 2943-2957.

Milanovic, P., Jacimovic, B. and Genic, S. (2006). Experimental measurement of fouling resistance in the heat exchanger of a geothermal heating system. *Geothermics*. 35(1), 79-86.

Morrissey, P. A., & O'Mahony, F. (1976). Heat stability of forewarmed milks: influence of κ-casein, serum proteins and divalent cations. *Journal of Dairy Research*, *43*(2), 267-274.

Nieuwenhuijse, J. A., Sjollema, A., van Boekel, M. A. J. S., Van Vliet, T., & Walstra, P. (1991). The heat stability of concentrated skim milk. *Netherlands Milk and Dairy Journal*, *45*, 193-224.

O'Connell, J.E. and Fox, P.F. (2003). Heat induced coagulation of milk. In Fox P.F., McSweeney P.L.H. (eds) *Advanced Dairy Chemistry—1 Proteins, 3rd edition*. 879-945. Plenum Press, New York.

On-Nom, N., Grandison, A. S., & Lewis, M. J. (2012). Heat stability of milk supplemented with calcium chloride. *Journal of Dairy Science*, *95*(4), 1623-1631.

Prakash, S., Datta, N. and Deeth, H. C. (2005). Methods of detecting fouling caused by heating of milk. *Food Reviews International*, *21(3),* 267-293.

Rose, D. (1961a). Factors affecting the pH-sensitivity of the heat stability of milk from individual cows. *Journal of Dairy Science*, *44*(8), 1405-1413.

Rose, D. (1961b). β-Lactoglobulin and pH-sensitivity of the heat stability of evaporated milk. *Journal of Dairy Science*, *44*(9), 1763.

Saget, M., de Almeida, C.F., Fierro, V., Celzard, A., Delaplace, G., Thomy, V., Coffinier, Y. and Jimenez, M. (2021). A critical review on surface modifications mitigating dairy fouling. *Comprehensive Reviews in Food Science and Food Safety*, *20*(5), 4324-4366.

Schmidt, R. H. (1981). Gelation, and coagulation. In Cherry J.P. (eds) *Protein Functionality in Foods*. 131-147. American Chemical Society, Washington DC.

Singh, H., and Creamer, L.K. (1991). Changes in Size and Composition of Protein Aggregates on Heating Reconstituted Concentrated Skim Milk at 120°C. *Journal of food science*, *56*(3), 671-677.

Smits, P., and Van Brouwershaven, J.H. (1980). Heat-induced association of β-lactoglobulin and casein micelles. *Journal of Dairy Research*, *47*(3), 313-325.

Sutariya, S.G., Huppertz, T. and Patel, H.A. (2017). Influence of milk pre-heating conditions on casein–whey protein interactions and skim milk concentrate viscosity. *International Dairy Journal*, *69*, 19-22.

Swartzel, K.R. (1983). The Role of Heat Exchanger Fouling in the Formation of Sediment in Aseptically Processed and Packaged Milk 1. *Journal of Food Processing and Preservation*, *7*(4), 247-257.

van Boekel, M. A. J. S., Nieuwenhuijse, J. A., & Walstra, P. (1989). The heat coagulation of milk, 1: Mechanisms. *Netherlands Milk and Dairy Journal, 43,* 97–127.

Visser, J. and Jeurnink, T. J. M. (1997). Fouling of heat exchangers in the dairy industry. *Experimental Thermal and Fluid Science*. 14(4), 407-424.

Wallhäußer, E., Hussein, W. B., Hussein, M. A., Hinrichs, J., & Becker, T. (2013). Detection of dairy fouling: Combining ultrasonic measurements and classification methods. *Engineering in life sciences*, *13*(3), 292-301.

Wiegand, J., (1971). Falling-film evaporators and their applications in the food industry. *Journal of Applied Chemistry and Biotechnology*, *21*(12), 351-358.

Xiong, Y.L. (1992). Influence of pH and ionic environment on thermal aggregation of whey proteins. *Journal of Agricultural and Food Chemistry*, *40*(3), 380-384.

Chapter 3

The impact of pH on fouling and related physicochemical properties of concentrated skim milk during heat treatment using a laboratory-scale fouling rig

Tara R. Murphy, Eoin W. Finnegan, Tom F. O'Callaghan, James A. O'Mahony

School of Food and Nutritional Sciences, University College Cork, Cork, Ireland

Declaration

This chapter was written by author Tara R. Murphy (TRM) and reviewed by all co-authors. TRM co-designed the study and performed all of the experimental work.

Abstract

Fouling of evaporators during the concentration of skim milk is a key challenge in the dairy industry that causes product loss, decline in equipment heat performance, reduced product quality and an increase in overall operating costs. The main objective of this work was to investigate the effect of pH on the heat-induced changes in concentrated skim milk, as related to evaporator fouling. The heat coagulation time of the concentrated skim milk solutions (30%, w/w, total solids) was determined at 120°C as a function of pH in the range pH 6.0-6.7. The skim milk solutions at pH 6.1, 6.3, 6.5 and 6.7 were recirculated in a custom-built fouling rig at 85°C for 90 min, and after recirculation, changes in viscosity, particle size distribution, sedimentation, and composition were measured. Composition and turbidity analysis of cleaning in place (CIP) chemicals used to clean the rig after fouling experiments was also performed. Foulant adhering to the heat exchanger of the fouling rig was collected and analysed for protein content and protein profile. The skim milk solutions at pH 6.1 and 6.3 fouled the heat exchanger most extensively, and had increased viscosity, particle size and sedimentation after recirculation, and in comparison, the skim milk solutions at pH 6.5 and 6.7 did not foul the heat exchanger. Compositional analysis of the skim milk solutions after recirculation, in addition to the CIP chemicals after the cleaning cycles, suggested that aggregated protein was the main contributor to fouling, as confirmed by SDS-PAGE analysis of the adhered foulant. These findings provide new insights into the impact of pH on fouling during evaporation of skim milk.

3.1. Introduction

In the dairy industry, the process of evaporation is used to concentrate skim milk before it is dried to produce skim milk powder (SMP) (Kelly *et al.,* 2003). Evaporation involves heating the milk under vacuum to temperatures ranging from 55-70°C. This heat treatment removes water from the milk and concentrates the liquid skim milk, typically achieving a total solids content of 48-50%, before it is spray-dried into a powder (Bylund, 2015). The dairy industry faces challenges related to fouling, particularly in the evaporation stage of the production of SMP. Fouling refers to the accumulation of undesired deposits in different parts of the thermal processing equipment, such as pipes, heat exchange surfaces, and other apparatus fittings (Fryer & Belmar-Beiny, 1991), in addition to such foulant material also being present in the finished product. In dairy processing, the formation of fouling involves a complex process that encompasses the aggregation of proteins and the formation of insoluble calcium phosphate within the fluid. The aggregated protein primarily forms deposits on heat transfer surfaces. A study by Georgiadis & Macchietto (2000) indicated that the deposition rate is influenced by the quantity of aggregated protein in the thermal boundary layer. A thicker deposit corresponds to a greater temperature difference (ΔT) between the heating medium and the product temperature. Another significant aspect of dairy fouling is the deposition of minerals, particularly calcium phosphate. As temperature increases, the solubility of calcium phosphate decreases, resulting in its precipitation and the formation of crystalline deposits on heat transfer surfaces (Hagsten *et al.,* 2016). Within fouling layers, calcium phosphate can bind to existing beta-lactoglobulin (β-lg) molecules, enhancing the stability of the fouling layer and facilitating protein-protein interactions through charge neutralization (Dalgleish & Law, 1989).

Fouling poses significant economic, operational, and environmental challenges for the dairy industry. The accumulation of deposits during production can increase thermal resistance, leading to a decline in equipment performance. This, in turn, obstructs fluid flow, increases pressure drop, and reduces the heat transfer coefficient (Schnöing *et al.,* 2020; Georgiadis *et al.,* 1998). As a result, the industry incurs higher operating costs due to more frequent cleaning requirements and increased energy consumption. The cleaning protocols needed to remove fouling deposits are time-consuming, causing extended downtimes and significant environmental impact due to the use of chemicals, water, and heat (Hagsten et al., 2016). Moreover, there is a risk of product quality deterioration, as the desired temperature may not be achieved (Holsinger *et al.,* 1997), and the erosion of fouling layers can lead to finished product containing foulant with the potential to contribute to insolubility and sedimentation

(Saget et al., 2021). Biofilm formation also poses a threat to microbial quality, as bacteria, including spoilage and pathogenic microorganisms, can adhere to stainless steel surfaces and reduce the microbial quality of the product (Hinton *et al.,* 2002). In addition to fouling, another important aspect during heat treatment is the physicochemical changes that can occur in the product resulting in significant effects on its organoleptic, nutritional, and functional properties (Fox *et al.,* 2015). Heat treatment leads to the denaturation of whey proteins, which involves the disruption of the protein's native structure, resulting in changes to their functional properties, in addition to challenges for processability (Anema & Li, 2000; McMahon *et al.*, 1993; Vasbinder & De Kruif, 2003).

Given the operational and environmental costs involved, it is important for the dairy industry to be able to measure or predict the presence, type, and intensity of fouling during thermal processes. This knowledge would assist in designing, improving, or adapting production processes to avoid unnecessary product or capital loss (Wallhäußer et al., 2013). However, fouling is a complex process influenced by various parameters that are challenging to measure accurately, making it difficult to quantify overall fouling resistance (Bott, 2001). Hence, the objective of this research was to examine how pH affects the heat stability and heat-induced changes in concentrated skim milk, aiming to assess the suitability and interconnectedness of potential measures and indicators of fouling. The heat coagulation time of the concentrated skim milk solutions (30%, w/w, total solids) was determined at 120°C as a function of pH in the range 6.0-6.7. These skim milk solutions at pH 6.1, 6.3, 6.5 and 6.7 were then recirculated in a custom-built fouling rig at 85°C for 90 min; during recirculation, continuous measurements of temperature, pH and conductivity were taken, and after recirculation, changes in viscosity, particle size distribution, sedimentation, and composition were measured. Composition and turbidity analysis of CIP chemicals used to clean the fouling rig after experiments was also performed. Adhered foulant formed in the heat exchanger of the fouling rig was collected and analysed for protein content and protein profile using sodium dodecyl sulphate-polyacrylamide gel electrophoresis (SDS-PAGE). From an analytical perspective, in this study, fouling is classified into two categories, *adhered fouling* and *non-adhered fouling*, whereby adhered fouling pertains to the accumulation of fouling deposits on thermal equipment, while non-adhered fouling encompasses any product changes resulting from heat-induced reactions associated with fouling or sedimentation of the fouling layer in the heat treated, concentrated product.

3.2. Materials and methods

3.2.1. Materials

Medium-heat skim milk powder (SMP) was provided by a local Irish dairy company. The total protein, fat, ash, and carbohydrate of the SMP were 34.1, 0.80, 8.00 and 57.1 % (w/w) respectively, as provided by the manufacturer. All chemicals and reagents, unless otherwise stated, were sourced from Sigma-Aldrich (Wicklow, Ireland) and were of analytical grade.

3.2.2. Preparation of high-solids skim milk solutions

Reconstituted skim milk was prepared by adding medium-heat SMP to ultrapure water over 1 h at 50ºC to attain 30% (w/w) total solids (TS) (and 9%, w/w, TS for research described in Section 3.2.3) while stirring using an overhead stirrer (Eurostar 60 control, IKA, Staufen, Germany) with a spiral mixing element (Visco Jet 3x spiral mixing element d = 80 mm, Küssaberg, Germany). During rehydration, the stirring speed was gradually increased from 100 to 250 rpm. The solutions were stirred under the conditions described above for a further 3 h at 200 rpm, after which the solutions were cooled to 20ºC while magnetically stirring for pH adjustment. The pH of the skim milk solutions were measured using a standard pH meter at 20°C (Mettler Toledo, FiveEasy pH/mV bench meter, F20, Switzerland).The skim milk solutions were adjusted to pH 6.1, 6.3, 6.5 and 6.7 using 1 N NaOH and HCl as appropriate (skim milk solutions were also adjusted to pH 6.0, 6.2, 6.4 and 6.6 for Section 3.2.3). The skim milk solutions were magnetically stirred for a further 2 h, after which pH was readjusted to the target pH, if required. The skim milk solutions were then stored at 4°C overnight, with low speed magnetic stirring, to facilitate complete rehydration. After overnight rehydration, the samples were equilibrated to 22ºC for 2 h, after which the pH was checked and re-adjusted to the target pH, as required.

3.2.3. Heat coagulation time as a function of pH

Heat coagulation time (HCT) of skim milk solutions at 9 and 30% (w/w) TS, was determined at 120°C as a function of pH in the range 6.0-6.7 using the method of Davies and White (1966). Samples (2 mL) were added to heat-resistant glass tubes and stoppered using a rubber bung, placed in a steel rack, and immersed in a silicone oil bath (Hettich ESP oilbaths;

Hettich Benelux BV). The HCT was recorded as the time elapsed between immersing the sample in the oil bath and the visible detection of aggregates within the sample.

3.2.4. Fouling of concentrated skim milk

Fouling behaviour of the skim milk solutions (4 L) at pH 6.1, 6.3, 6.5 and 6.7 was determined using a custom-built fouling rig, as per the method developed by Hebishy *et al.* (2019), with modifications detailed in Appendix 1. In brief, the fouling rig used in this study consisted of a stainless steel, shell and tube heat exchanger of length 90 cm and internal diameter 5 cm (Liam A. Barry Ltd., Cork, Ireland), connected to a circulating waterbath (Grant, LT ecocool™100, Cambridge, UK) which controlled temperature of the water used as the heating medium. Two electronic pressure transducers (PR-33X, Keller-druck, Dorchester, UK), one located immediately before and one immediately after the heat exchanger, were used to measure temperature and pressure in-line. Two analogue pressure gauges, on either side of the electronic pressure transducers, were used as an additional measure of pressure. The unit had a stainless steel feed vessel (capacity 4 L), connected directly to a positive displacement, progressive cavity pump (Torqueflow, Sydex, UK); the liquid flow rate through the heat exchanger was controlled by means of a variable speed drive. The pressure on the recirculating samples was set using a manual diaphragm throttling valve, with pressure recorded using an analogue pressure gauge (1107J486, WIKA, Los Angeles, CA, USA). The initial back pressure was set at 1 bar using the throttling valve and was not adjusted during the runs. pH and conductivity of the recirculating samples were measured using a pH/conductivity meter attached to the feed vessel (Metler Toledo, SevenGo Duo, SG23, Switzerland). Temperature of the samples was also measured using a thermocouple mounted to the feed vessel (Digitron 2024T Digital Thermometer Pt100, Port Talbot, UK). The fouling system was operated at a laminar flow rate (25 Hz) in batch recirculation mode. The samples were introduced to the fouling rig at an initial temperature of 25 ºC, and the fouling experiments were conducted at 90ºC (temperature of the heating medium) to simulate thermal processing and preheating of spray dryer liquid concentrate feeds during SMP processing and to enable sufficient denaturation and deposit build-up on the heat exchanger (Jimenez *et al*., 2013; Khalid *et al.,* 2013). The experiment was stopped after 90 min of recirculation, after which the recirculated samples were recovered for further analysis, summarised in Figure 3.1. After sample recovery, the fouling rig was visually inspected for fouling deposit and any deposit formed was collected for further analysis.

The system was cleaned in place (CIP) using a standardised CIP protocol. The system was first rinsed using deionised water (4 L) for 10 min, after which a caustic wash was performed using 4 L of 1% (v/v) NaOH solution containing sodium hypochlorite (5%) (Ansep CIP, Ecolab, Co. Meath, Ireland) at 64 ºC for 30 min to dissolve fat, protein, and carbohydrate deposits. After the caustic CIP step, the system was rinsed for 10 min with deionised water (4 L) to remove any residues of caustic. An acid wash was then performed using 4 L of 1% (v/v) acid solution containing nitric acid (>30%) and orthophosphoric acid (<5%) (Horolith V, Ecolab, Co. Meath, Ireland) at 46 ºC for 30 min to dissolve any remaining carbohydrate and mineral deposits. After the acid wash, the system was rinsed for 10 min with deionised water (4 L) to remove any residues of acid. The recirculated washes were recovered after each cleaning step for analysis of protein, ash, and turbidity.

3.2.5. Viscosity

The viscosity of the skim milk solutions (30%, w/w, TS; pH 6.1, 6.3, 6.5, 6.7) after each fouling experiment (detailed in Section 3.2.4), were measured using an AR-G2 controlled-stress rheometer (TA Instruments, Crawley, UK) equipped with a concentric cylinder geometry. Samples (25 g), at 25°C controlled by a Peltier apparatus (± 0.1°C), were subjected to a shear ramp from 0-300 s^{-1} for 4 min, followed by holding at 300 s^{-1} for 2 min, and a shear ramp from 300-0 s^{-1} for 4 min. Corresponding un-heated samples of the skim milk solutions were used as controls.

3.2.6. Particle size distribution

Particle size distribution (PSD) of the skim milk solutions (30%, w/w, TS; pH 6.1, 6.3, 6.5, 6.7) after each fouling experiment (detailed in Section 3.2.4), was measured using a laser light diffraction unit (Mastersizer 3000 S, Malvern Instruments Ltd., Worcestershire, UK) equipped with a 300 reverse Fourier lens and He–Ne laser (λ of 633 nm). The samples were introduced to the dispersing unit using ultrapure water as dispersant to reach an obscuration of 10% (± 1%). Analysis of PSD was performed using the generalised polydisperse model, with particle refractive index of 1.46, absorption of 0.1 and dispersant refractive index of 1.33. Non-heated samples of the skim milk solutions were used as controls.

3.2.7. Dry sediment

Sediment was measured following a centrifugation method of Chen *et al.* (2012), with minor modifications to adapt the method for high total solids material. After the fouling experiments, as detailed in Section 3.2.4., the skim milk solutions (30%, w/w, TS; pH 6.1, 6.3, 6.5, 6.7) were mixed to ensure a homogenous sample, and 20 g was accurately weighed and poured into a calibrated tube and centrifuged (Sorvall RC5C Plus, Massachusetts, United States) at 12,000 g for 1 h. After the supernatant was removed, the sediment was oven-dried at 105°C until a constant weight was obtained, to determine its percentage dry weight. The moisture content (%w/w) of the sediment was calculated by the difference in weight before and after oven drying the sediment. Unheated samples of the skim milk solutions were used as controls.

3.2.8. Composition of skim milk solutions, sediment, and cleaning in place solutions

Samples of the skim milk solutions after the fouling experiments (detailed in Section 3.2.4), the supernatant formed during the dry sediment method, and the cleaning in place (CIP) solutions used in cleaning cycles after the fouling experiments were analysed for protein (%, w/w) and ash content (%, w/w). Protein was determined using the Kjeldahl method with a nitrogen-to-protein conversion factor of 6.38 (IDF, 2001). Ash content was determined by dry ashing in a muffle furnace (Nabertherm GmbH, Lilienthal, Germany) at 650ºC until a white ash was obtained (IDF, 2008). The protein and ash content of the sediment was calculated as follows:

$$\textit{Skim milk solution crude protein} - \textit{Supernatant crude protein} = \textit{Sediment crude protein} \quad [3.1]$$

$$\textit{Skim milk solution ash} - \textit{Supernatant ash} = \textit{Sediment ash} \quad [3.2]$$

Samples of the skim milk solutions after the fouling experiments and the CIP solutions used in cleaning cycles after the fouling experiments were also analysed for total solids (%,w/w) by oven drying at 104°C until a constant weight was obtained (IDF, 2010).

3.2.9. Turbidity of cleaning in place solutions

The turbidity of the CIP solutions was measured at 600 nm using a Cary 300 bio UV-visible spectrophotometer (Varian Inc., CA, USA) which was equipped with a temperature

control system. CIP solutions were measured for turbidity immediately after the cleaning cycles of the fouling rig.

3.2.10. Electrophoretic analysis of protein profile

The protein profile of fouling material deposited in the heat exchanger by the skim milk solutions at pH 6.1 and 6.3 (Section 3.2.4) were analysed using sodium dodecyl sulphate-polyacrylamide gel electrophoresis (SDS-PAGE), as described by Laemmli (1970), with minor modifications. No fouling was observed in the heat exchanger after recirculating the skim milk solutions at pH 6.5 and 6.7, therefore SDS-PAGE was not performed on these samples. Prepared samples were analysed using pre-cast mini-protean Tetra Cell TGX 4-20% acrylamide gels (Bio-Rad Laboratories, Inc., Hercules, CA, US) at a constant voltage of 180 V, under reducing and non-reducing conditions. The solid fouling material was dissolved in SDS-buffer to obtain the desired protein load of 1 mg/ml in the individual gel loading wells. All gels were Coomassie-stained, before being de-stained with a solution of water, methanol, and acetic acid, 50:40:10, respectively, until a bright background was reached. Stained SDS-PAGE gels were scanned using a desktop flatbed scanner (HP Scanjet G4010, HP, Leixlip, Ireland).

3.2.11. Statistical analysis

All experimental analyses were conducted in triplicate, with samples produced from two independent trials for each pH, unless otherwise stated. Results are expressed as mean ± standard deviation. Analysis of variance (ANOVA; Tukey's HSD test) was performed using R i386 version 4.0.2 (R Foundation for Statistical Computing, Vienna, Austria) to identify statistically significant differences between mean values for different samples. The level of significance was determined at $p < 0.05$ to determine whether statistically significant differences existed between the mean values.

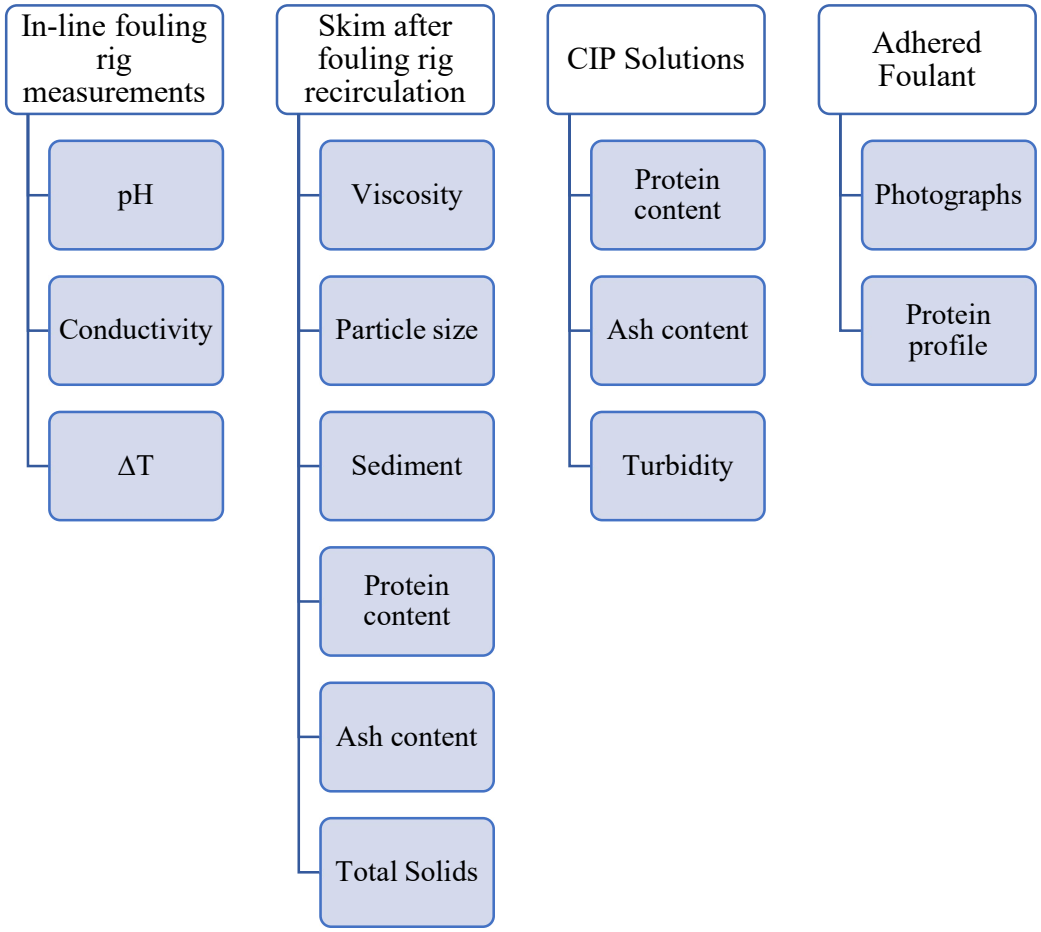

***Figure 3.1.**: Summary of analytical approaches used to identify and quantify fouling and heat-induced changes in concentrated skim milk solutions. Four categories of fouling analysis are outlined in this study: in-line measurements during fouling experiments, analysis of skim milk solutions after recirculation on the fouling rig, analysis of cleaning-in-place (CIP) solutions used in cleaning cycles after fouling experiments, and analysis of fouling deposit collected from the fouling rig heat exchanger after fouling experiments. The abbreviation ΔT is the difference in temperature between the heating medium and the skim milk solution in the fouling rig.*

3.3. Results and discussion

3.3.1. Heat stability of skim milk solutions

To determine the influence of concentration on the heat stability of the skim milk solutions, the heat coagulation time (HCT) was determined at 120°C as a function of pH in the range 6.0-6.7, at both 9 and 30% (w/w) TS, with results presented in Figure 3.2. The wide pH range used was deemed essential for this study, as in-house preliminary trials (data not shown) demonstrated that the pH of skim milk decreased markedly as TS increased during evaporation, in agreement with findings of Anema (2009), where a linear decrease in pH was observed when heating a 28.8% TS skim milk solution from 20 to 80°C. As evaporation increases the dry matter content of milk, the decrease in pH can be attributed to the resultant increase in ionic components, precipitation of calcium phosphate and resultant release of hydrogen ions from the casein micelle (Tanguy *et al.,* 2016).

In the present study, at 9% (w/w) TS, the maximum HCT was observed at pH 6.7, and as the samples were acidified, the HCT decreased. The samples had significantly higher ($p < 0.05$) HCT at pH between 6.5-6.7, compared to pH 6.0-6.4. In addition, between pH 6.5-6.7, the HCT differs significantly ($p < 0.05$), varying from 18.2 to 38.7 min. The heat stability of milk follows two trends: a maximum HCT at the natural pH of milk (pH 6.6-6.8) and a local minimum at pH 6.9-7.0, or the heat stability profile shows an increase in HCT with increasing pH (Huppertz, 2016). The control sample at 9% TS skim milk solution showed a maximum HCT at the natural pH of milk, which is the most dominant profile reported for skim milk (Fox and McSweeney, 2003). The higher heat stability observed in the samples between pH 6.5 and 6.7 is attributable to the stability of the casein micelles as the pH is within the region of the native pH of milk, making them less prone to aggregation due to denatured whey proteins adsorbed to the micelle surface, forming a less calcium sensitive steric barrier. The low heat stability of the samples between pH 6.0 and 6.4 can be attributed to 'salt-induced' coagulation. At low pH, the colloidal stability of casein micelles is lowered by a decrease in surface charge of casein micelles, reduced electrostatic repulsion, and a collapse of the hairy layer due to charge neutralisation. This results in an increased tendency towards aggregation (Anema *et al.,* 2004). An increase in calcium activity and ionic strength by the dissolution of colloidal calcium phosphate (CCP) also contributes to an increase in calcium-mediated bridging between casein micelles (McMahon & Oommen, 2008).

For the skim milk solution at 30% (w/w) TS, the maximum HCT was observed at pH 6.6, and as the samples were acidified, the HCT decreased, but not as severely as the decrease in HCT observed on acidification of the skim milk at 9% (w/w) TS. The samples at 30% (w/w) TS had significantly higher ($p < 0.05$) HCTs between pH 6.5-6.7, compared to pH 6.0-6.4. In addition, between pH 6.5-6.7 the HCTs differ significantly ($p < 0.05$) in a small range, varying from 8.04 to 9.27 min, which was much lower than the HCTs observed at 9% (w/w) TS in the same pH range. The HCT at 30% (w/w) TS was slightly higher between pH 6.0 and 6.4 compared to 9% (w/w) TS, and the HCT of the 30% (w/w) TS samples at pH 6.3 and 6.4 were significantly higher ($p < 0.05$) than the samples at pH 6.0, 6.1 and 6.2, which was not observed at 9% (w/w) TS, where there was no significant differences ($p > 0.05$) in this pH range

The explanation for the differences in HCT between low pH (6.0-6.4) and high pH (6.5-6.7) samples at 30% (w/w) TS is essentially the same as that described above for the 9% (w/w) TS samples. However, there have been several studies exploring why the heat stability of concentrated skim milk is lower than that of unconcentrated skim milk, as heat induced coagulation is a complex process with at least two stages (destabilisation and aggregation), being affected by multiple environmental conditions that mutually influence each other (Parris *et al.,* 1991). Dumpler (2018) found that the HCT of skim milk decreased significantly ($p < 0.05$) with increasing TS content, and efforts to improve the heat stability of concentrated skim milk by increasing pH through NaOH addition were shown to be less effective with increasing TS content. Other factors that have been shown to affect the heat stability of concentrated skim milk include an increase in protein content (McLean *et al.,* 1987), an increase in ionic strength proportional to volume reduction (Augustin & Clarke, 1990), and an increase in the concentration of soluble calcium (Anema, 2009; Hardy *et al.,* 1984). It has also been shown by Fourier transform infrared (FTIR) analysis that proteins in milk undergo considerable structural changes during concentration that make them more prone to destabilisation reactions during heating (Markoska *et al.,* 2019). All of these factors contribute to the increased susceptibility of concentrated skim milk to aggregation, and therefore a lower heat stability than unconcentrated skim milk.

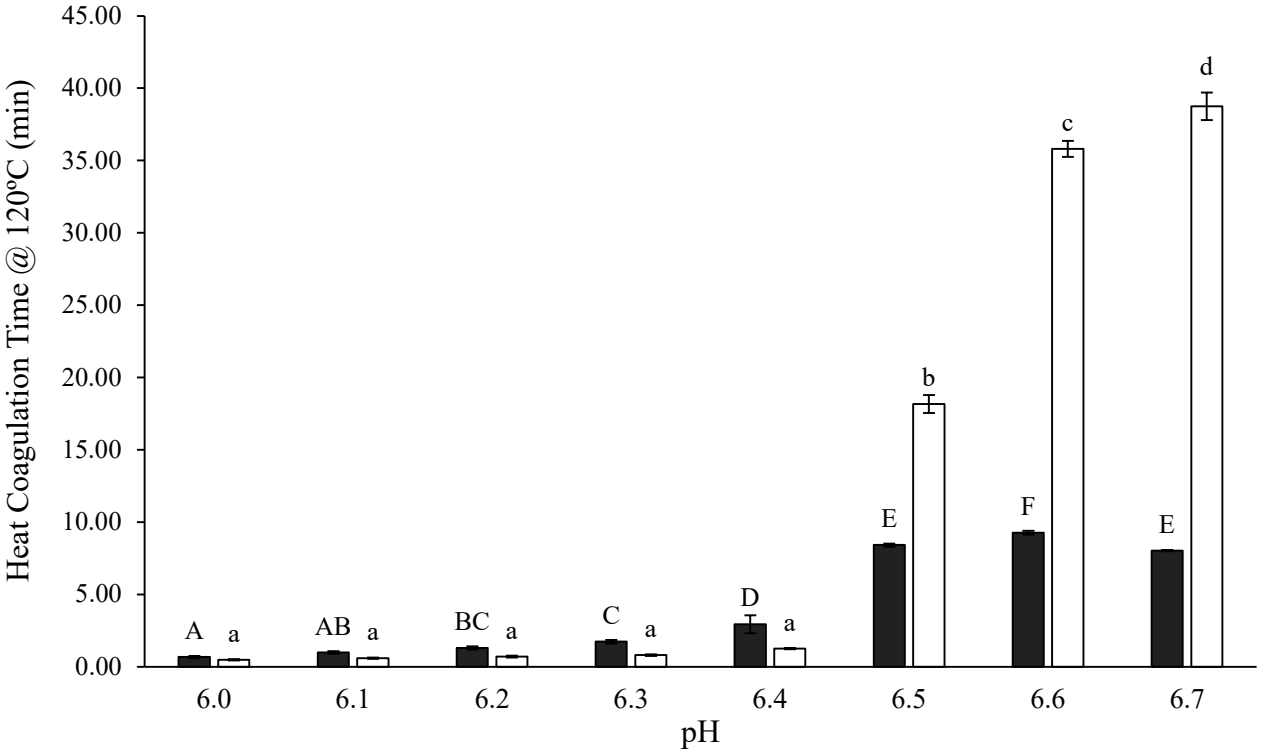

Figure 3.2.*: Heat coagulation time (HCT) at 120ºC as a function of pH for concentrated reconstituted skim milk at 30% total solids (TS) (■) and at 9% TS (□). Results are the means of data from three independent trials.* $^{A\text{-}F}$*Mean values at 30% TS with different superscript letters are significantly different (p < 0.05).* $^{a\text{-}d}$*Mean values at 9% TS with different superscript letters are significantly different (p < 0.05).*

3.3.2. Fouling rig

Concentrated skim milk solutions at pH 6.1, 6.3, 6.5 and 6.7 were chosen for fouling analysis by recirculation on the fouling rig based on the results from Section 3.2.1, as they represent the two distinct regions of the heat stability profile i.e., samples at pH 6.1 and 6.3 displayed low heat stability, whereas samples at pH 6.5 and 6.7 displayed high heat stability.

3.3.2.1. Inline pH and conductivity measurements

During recirculation of the skim milk samples on the fouling rig, pH and conductivity were measured at regular intervals to provide information on the effects of initial sample pH on the heat-induced changes during fouling (Figures 3.3 and 3.4). Recirculation of the samples

on the fouling rig resulted in a decrease in the pH of all samples (no significant differences ($p > 0.05$) in the extent of pH reduction between samples), with all samples decreasing in pH by ~0.36 units (Table 3.1). For all samples, the most extensive change in pH occurred during the initial heat-up phase of the fouling experiments (i.e., between 0-40 min), with a decrease in pH by ~0.31 units for all samples during this time. After the fouling rig experiments, the samples of concentrated skim milk were collected and cooled to 25°C for measurement of pH; all samples did not return to their starting pH after fouling rig recirculation, with each sample reading ~0.1 units less than their initial pH.

A different trend was observed for conductivity, with recirculation of the samples on the fouling rig resulting in an increase in conductivity for all samples. All samples had approximately the same conductivity (~8.07 mS/cm), with no significant differences ($p > 0.05$) between samples (Table 3.1). Conductivity increased from 8.07 to 9.09 mS/cm for the sample at pH 6.7, which was significantly different ($p < 0.05$) from the conductivity increase for the samples at pH 6.3 and 6.5, increasing to 9.24 and 9.18 mS/cm, respectively. The sample at pH 6.1 had the largest increase in conductivity, being significantly different from all other samples ($p < 0.05$), increasing from 8.09 to 9.40 mS/cm during recirculation. In a similar trend to pH, the conductivity of all samples did not return to the starting value when cooled to 25°C after the fouling rig trials, with all samples having a conductivity of ~8.23 mS/cm when cooled (no significant difference ($p > 0.05$) between samples, with an increase of ~0.16 mS/cm from the starting conductivity).

The observed decrease in sample pH during recirculation can be attributed to the precipitation of colloidal calcium phosphate (CCP), since the solubility of calcium and phosphate ions decreases with increasing temperature (Chaplin & Lyster, 1988) and the release of hydrogen ions that accompanies the precipitation of CCP causes the reduction in pH (Fox *et al.,* 2015). The samples at pH 6.1 and 6.3 displayed a build-up of adhered foulant and it can be safely assumed that there was a higher amount of free calcium ions in the serum phase of these samples (compared to the samples at pH 6.5 and 6.7) as the pH of the samples before recirculation on the fouling rig was sufficiently low to allow solubilisation of CCP and release of free calcium and phosphate ions into the serum phase (Pyne & McGann, 1960). Upon recirculation of the samples at pH 6.1 and 6.3 on the fouling rig, precipitation of CCP would still have occurred, causing a further decrease in pH, but the high amount of free calcium already in the serum phase would still be reactive and promote fouling through calcium-mediated bridging between casein micelles (Nieuwenhuijse *et al.*, 1991). As the samples at pH

6.1 and 6.3 further decreased in pH upon recirculation on the fouling rig, the colloidal stability of casein micelles would have been lowered by a decrease in surface charge of casein micelles, a reduced electrostatic repulsion, and a collapse of the casein micelle surface hairy layer due to charge neutralisation; combined, these effects result in an increased tendency towards aggregation (van Boekel *et al*. 1989). Further aggregation of casein micelles caused by association of denatured whey proteins with κ-casein via intermolecular disulphide bonds and hydrophobic interactions contributes to the formation of an adhered fouling layer after recirculation of samples at pH 6.1 and 6.3 (Haque & Kinsella, 1988; Singh, 1995).

Milk has conductive properties due to its charged constituents, particularly mineral salts (Mabrook & Petty, 2003). The electrical conductivity of milk is determined primarily by sodium and chloride ions (Mabrook and Petty, 2003) but also by other ions (Jenness and Koops, 1962), with the distribution of salt fractions between soluble and colloidal forms being of particular importance to the electrical conductivity (Pyne, 1962). The observed increase in conductivity during recirculation of all samples on the fouling rig can be attributed to changes in equilibria of buffer systems and solubilisation casein-bound calcium and phosphorus salts in milk due to the acidification of milk on heating (Mucchetti *et al.,* 1994). The greater increase ($p < 0.05$) in conductivity of the sample with an initial pH of 6.1 is due to the more extensive changes in mineral equilibrium and abundance of free ions as the pH of the sample decreased from 6.10 to 5.70 during recirculation on the fouling rig. These results show that conductivity is not directly related to fouling, rather it is a co-product of changes in pH, which has been shown here to be directly related to the occurrence of fouling. Therefore, in-line measurements of pH and ΔT (perhaps with conductivity measurements to coincide with pH readings) could be used in industry as an indicator of susceptibility to, and extent of fouling during thermal processing.

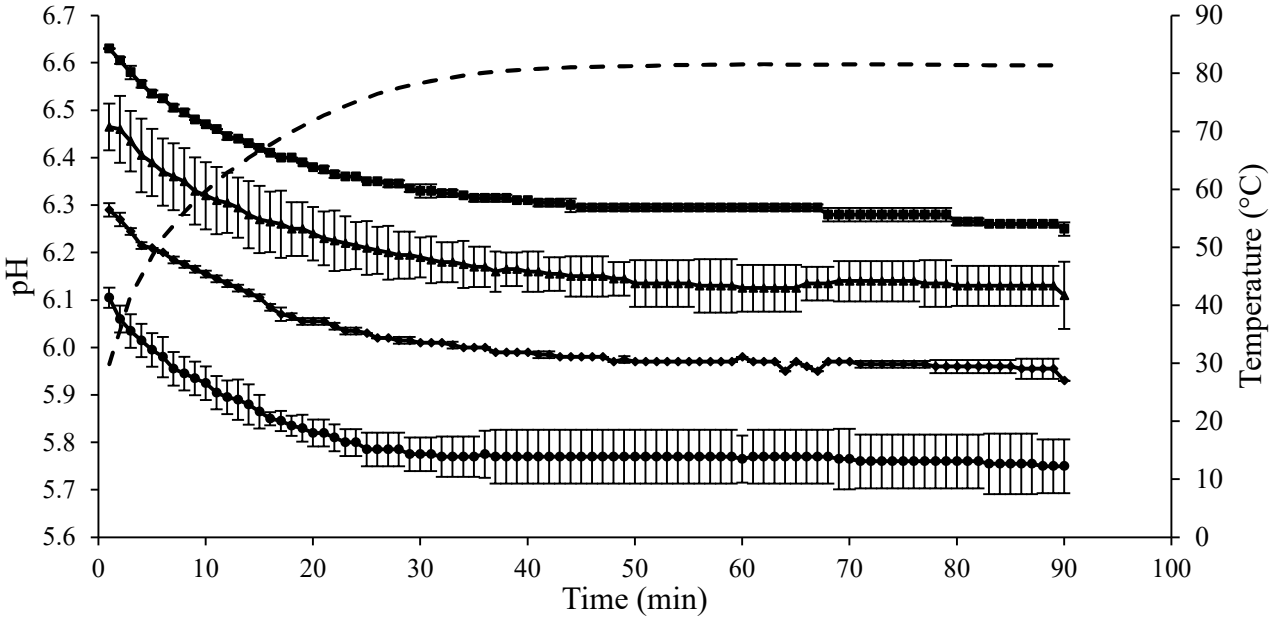

Figure 3.3.*: pH as a function of time of concentrated skim milk solutions (30% w/w, total solids) at a starting pH of 6.1 (●), 6.3 (♦), 6.5 (▲) and pH 6.7 (■) during recirculation on the fouling rig at 85°C. Temperature of the feed as a function of time (dashed line) is also shown. Results are the means of data from two independent trials.*

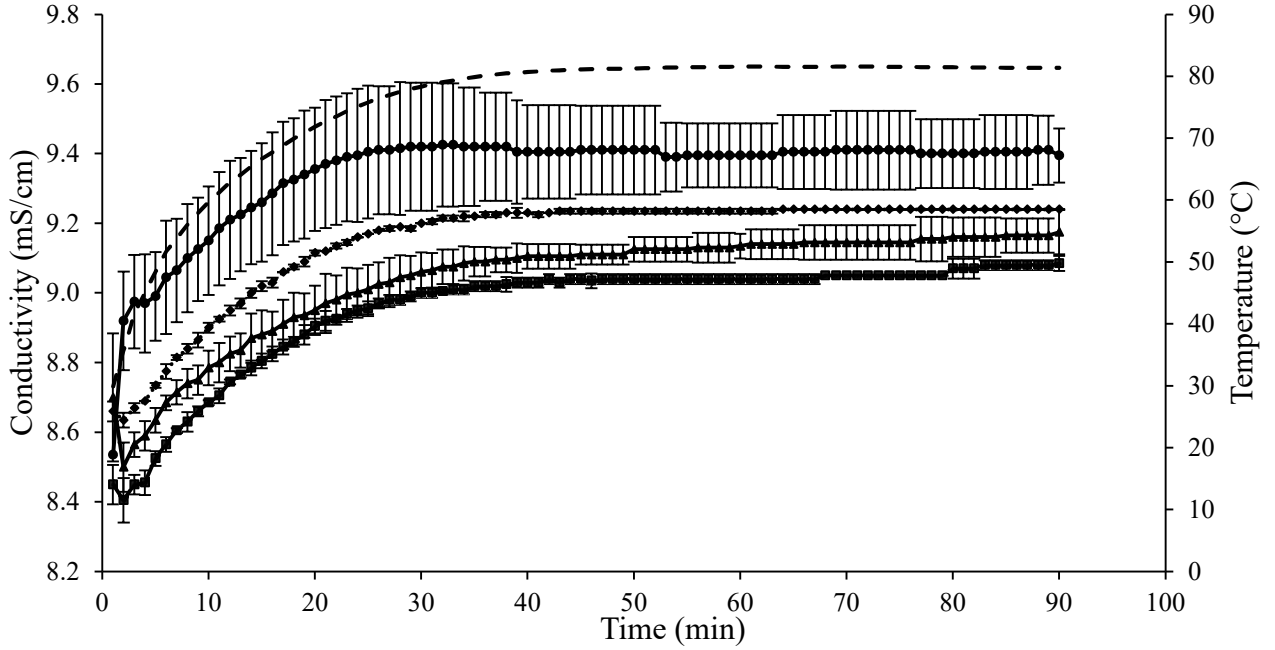

Figure 3.4.*: Conductivity (mS/cm) as a function of time for concentrated skim milk solutions at 30% w/w, total solids at starting pH of 6.1 (●), 6.3 (♦), 6.5 (▲) and pH 6.7 (■) during recirculation on the fouling rig at 85°C. Temperature of the feed as a function of time (dashed line) is also shown. Results are the means of data from two independent trials.*

***Table 3.1.**: In-line measurements of pH and conductivity (mS/cm) during recirculation of concentrated skim milk solutions at 30% w/w total solids at a starting pH of 6.1, 6.3, 6.5 and 6.7. Measured changes(Δ) in these parameters are shown. The abbreviations 't_0' and 't_{90}' indicate the measurements at the start (0 min) and end (90 min) of the fouling experiments.*

Sample pH	pH					Conductivity (mS/cm)					
	t_{90}	Cooled to 25ºC after run	Δ during run	Δ 0-40 min	Δ 40-90 min	t_0	t_{90}	Cooled to 25ºC after run	Δ during run	Δ 0-40 min	Δ 40-90 min
6.1	5.70 ± 0.13^{a}	6.00 ± 0.00^{a}	0.36 ± 0.08^{a}	0.34 ± 0.08^{a}	0.02 ± 0.00^{a}	8.09 ± 0.07^{a}	9.40 ± 0.08^{a}	8.21 ± 0.01^{a}	1.31 ± 0.01^{a}	0.87 ± 0.69^{a}	0.04 ± 0.01^{a}
6.3	5.93 ± 0.00^{b}	6.20 ± 0.00^{b}	0.36 ± 0.01^{a}	0.30 ± 0.01^{a}	0.06 ± 0.00^{a}	8.09 ± 0.00^{a}	9.24 ± 0.00^{b}	8.25 ± 0.00^{a}	1.15 ± 0.00^{b}	0.57 ± 0.03^{a}	0.01 ± 0.00^{a}
6.5	6.11 ± 0.07^{c}	6.36 ± 0.09^{b}	0.36 ± 0.02^{a}	0.31 ± 0.01^{a}	0.05 ± 0.03^{a}	8.04 ± 0.02^{a}	9.18 ± 0.06^{b}	8.24 ± 0.04^{a}	1.14 ± 0.08^{b}	0.41 ± 0.22^{a}	0.07 ± 0.03^{a}
6.7	6.25 ± 0.01^{d}	6.58 ± 0.04^{c}	0.38 ± 0.01^{a}	0.32 ± 0.00^{a}	0.06 ± 0.01^{a}	8.07 ± 0.05^{a}	9.09 ± 0.02^{c}	8.23 ± 0.02^{a}	1.02 ± 0.07^{c}	0.58 ± 0.07^{a}	0.06 ± 0.01^{a}

Results are the means of data from two independent trials. Mean values within a column not sharing a common superscript letter differ significantly ($p < 0.05$).

3.3.2.2. Temperature difference

During recirculation of the samples on the fouling rig, temperature was continuously measured to provide information on the efficiency of heat transfer across the stainless steel heat exchange surface. The heat transfer efficiency of thermal equipment is reduced as fouling deposit build up on the heat transfer surface, therefore the temperature of the heating medium must increase in order to maintain product temperature for product quality and safety; this temperature increase can be used as an indirect measure of fouling (Kastanas *et al.,* 1995). This concept was implemented and adapted in ultra-high temperature (UHT) fouling studies by Wadsworth & Bassette (1985) and Hill *et al.* (1997), where the temperature difference (ΔT) between the heating medium and the treated milk leaving the system was monitored, with an increase in this ΔT parameter indicating fouling deposit build-up. In this current study, the ΔT was measured differently, as the configuration meant that the heating medium remained at constant temperature and the reduction in product temperature was measured over time as an indicator of fouling (maintaining temperature was not a product quality requirement). The measured values for ΔT after the initial heat up time (i.e., 40 min of recirculation) for each sample are shown in Figure 3.5. The skim milk samples at pH 6.5 and 6.7 displayed similar development in ΔT after 40 min of initial recirculation; there was a gradual decrease in ΔT before plateauing at ~68 min and reaching a final ΔT of 7.80°C for both samples. The sample at pH 6.3 had a slightly different progression of ΔT compared to the samples at pH 6.5 and 6.7, whereby it decreased sharply before plateauing at 8.10°C after 60 min, followed by a slight increase to 8.20°C between 80-90 min. The sample at pH 6.1 had a very different progression of ΔT to all other samples; after a slight decrease in ΔT between 53-63 min, the ΔT increased steadily for the remainder of the experiment, peaking, and plateauing after 83 min at 10.8°C.

Upon visual inspection of the heat exchanger after the fouling experiments, no adhered foulant was observed after recirculation of the samples at pH 6.5 and 6.7 (Figure 3.6), demonstrating that the plateaued ΔT at 7.80°C is indicative of no visual fouling for this system. An 'acceptable' ΔT, i.e., suggestive of no fouling, is process and product specific, and for the experimental configuration used in this study, it was determined through several preliminary trials that a ΔT between 2-8°C is associated with no visible adhered fouling. The higher final ΔT at pH 6.3 (Table 3.1) can be attributed to the small amount of fouling deposit built up on the heat exchanger, impeding the heat transfer (Figure 3.4). The final ΔT after recirculation of the sample at pH 6.1 was significantly higher ($p < 0.05$) than the samples at a higher pH (Table 3.1), and this coincides with the considerable amount of adhered foulant deposited on the heat

exchanger by the sample at pH 6.1 (Figure 3.4). The foulant material formed at pH 6.1 and 6.3 were characteristic of 'type-A deposit' (Burton, 1968), which is a soft, curd-like material that forms at temperatures between 70-110ºC. A similar deposit was formed in a fouling study by Jeurnink *et al.* (1996), and it was determined that the deposit consisted mainly of whey proteins, followed by minerals and caseins; the authors also reported that lowering the pH of milk results in severe fouling caused by casein micelles. Therefore, it can be hypothesised that the foulant formed in this current study is attributable to mutual interactions of casein micelles due to aggregation facilitated by denatured whey proteins and calcium phosphate (Rosmaninho & Melo, 2008). This reaction, in conjunction with heat-induced disulphide bonding between whey proteins and κ-caseins, results in a significant degree of protein aggregation that can contribute to fouling (Lowe *et al.,* 2004). No adhered foulant was formed by the samples at pH 6.5 and 6.7, further supporting the hypothesis that the build-up of foulant is due to association of denatured whey proteins and casein micelles. As the pH approached the native pH of milk, the micelle surface charge will increase, reducing the tendency of the denatured whey proteins and casein micelles to associate (Anema & Li, 2003).

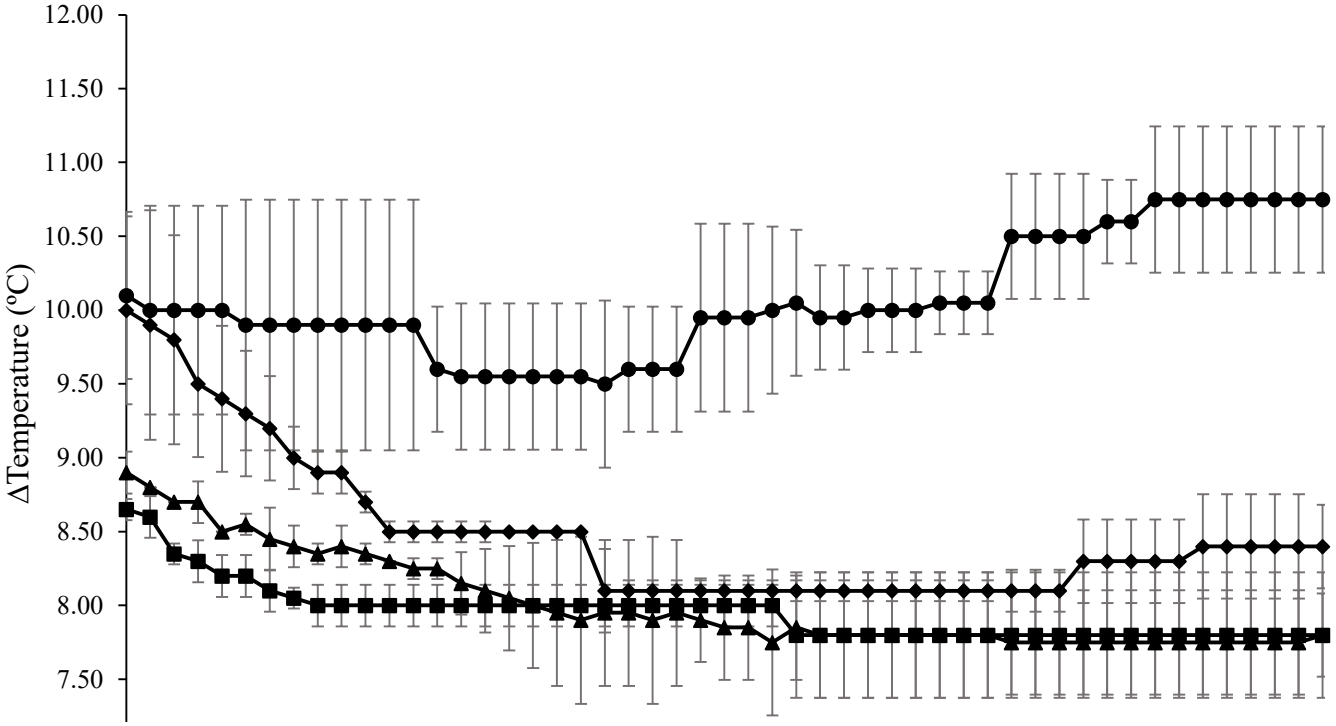

Figure 3.5.*: Difference in temperature of heating medium and product as a function of recirculation time for concentrated skim milk solutions at 30% w/w, total solids at pH 6.1 (●), 6.3 (♦), 6.5 (▲) and pH 6.7 (■), after the initial 40 minute heat up time of the fouling experiment. Results are the means of data from two independent trials.*

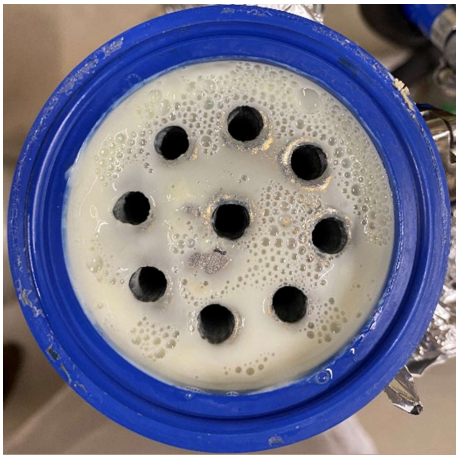

pH 6.1

pH 6.3

pH 6.5

pH 6.7

Figure 3.6.*: Images of the surface of the heat exchanger outlet after recirculation of concentrated skim milk solutions at 30% w/w, total solids at pH 6.1, 6.3, 6.5, and 6.7 at 85°C for 90 min.*

3.3.3. Viscosity

Measurements of viscosity of the concentrated skim milk samples at initial pH of 6.1, 6.3, 6.5 and 6.7 were performed immediately after recirculation on the fouling rig (Figure 3.7). The viscosity of samples at pH 6.5 and 6.7 (9.68 and 7.34 mPa.s, respectively) after the fouling experiments did not differ significantly ($p > 0.05$) from that of the unheated control (7.54 mPa.s). Both the samples at pH 6.1 and 6.3 had significantly higher ($p < 0.05$) viscosity after the fouling experiments when compared to the unheated control, while also being significantly different ($p < 0.05$) from each other with viscosity values of 47.8 and 22.1 mPa.s for the sample at pH 6.1 and pH 6.3, respectively. The significant increase in viscosity for the samples at pH 6.1 and 6.3 can be attributed to a greater extent of association of whey protein with the casein micelles during heat treatment, as reported by Anema *et al.* (2004) who showed a similar effect when the pH of skim milk samples were adjusted to pH 6.5 and 7.1 prior to heat treatment, resulting in a higher viscosity being observed at pH 6.5 after heat treatment when compared to pH 7.1. A later study by Anema *et al.* (2014) also reported the same phenomenon in a concentrated skim milk system, with a greater increase in viscosity being observed for samples heated at low pH. This more extensive increase in viscosity at low pH can be attributed to an increase in volume fraction and casein micelle voluminosity, as well as decreased electrostatic repulsion between micelles. When milk is heated, conformational changes in the tertiary structure of whey protein cause the proteins to denature and unfold , exposing the reactive thiol groups that interact with each other to form disulphide bonds, resulting in association with κ-casein, hydrophobic regions of the casein micelle, and other whey proteins. These interactions cause protein aggregation, which results in an increase in the volume fraction and voluminosity of the casein micelles (Nair *et al.,* 2013; Ho *et al.,* 2018).

More adhered foulant was visually apparent after recirculation of the skim milk sample at pH 6.1, when compared to the adhered foulant formed by the sample at pH 6.3 (Figure 3.4), which coincides with the higher viscosity of the sample at pH 6.1 after recirculation. Concentrated dairy systems with high viscosity are associated with fouling of heat exchangers and reduction in heat transfer during evaporation (Bienvenue *et al.,* 2003; Bista *et al.,* 2021). As the samples at pH 6.1 and 6.3 resulted in adhered foulant in the heat exchanger of the fouling rig, which did not occur for samples at pH 6.5 and 6.7, it can be hypothesised that the increased viscosity, driven by the denaturation/aggregation of proteins is a key factor in the build-up of adhered foulant in thermal processing equipment.

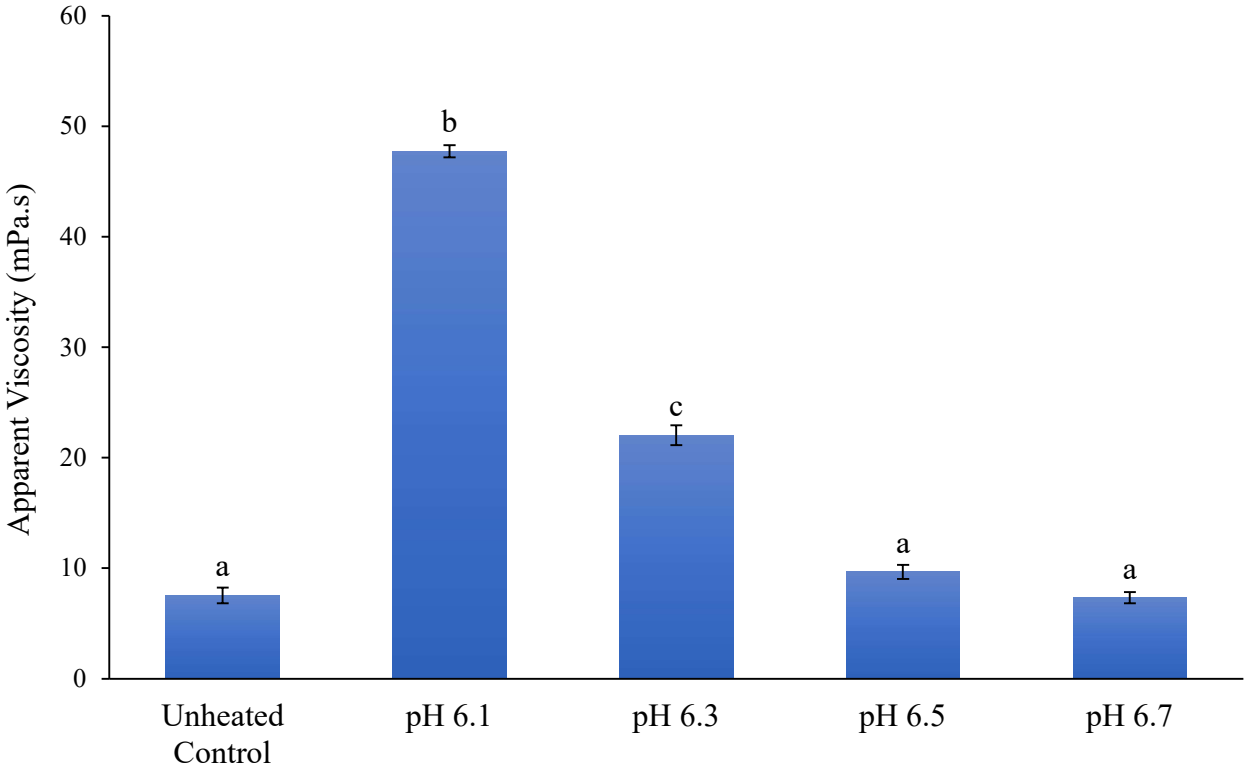

***Figure 3.7.**: Apparent viscosity at a shear rate 300 s^{-1} and 25°C for concentrated skim milk solutions at 30% w/w, total solids, and pH 6.1, 6.3, 6.5 or 6.7 after 90 min of recirculation in the fouling rig at 85°C. The unheated control was not subjected to heat treatment on the fouling rig. Results are the means of data from two independent trials. Mean values not sharing a common letter differ significantly ($p < 0.05$).*

3.3.4. Particle size distribution

Particle size analysis was conducted to assess the extent of protein aggregation in the concentrated skim milk solutions that fouled the heat exchanger of the fouling rig (pH 6.1 and 6.3), in comparison with samples that did not foul the heat exchanger (pH 6.5 and 6.7). The unheated control and the recirculated samples at pH 6.5 and 6.7 displayed monomodal particle size distributions (PSD's), with one peak identified between 0.01 and 1 μm (Figure 3.8). At pH 6.3, an additional shoulder was observed between 1 and 300 μm, indicating a moderate level of protein denaturation and aggregation. The recirculated sample at pH 6.1 was poly-disperse, displaying multiple large peaks between 0.1 and 1000 μm. The large standard deviations observed in the particle size distribution analysis of the recirculated sample at pH 6.1 can be attributed to the heterogenous nature of the sample, with aggregates of varying size. These results show that as the pH of concentrated skim is decreased, the degree of protein denaturation and aggregation increases (Anema & Li, 2003), resulting in increased extent of fouling.

There were no significant differences ($p > 0.05$) in volume mean diameter (D [4,3]) between the unheated control and the recirculated samples at pH 6.5 and 6.7 (Table 3.2). The recirculated samples at pH 6.1 and 6.3 showed significantly higher ($p < 0.05$) values for D[4,3], at 17.6 and 2.96 μm, respectively. The D[4,3] of the recirculated sample at pH 6.1 was significantly higher ($p < 0.05$) than that of the recirculated sample at pH 6.3 due to the dominance of very large, aggregated particles present (Table 3.2). These results are in agreement with previous studies that showed an increase in particle size of heated skim milk with a decrease in pH (Anema, 2007; Anema *et al.* (2004)). It was also observed that the span for the recirculated sample at pH 6.1 was significantly larger ($p < 0.05$) than all other samples, as it displayed the most polydisperse PSD. It can be concluded there is a pH-dependent increase in particle size of concentrated skim milk on heating. At low pH (i.e., at pH 6.1 and 6.3), heat-induced whey protein association with casein micelles occurs, resulting in an increase in protein particle size due to aggregation of whey proteins with caseins, as well as with other whey proteins, (Anema & Li, 2003; Beaulieu *et al.,* 1999), which is reflected in the formation of adhered foulant in the heat exchanger of the fouling rig.

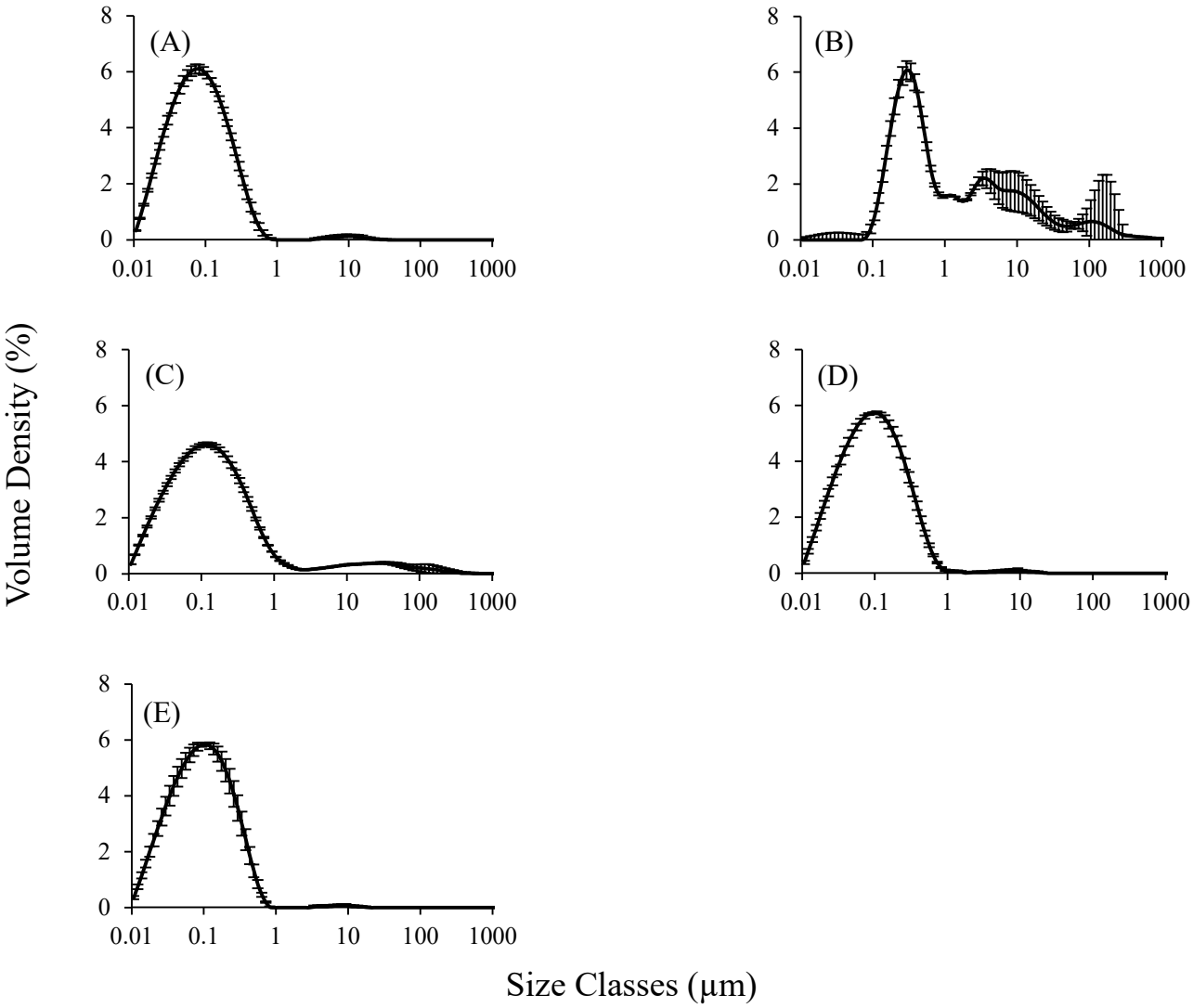

***Figure 3.8.**: Particle size distribution of concentrated skim milk solutions at 30% w/w, total solids after 90 min of recirculation in the fouling rig at 85°C at pH 6.1 (B), pH 6.3 (C), pH 6.5 (D), and pH 6.7 (E). The unheated control (A) was not subjected to heat treatment on the fouling rig. Results are the means of data from two independent trials.*

***Table 3.2.**: Particle size distribution parameters for concentrated skim milk solutions at 30% w/w total solids after 90 min of recirculation in the fouling rig at 85°C. The unheated control was not subjected to heat treatment on the fouling rig.*

Sample	D[3,2]	D[4,3]	Dv(10)	Dv(50)	Dv(90)	Span
			(µm)			
Unheated Control	0.05 ± 0.00[a]	0.24 ± 0.09[a]	0.02 ± 0.00[a]	0.08 ± 0.00[a]	0.26 ± 0.02[a]	3.06 ± 0.18[a]
pH 6.1	0.46 ± 0.01[b]	17.6 ± 7.68[b]	0.19 ± 0.00[b]	0.65 ± 0.05[b]	25.2 ± 5.88[b]	38.5 ± 6.41[b]
pH 6.3	0.07 ± 0.01[a]	2.96 ± 0.62[c]	0.03 ± 0.00[a]	0.13 ± 0.00[a]	0.94 ± 0.13[a]	7.26 ± 0.94[c]
pH 6.5	0.06 ± 0.00[a]	0.19 ± 0.06[a]	0.03 ± 0.00[a]	0.09 ± 0.00[a]	0.31 ± 0.01[a]	3.19 ± 0.11[a]
pH 6.7	0.06 ± 0.00[a]	0.18 ± 0.03[a]	0.02 ± 0.00[a]	0.09 ± 0.00[a]	0.29 ± 0.01[a]	3.16 ± 0.07[a]

Results are the means of data from two independent trials. Mean values within a column not sharing a common superscript letter differ significantly ($p < 0.05$).
D[4,3] = volume-weighted mean particle diameter.
D[3,2] = surface-weighted mean particle diameter.
Dv(10) = particle size below which 10% of sample volume is found.
Dv(50) = particle size below which 50% of sample volume is found.
Dv(90) = particle size below which 90% of sample volume is found

3.3.5. Sediment formation

Sediment is formed during heating of concentrated skim milk by casein micelle and/or whey protein aggregation (Chen & O'Mahony, 2016), and is an indicator of poor heat stability (Chen *et al.*, 2012). Previous studies have shown that the dry weight of sediment formed in samples of reconstituted milk heated and dialysed at 115°C for 30 min consisted of 50-60% protein, with all the major whey protein and casein fractions being identified in the sediment (On-Nom *et al.,* 2012). Lewis *et al.* (2011) found that calcium ions are also a predominant factor influencing sediment formation, as ultra heat-treated milk with calcium chloride additions had significantly more sediment formation than milk without added calcium.

In this study, sediment was quantified as a measure of the extent of fouling, as transfer of the fouling deposit into evaporated milk products is a common occurrence in the dairy industry as excessive sediment formation reduces product quality (Dumpler & Kulozik, 2016; Kasinos *et al.,* 2014; Swartzel, 1983). The sediment formation in the unheated control was significantly different ($p < 0.05$) from the heated samples with pH at 6.1 and 6.3, whereas samples at pH 6.5 and 6.7 did not differ significantly ($p > 0.05$) from the unheated control (Figure 3.8). The largest amount of sediment was formed at pH 6.1, followed by pH 6.3, with significantly different ($p < 0.05$) sediment values of 35.5 and 17.4% respectively. These results align with those of On-Nom *et al.* (2012), where no significant sediment was formed in heated samples of reconstituted skim milk if the pH was maintained above 6.3. The large amount of sediment formation in the low pH range can be attributed to protein aggregation, as evidenced in the earlier particle size analysis. Havea (2006) used a similar method for determining sediment, in which milk protein concentrate was separated into two parts: the supernatant which consisted of the soluble protein, and the sediment which consisted of the insoluble protein, with the aggregated proteins defined as the insoluble protein, forming the sediment.

The protein, ash, and moisture content of the sediment, presented as a percentage of the total sediment formed, provides insights into how the composition of the sediment formed in concentrated skim milk varies with pH (Figure 3.9). For all sediment formed, protein and moisture were found to be the main components. The unheated control had a very small percentage of moisture in the sediment, as the sediment formed was extremely compact and firm. As pH of the concentrated milk was reduced, the amount of protein and moisture in the sediment increased. The higher percentage protein present in the sediments formed at pH 6.1 and 6.3 can be attributed to extensive protein aggregation that occurs at low pH as the proteins become destabilised; consistent with previous hypotheses that sediment consists of mainly

aggregated protein (Chen & O'Mahony, 2016; On-Nom *et al*., 2012). The high moisture content in the sediments formed at pH 6.1 and 6.3 can be attributed to the presence of large protein aggregates resulting in a less compact and porous sediment layer. These large aggregates could have prevented the sediment compacting as firmly as the unheated control during centrifugation, resulting in a large amount of trapped moisture in the sediment. The sediment formed by the sample at pH 6.1 had the highest ash content; all other samples had ash contents comparable to the unheated control. This to be expected, as the low pH of the sample would promote calcium activity by dissolution of the CCP (Nieuwenhuijse *et al.,* 1991), suggesting that the significant amount of sediment formed at pH 6.1 was due to calcium mediated-bridging between casein micelles, as well as denatured whey proteins associated with κ-casein. Overall, these results coincide with previous results in studies of sediment formation in unconcentrated and concentrated milk on heating (Chen & O'Mahony, 2016; Havea, 2006; Lewis *et al.,* 2011; On-Nom *et al.,* 2012), which concluded that the amount of sediment formed in heated milk systems increases with decreasing product pH, and that the sediment consists mainly of aggregated protein, followed by minerals. These studies, as well as the current study, have established a clear link between product instability and sediment formation. In this study, the samples that caused the most fouling (as discussed in Section 3.3.2) also had the highest amount of sediment formation (i.e., samples at pH 6.1 and 6.3), showing that sediment formation is strongly linked with fouling.

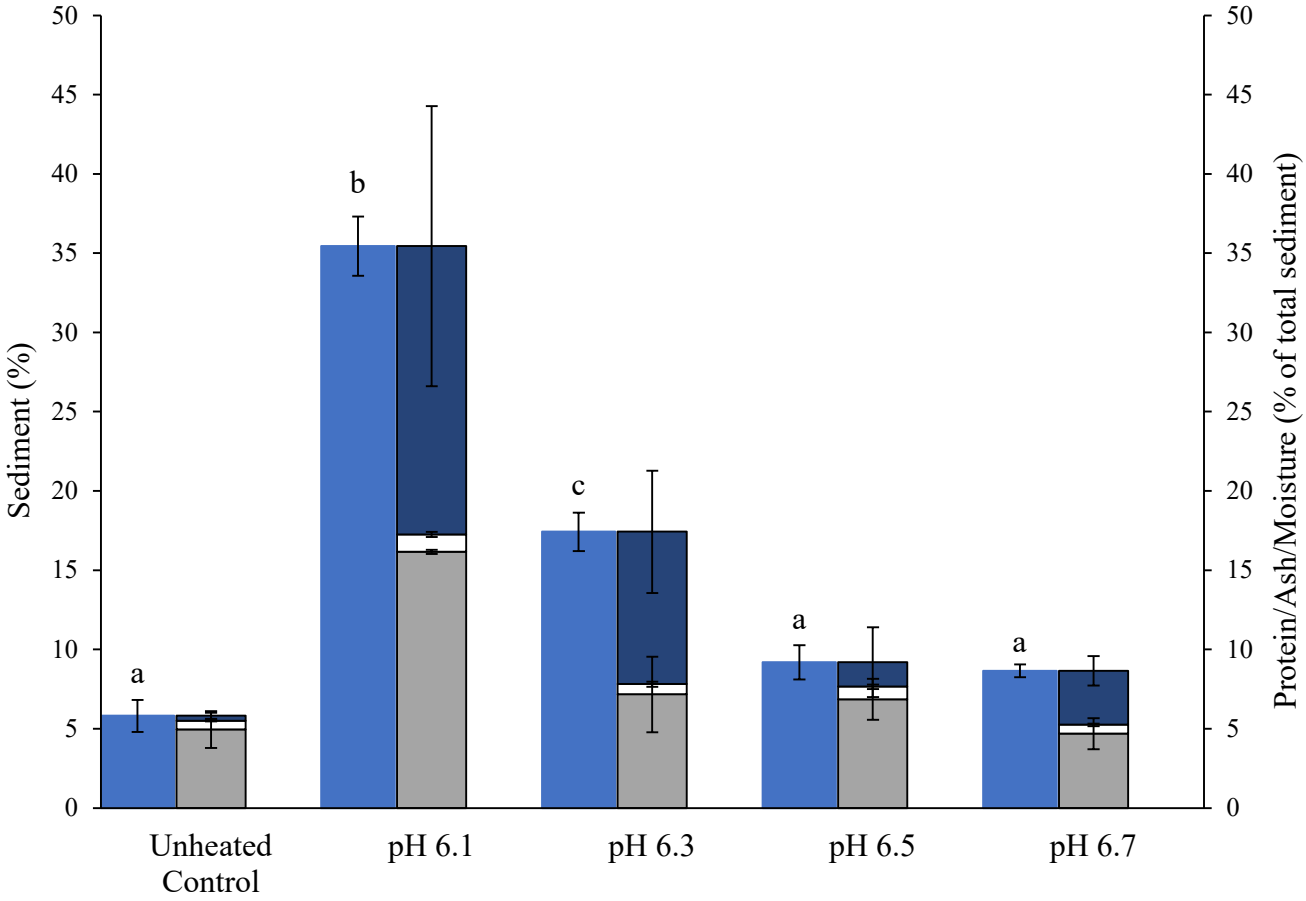

***Figure 3.9.**: The relationship between pH and sediment (■) formation (%) following recirculation of concentrated skim milk solutions at 30% w/w total solids on the fouling rig at 85°C for 90 min. The protein (■), ash (□) and moisture (■) content of the sediments is expressed as a percentage of the total sediment formed for each sample. The unheated control was not subjected to any heat treatment. Results are the means of data from two independent trials. Mean values for sediment formation (%) with different superscript letters are significantly different (p <*

3.3.6. Composition of the concentrated skim milk solutions following fouling rig recirculation

To determine what components of the concentrated skim milk solutions contributed to fouling, measurement of the total solids, protein, and ash content of the samples before and after recirculation on the fouling rig was performed (Table 3.3). The total solids, protein and ash content of the starting material was 30.3, 9.45, and 2.00% respectively. The total solids content was significantly lower ($p < 0.05$) after recirculating the samples at pH 6.1, 6.3. 6.5 and 6.7, reducing to 23.3, 24.0, 24.6, and 24.9% respectively. After recirculating the sample at pH 6.1, the protein content decreased significantly ($p < 0.05$) to 7.87%, whereas a less extensive, but significantly different ($p < 0.05$), change in protein content was observed after recirculating the sample at pH 6.3, with the protein content reducing to 8.02%. After recirculation at pH 6.5 and 6.7, the protein contents (8.20 and 8.50%, respectively) were significantly different ($p < 0.05$) from both the unheated control and the recirculated sample at pH 6.1, but not significantly different ($p > 0.05$) from the recirculated sample at pH 6.3. The ash content was also significantly lower ($p < 0.05$) after recirculating the samples at pH 6.1, 6.3, 6.5, and 6.7 reducing to 1.67, 1.74, 1.74 and 1.76% respectively, with only the recirculated sample at pH 6.1 having a significantly different ($p < 0.05$) ash content from the other samples after recirculation. This indicates that minerals were a contributing factor to fouling caused by concentrated skim milk only at very low pH (pH 6.1), as both the mildly fouled (pH 6.3) and unfouled samples (pH 6.5 and 6.7) had similar ash contents after recirculation, further supporting that the fouling deposit was caused mainly by aggregated proteins, i.e., 'type A fouling'. The reduction in ash content between the starting material and the samples drained from the fouling rig could be attributed to casein micelles in the fouling layer that contain a relatively large amount of minerals, as well as small amounts of solubilised calcium phosphate from the casein micelle facilitating protein-protein interactions (Khaldi *et al.,* 2018; Koutina *et al.,* 2014).

***Table 3.3**: Protein, ash, and total solids content (% w/w) of concentrated skim milk solutions at 30% w/w total solids at pH 6.1, 6.3, 6.5 and 6.7 after heating through recirculation through the fouling rig at 85°C for 90 min. Unheated control was not subjected to any heat treatment. Samples analysed after heating are abbreviated to 'AH'.*

Sample	Total solids	Protein	Ash
	(%w/w)		
Unheated Control	30.3 ± 0.17^{a}	9.45 ± 0.34^{a}	2.00 ± 0.02^{a}
pH 6.1 AH	23.3 ± 0.48^{b}	7.87 ± 0.77^{b}	1.67 ± 0.07^{b}
pH 6.3 AH	24.0 ± 0.82^{bc}	8.02 ± 0.72^{c}	1.74 ± 0.02^{c}
pH 6.5 AH	24.6 ± 0.82^{bc}	8.20 ± 1.29^{c}	1.74 ± 0.04^{c}
pH 6.7 AH	24.9 ± 0.32^{c}	8.5 ± 0.46^{c}	1.76 ± 0.07^{c}

Results are the means of data from two independent trials. Mean values with different superscript letters within a column are significantly different ($p < 0.05$).

3.3.7. Cleaning in place analysis

3.3.7.1. Composition of the recovered cleaning in place solutions

The recovered cleaning in place (CIP) solutions obtained after applying the CIP protocols were analysed for protein and ash content to further investigate the components of concentrated skim milk contributing to fouling (Figure 3.10 and 3.11). The protein and ash content of the water rinses differed significantly ($p < 0.05$) only after recirculation at pH 6.7, with the higher protein and ash content of the water rinse being attributed to any remaining deposit after recirculation being loosely bound (Vasbinder & De Kruif, 2003). A significant difference ($p < 0.05$) was observed in the protein content of the caustic wash after recirculation of the sample at pH 6.1 (0.24%), when compared to the protein content of the caustic washes after recirculation of samples at pH 6.3, 6.5 and 6.7. This demonstrates that considerably more protein adhered to the stainless-steel surfaces within the fouling rig at pH 6.1, further confirming that heat induced protein denaturation contributes to fouling and that the reactions are promoted at low pH (De Wit, 1990). The ash content of the acid washes differed significantly ($p < 0.05$) between all samples, with the highest percentage ash being observed after the CIP regime for the recirculation of the skim milk solution at pH 6.1 (1.06%). A linear trend was observed for the ash content of the acid washes, whereby as the pH of the recirculated samples increased, the ash content of the acid washes decreased. This indicates that minerals play a more significant role in heat-induced reactions at low pH; further supporting the hypothesis that solubilised calcium phosphate is involved in the formation of fouling deposits caused by concentrated skim milk at low pH (Guérin *et al.,* 2007). As the natural pH of milk (pH 6.7) decreases towards its iso-electric point, the net charge of the casein micelle decreases. This causes progressive protonation of organic and inorganic phosphate present in the casein micelles resulting in dissolution of the CCP (Petit *et al.,* 2011).

3.3.7.2 Turbidity of the recovered CIP solutions

The results from turbidity analysis of recovered CIP solutions obtained after applying the CIP protocols were in good agreement with the protein and ash contents of the CIP solutions (Tables 3.4 and 3.5). The turbidity of the water rinses after recirculation of the samples at pH 6.5 and 6.7 (2.96 and 3.27, respectively) were significantly higher ($p < 0.05$) than the turbidity of the water rinses at pH 6.1 and 6.3 (2.91 and 2.91, respectively). This can be attributed to the higher protein and ash content of the water rinses at pH 6.5 and 6.7. The turbidity of the caustic wash used in the CIP regime after recirculation of the sample at pH 6.1 was significantly higher

($p < 0.05$) than all other samples, which can be attributed to the significantly higher ($p < 0.05$) amount of protein dissolved by the caustic wash after recirculation of concentrated skim milk at pH 6.1. The turbidity of the acid washes were significantly different ($p < 0.05$) for all samples, following a linear trend with a decrease in turbidity being observed with increasing sample pH, which is in agreement with the trend observed in ash content of the acid washes. These results show a direct correlation between the turbidity and protein and ash content of the CIP solutions, i.e., the more fouling material dissolved by the CIP solutions, the more turbid the solutions were. Other fouling studies have monitored the cleaning procedure after fouling has occurred through turbidity measurements, proving it to be a convenient and efficient method for promptly assessing the cleaning effectiveness. Guerrero-Navarro *et al.* (2019) found that analysing turbidity to compare the effectiveness of different cleaning strategies for fouling served as an efficient and effective indicator of the cleaning process's advancement, facilitating optimization efforts. Van Asselt et al. (2002) employed real-time turbidity monitoring via spectrophotometry in an automated CIP system to evaluate the elimination of protein fouling. Similarly, Fickak et al. (2011) utilized turbidity and conductivity measurements during the rinsing phase to assess the effectiveness of the cleaning process. The results of this study, coinciding with other fouling research, shows that measuring turbidity of CIP solutions after cleaning cycles can be used to analyse the cleaning effectiveness after fouling, i.e., critical turbidity values could indicate the degree of protein or mineral deposit removal. It is important to ensure cleaning regimes are effective in completely removing the fouling deposits, as any remaining deposit in the system will facilitate the formation of biofilms and allow for fouling reactions within the product to occur more quickly, as the protein and minerals have a reactive surface to bind to (Tuoc, 2015).

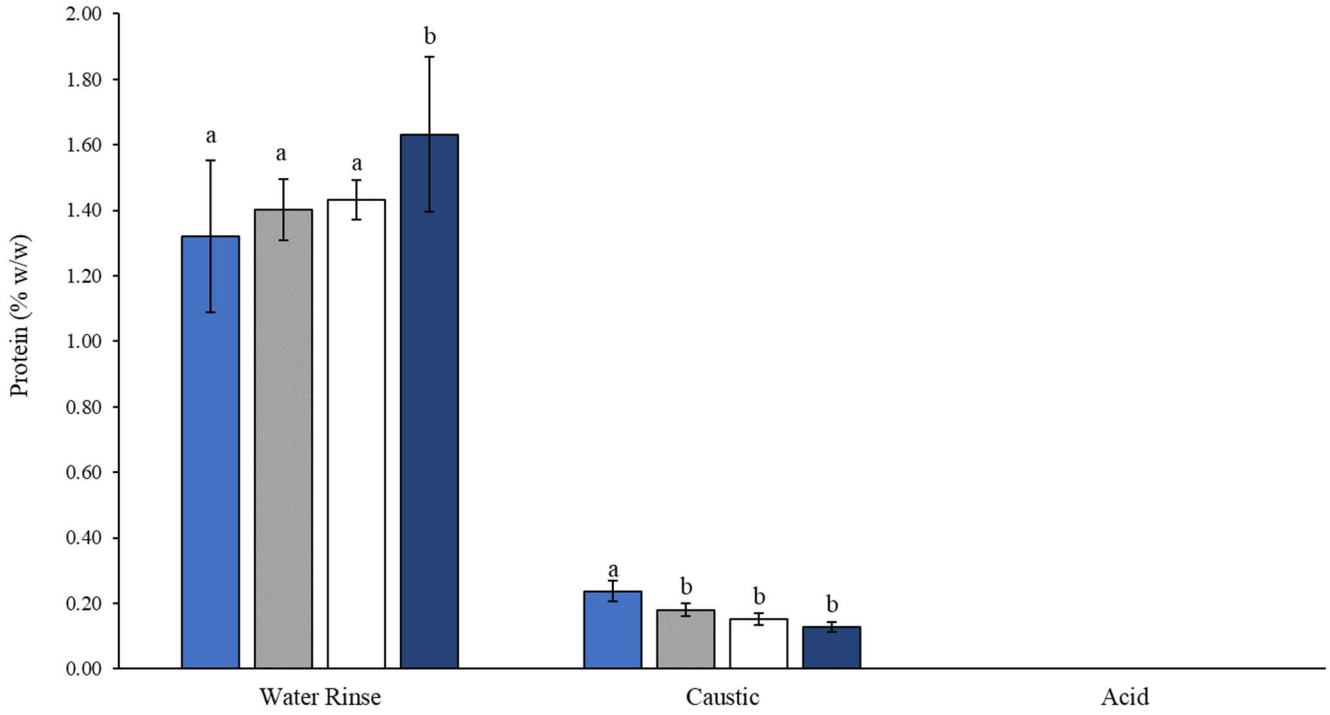

***Figure 3.10.**: Protein content (% w/w) of cleaning solutions recovered after applying a cleaning in place (CIP) protocol to the fouling rig after recirculation of concentrated skim milk solutions at 30% w/w total solids at pH 6.1 (■), 6.3 (■), 6.5 (□), and 6.7 (■) on the fouling rig at 85°C for 2 h. Results are the means of data from two independent trials. Mean values within each individual cleaning step (i.e., water rinse) with different superscript letters are significantly different ($p < 0.05$)..*

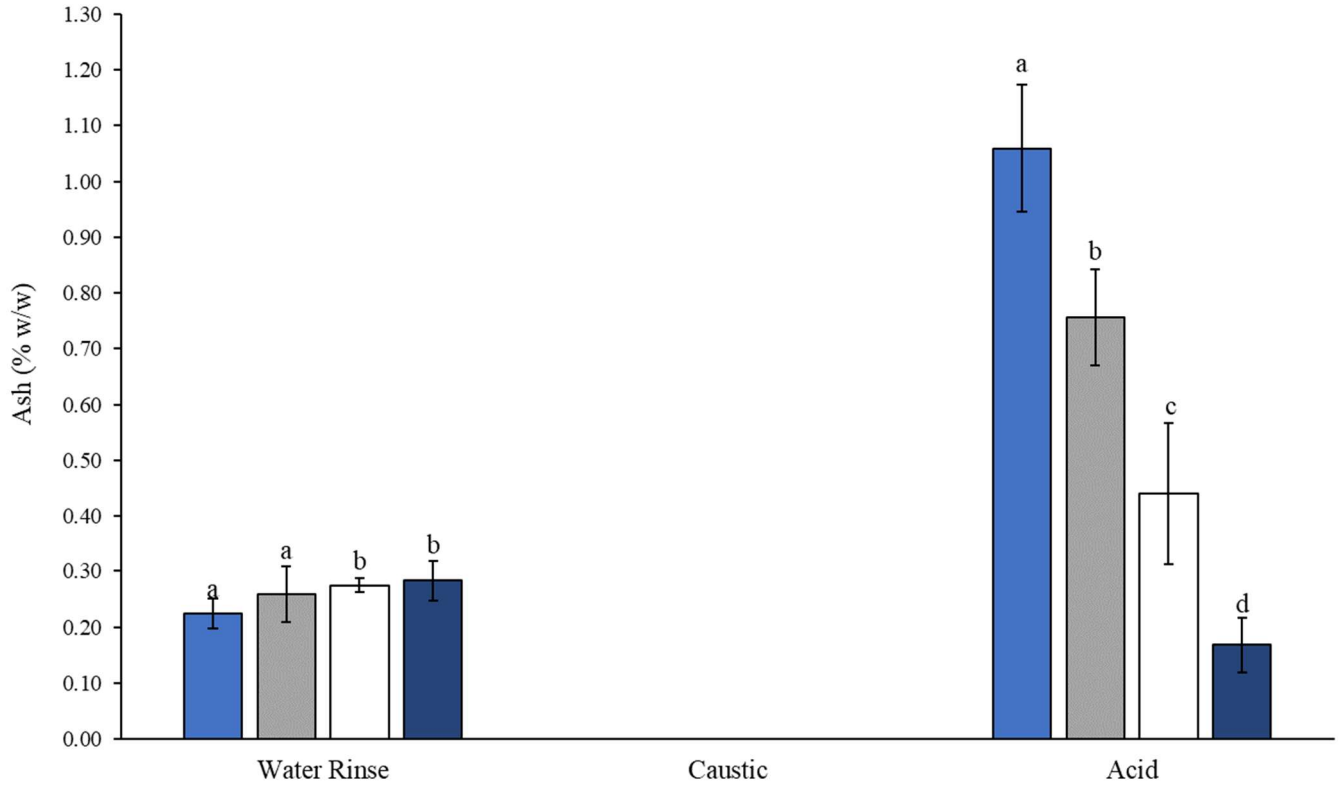

Figure 3.11.: *Ash content (% w/w) of cleaning solutions recovered after applying a cleaning in place (CIP) protocol to the fouling rig after recirculation of concentrated skim milk solutions at 30% w/w total solids at pH 6.1 (■), 6.3 (■), 6.5 (□), and 6.7 (■) on the fouling rig at 85°C for 2 h. Results are the means of data from two independent trials. Mean values within each individual cleaning step (i.e., water rinse) with different superscript letters are significantly different ($p < 0.05$).*

***Table 3.4.**: Turbidity (optical density @ 600 nm) of cleaning solutions recovered after applying a cleaning in place protocol to the fouling rig after recirculation of concentrated skim milk solutions at 30% w/w total solids at pH 6.1, 6.3, 6.5, and 6.7 on the fouling rig at 85°C for 2 h.*

	Turbidity (OD @ 600 nm)		
Circulated Milk pH	**Water Rinse**	**Caustic Wash**	**Acid Wash**
pH 6.1	2.91 ± 0.02^{a}	0.14 ± 0.01^{a}	0.76 ± 0.13^{a}
pH 6.3	2.91 ± 0.00^{a}	0.10 ± 0.02^{b}	0.63 ± 0.18^{b}
pH 6.5	2.96 ± 0.01^{b}	0.09 ± 0.01^{b}	0.31 ± 0.02^{c}
pH 6.7	3.27 ± 0.01^{c}	0.09 ± 0.01^{b}	0.18 ± 0.03^{d}

Results are the means of data from two independent trials. Mean values within a column with different superscript letters are significantly different ($p < 0.05$).

***Table 3.5.**: Images of cleaning solutions recovered after applying a cleaning in place (CIP) protocol to the fouling rig after recirculation of concentrated skim milk solutions at 30% w/w, total solids at pH 6.1, 6.3, 6.5, and 6.7 on the fouling rig at 85°C for 2 h.*

CIP solution	**pH of concentrated skim milk sample recirculated before CIP regime**			
	pH 6.1	pH 6.3	pH 6.5	pH 6.7
Water Rinse				
Caustic Wash				
Acid Wash				

3.3.7. Protein profile of foulant material

The fouling material built up in the heat exchanger after recirculation of the concentrated skim milk at pH 6.1 and 6.3 (Figure 3.4) was analysed electrophoretically under reducing and non-reducing conditions (Figure 3.12). From SDS-PAGE analysis, it can be observed that the protein profile of the fouling material deposited by the samples at pH 6.1 and 6.3 was similar. The bands corresponding to the caseins were the strongest in intensity in both the reducing and non-reducing gel, indicating that casein is one of the most dominant proteins in fouling deposit formed by concentrated skim milk. The intensity of bands corresponding to β-lg were markedly more prominent in the reducing gel compared to the non-reducing gel, indicating that denatured β-lg was a key component of the large aggregates present in the loading well of the non-reducing gel. The bands corresponding to α-lactalbumin (α-lac) were slightly more intense in the reducing gel, indicating that a small extent of denatured α-lac was also present in the fouling material. During the fouling process for concentrated milk, β-lg undergoes unfolding and denaturation due to heating, exposing the reactive thiol group (-SH) present in β-lg, which can interact with other milk proteins such as casein and α-lac, leading to the formation of aggregates and deposits (Changani et al., 1997; Oldfield et al., 2005; Visser and Jeurnink, 1997). Comparing the bands between 50-75 kDa in the reducing and non-reducing gels indicates the presence of protein aggregates in this region. In the non-reducing gel, there is only one major protein band below the 75 kDa band; however, in the reducing gel, this band is less intense and there are also additional bands, signifying the presence of other minor whey proteins such as bovine serum albumin (BSA) and lactoferrin; these bands were essentially absent in the non-reducing gel, indicating that these proteins could also have reacted in forming the large aggregates present in the loading well of the non-reducing gel. BSA, like β-lg, possesses a single free -SH group (Go et al., 2011); this -SH group in BSA can participate in intramolecular disulfide bonds with other protein molecules (Huggins et al., 1951; Nikkel and Foster, 1971), triggering the formation of large aggregates (Kelly and Zydney, 1994). The differences in the intensity of the bands between the reducing and non-reducing gels indicates that there was a significant amount of disulphide bonding between the caseins and denatured whey proteins. In previous studies where the composition of fouling deposits were analysed, it was found that whey proteins account for more than 50% of the fouling deposits in type A fouling, with β-lg being the dominant protein due to its sensitivity to heat (Lalande *et al.*, 1985; Gotham *et al.*, 1992).

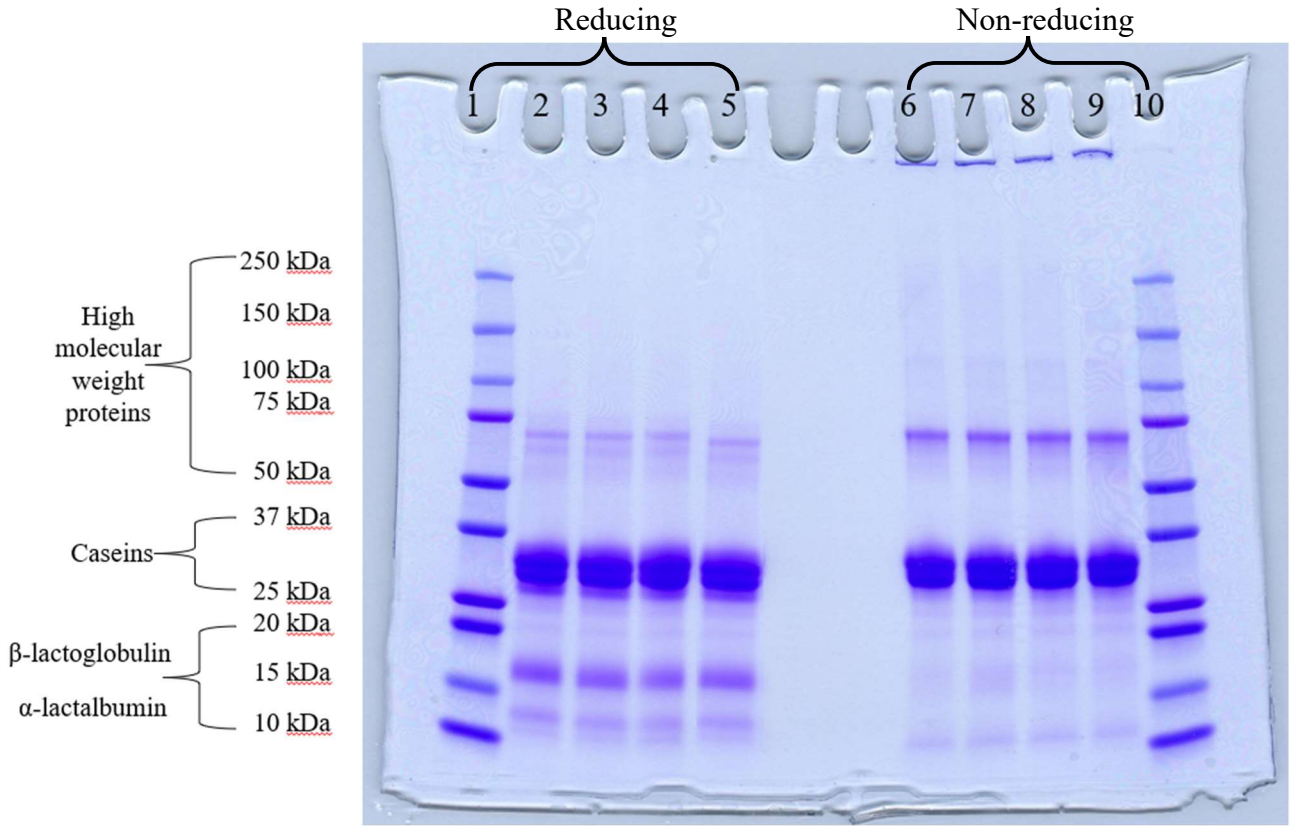

***Figure 3.12.**: Sodium dodecyl sulphate-polyacrylamide gel electrophoresis (SDS-PAGE) electrophoretograms of fouling material recovered from the heat exchanger of the fouling rig after recirculation of concentrated skim milk solutions at 30% w/w total solids at pH 6.1 and 6.3 at 85°C for 90 min: lane 1 and 10, molecular weight marker; lanes 2-3 and 6-7, foulant at pH 6.1; lanes 4-5 and 8-9, foulant at pH 6.3.*

3.4. Conclusion

This study successfully illustrated the intricate relationships among pH, heat stability, viscosity, particle size, sedimentation, and fouling in concentrated skim milk during thermal processing. As the initial pH of the concentrated skim milk solutions decreased, the heat stability decreased. Under the conditions of the study, fouling was induced in concentrated skim milk samples at pH 6.1 and 6.3 (i.e., those with low heat stability), but not at pH 6.5 and 6.7. Severe fouling was visibly evident and confirmed by a high ΔT for the sample at pH 6.1, and less so for the sample at pH 6.3. Although no significant differences in the degree of pH and conductivity change during fouling rig recirculation were observed between samples, it is important to note that all samples showed reductions in pH of ~0.36 units, highlighting the importance of monitoring pH during thermal processing. The concentrated skim milk samples that displayed fouling had higher viscosity, larger particle size distribution, and more sediment formation when compared to the unheated control and the samples that did not demonstrate fouling. Analysis of the composition of the concentrated skim milk solutions after recirculation on the fouling rig revealed reduced protein and ash content compared to the initial material, with this reduction being more significant at pH 6.1 and 6.3. These findings, along with compositional analysis of cleaning in place (CIP) solutions and SDS-PAGE analysis of the adhered foulant, demonstrated that the fouling deposits consisted primarily of aggregated protein, with the relatively high ash content of the CIP solutions indicating some calcium phosphate binding facilitated by the low pH. Through a combination of analytical approaches and tools, a deeper understanding of fouling was achieved, aiding in the identification of strategies to mitigate its occurrence in the future. Moreover, this study established the efficacy of the custom-fabricated fouling rig as a powerful tool for investigating the fouling behaviour of concentrated skim milk and cleaning of dairy heat exchangers. The rig's modular design facilitated the generation of deposits under high-temperature short-time conditions for compositional characterization and assessment of cleaning in place solutions. In the future, the fouling rig could be employed to explore potential process modifications aimed at reducing the occurrence of fouling.

3.4. Acknowledgements

The authors would like to acknowledge the Dairy Processing Technology Centre (DPTC), an Enterprise Ireland initiative, for financial support and permission to publish this work (Grant Number TC/2020/0028). The authors would also like to acknowledge Dr. Mestawet Taye Asfaw for her help with SDS-PAGE analysis.

3.6. References

Anema, S. G. (2007). Role of κ-casein in the association of denatured whey proteins with casein micelles in heated reconstituted skim milk. *Journal of Agricultural and Food Chemistry*, *55*(9), 3635-3642.

Anema, S.G. (2009). Effect of milk solids concentration on the pH, soluble calcium, and soluble phosphate levels of milk during heating. *Dairy Science and Technology*, *89*(5), 501-510.

Anema, S.G. and Li, Y. (2003). Effect of pH on the association of denatured whey proteins with casein micelles in heated reconstituted skim milk. *Journal of Agricultural and Food Chemistry*, *51*(6), 1640-1646.

Anema, S. G., Lowe, E. K., & Lee, S. K. (2004). Effect of pH at heating on the acid-induced aggregation of casein micelles in reconstituted skim milk. *LWT-Food Science and Technology*, *37*(7), 779-787.

Anema, S. G., Lowe, E. K., Lee, S. K., & Klostermeyer, H. (2014). Effect of the pH of skim milk at heating on milk concentrate viscosity. *International Dairy Journal*, *39*(2), 336-343.

Anema, S. G., Lowe, E. K., & Li, Y. (2004). Effect of pH on the viscosity of heated reconstituted skim milk. *International Dairy Journal*, *14*(6), 541-548.

Augustin, M.A. and Clarke, P.T. (1990). Effects of added salts on the heat stability of recombined concentrated milk. *Journal of Dairy Research*, *57*(2), 213-226.

Bienvenue, A., Jiménez-Flores, R., & Singh, H. (2003). Rheological properties of concentrated skim milk: importance of soluble minerals in the changes in viscosity during storage. *Journal of Dairy Science*, *86*(12), 3813-3821.

Bista, A., McCarthy, N., O'Donnell, C. P., & O'Shea, N. (2021). Key parameters and strategies to control milk concentrate viscosity in milk powder manufacture. *International Dairy Journal*, *121*, 105120.

Burton, H., (1968). Section G. Deposits from whole milk in heat treatment plant—a review and discussion. *Journal of Dairy Research*, *35*(2), 317-330.

Bylund, G. (2015). *Dairy Processing Handbook*. Tetra Pak Processing Systems AB.

Changani, S. D., Belmar-Beiny, M. T., & Fryer, P. J. (1997). Engineering and chemical factors associated with fouling and cleaning in milk processing. *Experimental Thermal and Fluid Science*, *14*(4), 392-406.

Chaplin, L. G., & Lyster, R. L. (1988). Effect of temperature on the pH of skim milk. *Journal of Dairy Research*, *55*(2), 277-280.

Chen, B. Y., Grandison, A. S. and Lewis, M. J. (2012). Comparison of heat stability of goat milk subjected to ultra-high temperature and in-container sterilization. *Journal of Dairy Science*, 95(3), 1057-1063.

Chen, B., & O'Mahony, J.A. (2016). Impact of glucose polymer chain length on heat and physical stability of milk protein-carbohydrate nutritional beverages. *Food Chemistry*, *211*, 474-482.

Davies, D. T., & White, J. C. D. (1966). The stability of milk protein to heat: I. Subjective measurement of heat stability of milk. *Journal of Dairy Research*, 33, 67-81.

Dalgleish, D.G. and Law, A.J. (1989). pH-induced dissociation of bovine casein micelles. II. Mineral solubilization and its relation to casein release. *Journal of Dairy Research*, *56*(5), 727-735.

De Wit, J. N. (1990). Thermal stability and functionality of whey proteins. *Journal of Dairy Science*, *73*(12), 3602-3612.

Dumpler, J. (2018). Heat stability of concentrated skim milk on lab scale. *Heat Stability of Concentrated Milk Systems: Kinetics of the Dissociation and Aggregation in High Heated Concentrated Milk Systems*. (pp. 47-61). Springer.

Fickak, A., Al-Raisi, A., & Chen, X. D. (2011). Effect of whey protein concentration on the fouling and cleaning of a heat transfer surface. *Journal of Food Engineering*, *104*(3), 323-331.

Fox, P. F. & McSweeney, P. L. H. (2003). *Advanced Dairy Chemistry—1 Proteins, 3rd edition.* Plenum Press, New York.

Fox, P. F., Uniacke-Lowe, T., McSweeney, P. L. H., O'Mahony, J. A., Fox, P. F., Uniacke-Lowe, T., ... & O'Mahony, J. A. (2015). Salts of milk. *Dairy Chemistry and Biochemistry*, 241-270.

Fryer, P. J., & Belmar-Beiny, M. T. (1991). Fouling of heat exchangers in the food industry: a chemical engineering perspective. *Trends in Food Science & Technology*, *2*, 33-37.

Georgiadis, M. C., Rotstein, G. E., & Macchietto, S. (1998). Optimal design and operation of heat exchangers under milk fouling. *AIChE Journal*, *44*(9), 2099-2111.

Go, E. P., Zhang, Y., Menon, S., & Desaire, H. (2011). Analysis of the disulfide bond arrangement of the HIV-1 envelope protein CON-S gp140 ΔCFI shows variability in the V1 and V2 regions. *Journal of Proteome Research*, *10*(2), 578-591.

Gotham, S.M., Fryer, P.J. and Pritchard, A.M. (1992). β-lactoglobulin denaturation and aggregation reactions and fouling deposit formation: a DSC study. *International Journal of Food Science & Technology*, *27*(3), 313-327.

Guérin, R., Ronse, G., Bouvier, L., Debreyne, P., & Delaplace, G. (2007). Structure and rate of growth of whey protein deposit from in situ electrical conductivity during fouling in a plate heat exchanger. *Chemical Engineering Science*, *62*(7), 1948-1957.

Guerrero-Navarro, A. E., Ríos-Castillo, A. G., Avila, C. R., Hascoët, A. S., Felipe, X., & Jerez, J. R. (2019). Development of a dairy fouling model to assess the efficacy of cleaning procedures using alkaline and enzymatic products. *LWT*, *106*, 44-49.

Hagsten, C., Altskär, A., Gustafsson, S., Lorén, N., Hamberg, L., Innings, F., ... & Nylander, T. (2016). Composition and structure of high temperature dairy fouling. *Food Structure*, *7*, 13-20.

Hardy, E. E., Muir, D. D., Sweetsur, A. M., & West, I. G. (1984). Changes of calcium phosphate partition and heat stability during manufacture of sterilized concentrated milk. *Journal of Dairy Science*, *67*(8), 1666-1673.

Haque, Z., & Kinsella, J. E. (1988). Interaction between heated κ-casein and β-lactoglobulin: predominance of hydrophobic interactions in the initial stages of complex formation. *Journal of Dairy Research*, *55*(1), 67-80.

Hebishy, E., Joubran, Y., Murphy, E. and O'Mahony, J.A. (2019). Influence of calcium-binding salts on heat stability and fouling of whey protein isolate dispersions. *International Dairy Journal*, *91*, 71-81.

Hill, J.P., Boland, M.J. and Smith, A.F. (1997). The effect of beta-lactoglobulin variants on milk powder manufacture and properties. In *Milk protein polymorphism, Palmerston North (New Zealand), Feb 1997*. International Dairy Federation.

Hinton, A. R., Trinh, K. T., Brooks, J. D., & Manderson, G. J. (2002). Thermophile survival in milk fouling and on stainless steel during cleaning. *Food and Bioproducts Processing*, *80*(4), 299-304.

Ho, Q. T., Murphy, K. M., Drapala, K. P., O'Callaghan, T. F., Fenelon, M. A., O'Mahony, J. A., & McCarthy, N. A. (2018). Effect of pH and heat treatment on viscosity and heat coagulation properties of milk protein concentrate. *International Dairy Journal*, *85*, 219-224.

Holsinger, V. H., Rajkowski, K. T., & Stabel, J. R. (1997). Milk pasteurisation and safety: a brief history and update. *Revue Scientifique et Technique-Office International des Epizooties*, *16*(2), 441-466.

Huggins, C., Tapley, D. F., & Jensen, E. V. (1951). Sulphydryl-disulphide relationships in the induction of gels in proteins by urea. *Nature*, *167*, 592-593.

Huppertz, T. (2016). Heat stability of milk. *Advanced Dairy Chemistry: Volume 1B: Proteins: Applied Aspects*, 179-196.

International Dairy Federation (IDF) (2001). Milk. Determination of nitrogen content, ISO 8968-5. IDF standard 020-5:2001.

International Dairy Federation (IDF) (2010). Milk, cream, and evaporated milk – Determination of total solids content, ISO 6731. IDF standard 21:2010.

Jenness, R. (1962). Preparation and properties of a salt solution which simulated milk ultrafiltrate. *Netherlands Milk and Dairy Journal*, *16*, 153-164.

Jeurnink, T.J., Walstra, P. and De Kruif, C.G. (1996). Mechanisms of fouling in dairy processing. *Netherlands Milk and Dairy Journal*, *50*, 407-426.

Jimenez, M., Delaplace, G., Nuns, N., Bellayer, S., Deresmes, D., Ronse, G., *et al*. (2013). Toward the understanding of the interfacial dairy fouling deposition and growth mechanisms

at a stainless steel surface: A multiscale approach. *Journal of Colloid and Interface Science*, 404, 192-200.

Kelly, A. L., O'Connell, J. E., & Fox, P. F. (2003). Manufacture and properties of milk powders. *Advanced Dairy Chemistry—1 Proteins: Part A/Part B*, 1027-1061.

Kelly, S. T., & Zydney, A. L. (1994). Effects of intermolecular thiol–disulfide interchange reactions on bsa fouling during microfiltration. *Biotechnology and bioengineering*, *44*(8), 972-982.

Khaldi, M., Croguennec, T., André, C., Ronse, G., Jimenez, M., Bellayer, S., Blanpain-Avet, P., Bouvier, L., Six, T., Bornaz, S., Jeantet, R. and Delaplace, G. (2018). Effect of the calcium/protein molar ratio on β-lactoglobulin denaturation kinetics and fouling phenomena. *International Dairy Journal*. 78, 1-10.

Koutina, G., Knudsen, J. C., Andersen, U., & Skibsted, L. H. (2014). Temperature effect on calcium and phosphorus equilibria in relation to gel formation during acidification of skim milk. *International Dairy Journal*, **36**(1), 65– 73.

Laemmli, U. (1970). Most commonly used discontinuous buffer system for SDS electrophoresis. *Nature, 227,* 680–686.

Lalande, M. and Tissier, J.P. (1985). Fouling of heat transfer surfaces related to β-lactoglobulin denaturation during heat processing of milk. *Biotechnology progress*, *1*(2), 131-139.

Lewis, M., Grandison, A., Lin, M., & Tsioulpas, A. (2011). Ionic calcium and pH as predictors of stability of milk to UHT processing. *Milchwissenschaft*, *66*(2), 197-200.

Lowe, E. K., Anema, S. G., Bienvenue, A., Boland, M. J., Creamer, L. K., & Jiménez-Flores, R. (2004). Heat-induced redistribution of disulfide bonds in milk proteins. 2. Disulfide bonding patterns between bovine β-lactoglobulin and κ-casein. *Journal of Agricultural and Food Chemistry*, *52*(25), 7669-7680.

Mabrook, M. F., & Petty, M. C. (2003). Effect of composition on the electrical conductance of milk. *Journal of Food Engineering*, *60*(3), 321-325.

McLean, D. M., Graham, E. B., Ponzoni, R. W., & Mckenzie, H. A. (1987). Effects of milk protein genetic variants and composition on heat stability of milk. *Journal of Dairy Research*, *54*(2), 219-235.

McMahon, D. J., & Oommen, B. S. (2008). Supramolecular structure of the casein micelle. *Journal of Dairy Science*, *91*(5), 1709-1721.

Mucchetti, G., Gatti, M., & Neviani, E. (1994). Electrical conductivity changes in milk caused by acidification: determining factors. *Journal of Dairy Science*, *77*(4), 940-944.

Nair, P. K., Dalgleish, D. G., & Corredig, M. (2013). Colloidal properties of concentrated heated milk. *Soft Matter*, *9*(14), 3815-3824.

Nieuwenhuijse, J. A., Sjollema, A., van Boekel, M. A. J. S., Van Vliet, T., & Walstra, P. (1991). The heat stability of concentrated skim milk. *Netherlands Milk and Dairy Journal*, *45*, 193-224.

Nikkel, H. J., & Foster, J. F. (1971). Reversible sulfhydryl-catalyzed structural alteration of bovine mercaptalbumin. *Biochemistry*, *10*(24), 4479-4486.

Oldfield, D. J., Singh, H., & Taylor, M. W. (2005). Kinetics of heat-induced whey protein denaturation and aggregation in skim milks with adjusted whey protein concentration. *Journal of Dairy Research*, *72*(3), 369-378.

On-Nom, N., Grandison, A. S., & Lewis, M. J. (2012). Heat stability of milk supplemented with calcium chloride. *Journal of Dairy Science*, *95*(4), 1623-1631.

Parris, N., Purcell, J. M., & Ptashkin, S. M. (1991). Thermal denaturation of whey proteins in skim milk. *Journal of Agricultural and Food Chemistry*, *39*(12), 2167-2170.

Petit, J., Herbig, A. L., Moreau, A., & Delaplace, G. (2011). Influence of calcium on β-lactoglobulin denaturation kinetics: Implications in unfolding and aggregation mechanisms. *Journal of Dairy Science*, *94*(12), 5794-5810.

Pyne, G. T. (1962). Section C. Dairy Chemistry: some aspects of the physical chemistry of the salts of milk. *Journal of Dairy Research*, *29*(1), 101-130.

Pyne, G. T., & McGann, T. C. A. (1960). The colloidal phosphate of milk: II. Influence of citrate. *Journal of Dairy Research*, *27*(1), 9-17.

Rosmaninho, R., & Melo, L. F. (2008). Protein–calcium phosphate interactions in fouling of modified stainless-steel surfaces by simulated milk. *International Dairy Journal*, *18*(1), 72-80.

Schnöing, L., Augustin, W., & Scholl, S. (2020). Fouling mitigation in food processes by modification of heat transfer surfaces: A review. *Food and Bioproducts Processing*, *121*, 1-19.

Singh, H. (1995). Heat-induced changes in casein, including interactions with whey proteins. *Heat-induced Changes in Milk.*, (Ed. 2), 86-104.

Tanguy, G., Siddique, F., Beaucher, E., Santellani, A. C., Schuck, P., & Gaucheron, F. (2016). Calcium phosphate precipitation during concentration by vacuum evaporation of milk ultrafiltrate and microfiltrate. *LWT-Food Science and Technology*, *69*, 554-562.

Tuoc, T. K. (2015). Fouling in Dairy Processes. In *Mineral Scales and Deposits* (pp. 533-556). Elsevier.

van Boekel, M. A. J. S., Nieuwenhuijse, J. A., & Walstra, P. (1989). The heat coagulation of milk, 1: Mechanisms. *Netherlands Milk and Dairy Journal, 43,* 97–127.

Van Asselt, A. J., Van Houwelingen, G., & Te Giffel, M. C. (2002). Monitoring system for improving cleaning efficiency of cleaning-in-place processes in dairy environments. *Food and Bioproducts Processing*, *80*(4), 276-280.

Vasbinder, A. J., & De Kruif, C. G. (2003). Casein–whey protein interactions in heated milk: the influence of pH. *International Dairy Journal*, *13*(8), 669-677.

Visser, J., & Jeurnink, T. J. (1997). Fouling of heat exchangers in the dairy industry. *Experimental Thermal and Fluid Science*, *14*(4), 407-424.

Wadsworth, K. D., & Bassette, R. (1985). Laboratory-scale system to process ultrahigh-temperature milk. *Journal of Food Protection*, *48*(6), 530-531.

Wallhäußer, E., Hussein, W. B., Hussein, M. A., Hinrichs, J., & Becker, T. (2013). Detection of dairy fouling: Combining ultrasonic measurements and classification methods. *Engineering in Life Sciences*, *13*(3), 292-301.

Chapter 4

General Discussion and Conclusions

Tara R. Murphy, Eoin W. Finnegan, Tom F. O'Callaghan, James A. O'Mahony

School of Food and Nutritional Sciences, University College Cork, Cork, Ireland

Declaration

This chapter was written by author Tara R. Murphy (TRM) and reviewed by all co-authors.

4.1. General discussion and conclusions

The production of skim milk powder involves the concentration of milk through evaporation, followed by drying to remove most of the remaining water. However, the evaporation process is often impacted by the challenge of fouling, which significantly impacts the efficiency and sustainability of the production process, while also often having undesirable implications for finished product quality (e.g., insolubility and sediment formation). Evaporator fouling refers to the unwanted deposition of solids on the heat transfer surfaces within the evaporator system. Over time, the fouling deposits accumulate, leading to reduced heat transfer efficiency, increased energy consumption, and decreased production capacity. The presence of fouling in the evaporator not only hampers the overall process efficiency but also poses a considerable economic burden for dairy processors. The accumulation of fouling deposits necessitates more frequent cleaning (with associated chemical and water usage), which translates into downtime, increased costs, and decreased profitability. Therefore, understanding the causes and mechanisms of evaporator fouling in skim milk powder production is of paramount importance to mitigate its adverse effects and optimize process performance. This thesis aimed to investigate evaporator fouling by exploring its underlying mechanisms and the factors influencing its formation. The studies described in this thesis systematically investigate the use of pH and lab-scale analysis to predict fouling; the results report on the heat-induced changes during heat treatment, and the impact of pH on the heat stability and physicochemical properties of concentrated skim milk and how it can be extrapolated to large scale evaporators.

The study described in Chapter 2 demonstrated the influence of pH (6.0-6.7) on the heat stability and physicochemical properties of concentrated skim milk after high temperature short time (HTST) processing using a rheometer. The objective of this study was to assess the contribution of pH and heat-induced changes in concentrated skim milk to the occurrence of fouling. As the pH of the concentrated skim milk solutions decreased, heat stability decreased, viscosity development on heating increased, particle size after heating increased, and formation of sediment in solution after heating increased. The poor heat stability and significant increase in viscosity, particle size, and sediment formation after heat treatment of samples between pH 6.0-6.3 can be attributed to aggregation of the principal milk proteins, caseins, and whey proteins. Indeed, the colloidal stability of casein micelles is lowered by a decrease in surface charge of casein micelles, a reduced electrostatic repulsion, and a collapse of the hairy layer due to charge neutralisation. The denaturation of whey proteins due to the high heat treatment

resulted in exposure of sulfhydryl (-SH) groups and hydrophobic regions, promoting interaction with the destabilised casein micelles, facilitating extensive protein aggregation, ultimately leading to an increase in viscosity and particle size of concentrated skim milk. This trend in the results of increasing extent of heat-induced physicochemical changes with decreasing pH was replicated when the analysis at two pH points (6.2 and 6.6) was upscaled from the rheometer to a custom built fouling rig. Heat treatment of concentrated skim milk at pH 6.2 on the fouling rig resulted in severe fouling, and analysis of the concentrated skim milk after recirculation on the fouling rig for particle size and sedimentation showed results consistent with the initial laboratory-scale heat treatment analysis. Fouling did not occur when concentrated skim milk was recirculated on the fouling rig at pH 6.6, and particle size and sedimentation did not increase significantly when compared with an unheated control. By conducting compositional analysis of the concentrated skim milk and cleaning-in-place solutions after recirculation on the fouling rig, it was hypothesized that the fouling deposit formed was mainly comprised of aggregated protein, comprised mainly of casein and whey proteins.

Building on the conclusions from Chapter 2, the study described in Chapter 3 focused on further characterising evaporator fouling and more systematically developing the inter-relationships between heat stability, viscosity, particle size and fouling across both laboratory (i.e., rheometer) and pilot (i.e., fouling rig) scales. Concentrated skim milk samples at pH 6.1, 6.3, 6.5 and 6.7 were recirculated on the fouling rig while in-line measurements of pH, conductivity and temperature were performed, followed by analysis of the concentrated skim milk samples, cleaning-in-place chemicals and adhered foulant on the heat exchanger after the fouling experiments. The objective of this study was to identify the effect of pH on the heat-induced physicochemical reactions contributing to fouling of concentrated skim milk during heat treatment and to develop laboratory-scale predictors for fouling taking place at pilot scale. This approach was effective in differentiating between the distinct pH regions in milk in which fouling was extensive (pH 6.1-6.3), in comparison with pH regions in which fouling was much more limited (pH 6.5-6.7). Continuous pH measurements carried out during the heat treatment of concentrated skim milk on the fouling rig revealed a significant decrease in pH for all samples during recirculation. This emphasizes the importance of pH monitoring during thermal processing, as a decline in pH within the threshold associated with protein aggregation corresponds to fouling occurrence. It was observed that the samples of concentrated skim milk that caused fouling also showed increased viscosity, particle size and sedimentation when

compared to the samples with limited/no fouling. Expanding upon the hypothesis that the fouling deposit was comprised largely of aggregated protein (Chapter 2), sodium dodecyl sulphate-polyacrylamide gel electrophoresis (SDS-PAGE) analysis of adhered foulant formed by concentrated skim milk at pH 6.1 and 6.3 was conducted and confirmed the prominence of denatured β-lactoglobulin and α-lactalbumin, as well as a strong presence of caseins. In conclusion, maintaining the pH of concentrated skim milk above pH 6.3 was effective in preventing the occurrence of fouling during heat treatment. Simple analysis of physicochemical properties related to protein aggregation, i.e., viscosity, particle size, and sedimentation, could be used as a preventative measure for fouling by predicting the likelihood of the concentrated skim milk to foul. These results emphasise the importance of monitoring pH during thermal processing to predict and control heat-induced fouling. Thus, the findings presented in this thesis are of significance in facilitating a better understanding of the role of protein-protein interactions in the formation of fouling deposits by concentrated skim milk.

Through a combination of experimental analysis and theoretical investigation, this study contributes to the existing body of knowledge by uncovering the fundamental causes of evaporator fouling. The findings will not only benefit dairy industry processors but also facilitate the development of innovative mitigation solutions. Ultimately, this thesis aims to shed light on the complex interplay between skim milk composition, processing conditions, and evaporator fouling, providing a scientific foundation for enhancing the efficiency, productivity, and sustainability of skim milk powder production.

4.2. Suggestions for future research

From the findings of the studies conducted in this thesis, it is evident that an area that requires further research is methods to improve the heat stability of concentrated skim milk. Application of these methods to the fouling rig could further develop the relationship between heat stability and fouling, as well as to facilitate the development of fouling mitigation strategies. Various approaches have been identified and proposed to improve the heat stability of milk:

- The utilization of enzymatic cross-linking, such as with transglutaminase, has demonstrated the ability to enhance the heat stability of milk by cross-linking denatured whey proteins, thereby inhibiting protein aggregation, and thus reducing fouling (O'Sullivan, 2002; Smiddy *et al.,* 2006).

- The heat stability of concentrated skim milk can be both positively and negatively influenced through heat-induced changes. Exposure to high temperatures with no pre-treatments (i.e., pre-heat treatment) can lead to extensive protein-protein interactions leading to aggregation. Alternatively, milk subjected to pre-heat treatments with lower controlled temperatures can facilitate protein interactions which can improve heat-stability. The heat stability of milk proteins, through preheating has been found to be an effective strategy by controlling heat induced Maillard conjugation between milk protein and sugar (Wu *et al.,* 2021a). Therefore, employing this approach may be a promising method to improve the heat stability of concentrated skim milk, and thus reduce the occurrence of fouling (Singh & Tokley, 1990; Sweetsur & Muir, 1980; Tan-Kintia & Fox, 1999; Wu *et al.,* 2021b).
- The addition of stabilisers e.g., disodium phosphate, trisodium phosphate, trisodium citrate, has been shown to increase the pH and, consequently, the heat stability of concentrated skim milk through analysis of the heat coagulation time at 120ºC (Sweetsur & Muir, 1980). In addition to their effect on pH, they have the ability to bind cations (e.g., calcium) which have been shown to mediate protein-protein aggregation. Thus, their addition to skim milk prior to heat treatment should be a potential mitigator of fouling

Another area that requires additional investigation would be to apply the findings related to pH and analysis of physicochemical properties associated with protein aggregation from this thesis to a pilot scale evaporator mimicking the evaporation stage in the production of skim milk powder. Monitoring the pH of skim milk during evaporation could identify the point in the process in which the pH drops to a level that promotes fouling (i.e., below pH 6.3). Through the collection of skim milk samples at various stages of evaporation and subsequent assessment of parameters such as viscosity, particle size, and sedimentation (as outlined within this thesis), it would be possible to determine the specific temperature and total solids content within the evaporation process at which milk fouling tendencies are most pronounced. Further detailed studies into the effects of process variables on fouling phenomena could provide a more comprehensive understanding of strategies for mitigating fouling.

The use of antifouling surfaces has been suggested as a solution to prevent fouling during thermal processing (Barish & Goddard, 2014; Mérian & Goddard, 2012; Rosmaninho *et al.,* 2007). However, the main challenge lies in reducing adhesion, which is crucial for antifouling effectiveness and depends on the properties of the substances attaching to the surface.

Moreover, modified surfaces and coatings introduce extra costs for fabrication and installation, which must be taken into account when assessing their fouling and cleaning performance. There is ample literature available on various antifouling coatings shown to mitigate dairy fouling, such as polytetrafluoroethylene and titanium dioxide nanoparticles (Bangavadi Munivenkatappa *et al.,* 2022), biomimetic surface modifications (Zouaghi *et al.,* 2019), and amphiphilic silicone coatings (Zouaghi *et al.,* 2018). However, few researchers have experimented with the effectiveness of antifouling coatings in mitigating the fouling of concentrated skim milk. Therefore, a study investigating the ability of different antifouling coatings to prevent fouling of concentrated skim milk using the fouling rig would provide useful information as a potential fouling mitigation strategy.

In Chapter 1, a range of in-line process analytical technologies (PAT) used to monitor fouling were reviewed, including ultrasonic sensors (Hay & Rose 2003; Mairal *et al.,* 1999), acoustic sensors (Dam Madsen, 1994; Lohr & Rose, 2003; Merheb *et al.,* 2007), voltametric methods (Fysun *et al.,* 2020; Roscoe *et al.,* 1993), sensors based on local differential thermal analysis (Crattelet *et al.,* 2013) and spectroscopic techniques (Blanpain-Avet *et al.,* 2012; Caponigro *et al.,* 2019; Fysun *et al.,* 2019). The research conducted on these PAT tools was primarily focused on fouling of skim milk and whey protein solutions; therefore, further research is required on the applicability of these PAT tools to fouling of concentrated skim milk. The modular design of the fouling rig used in this thesis allows for easy modification and addition of PAT tools to enable research on different aspects of fouling. A study comparing the applicability of different PAT tools in detecting fouling of concentrated skim milk would be easily facilitated using the fouling rig, as different technologies could be added and removed as needed, resulting in identification of the most effective PAT approach for monitoring fouling of concentrated skim milk.

Effective management of cleaning in place protocols offers significant potential for optimizing processes that are prone to fouling. The choice of the most suitable cleaning technique depends on the characteristics of the fouling deposit, and through an understanding of the fundamental mechanisms involved in deposit removal, these methods can often be considerably enhanced (Piepiórka-Stepuk *et al.,* 2012). There is a diverse array of cleaning in place methods available to the dairy industry; however, in many instances, the cleaning procedures currently used rely primarily on past experience and due to the absence of dependable monitoring tools, the cleaning time often tends to be longer than actually required, which has undesirable environmental and financial impacts. Many researchers who investigate

the cleaning process tend to optimize it primarily with regard to cleaning quality, specifically surface cleanliness. They take into account various factors that affect the process, such as flow velocity, temperature, and chemical concentration, and analyse their impact on the duration of cleaning. A significant portion of the literature focuses on the elimination of milk fouling from production surfaces, as post-production sediments encountered in food processing pose the greatest challenge for removal. For instance, Gillham et al. (1999) discovered a strong dependence of whey protein deposit removal from stainless steel pipes on temperature. Some authors have identified optimal chemical concentrations that minimize cleaning time (Fryer et al., 2006), while others have directed their attention towards mechanical influences (Changani et al., 1997). While all this previous research provides important insights into optimisation of cleaning for dairy systems, there is limited specific research regarding cleaning after fouling of concentrated skim milk. The fouling rig used in this thesis offers a useful medium for testing various cleaning in place protocols to optimise and specify a particular protocol that is most suited to fouling caused by concentrated skim milk.

4.3 References

Bangavadi Munivenkatappa, M., Franklin, M.E.E., Dhotre, A.V., Pushpadass, H.A., Shivanand, Anthonysamy, A., Mandhyan, P.K. and Patil, P.G. (2022). Mitigation of fouling during milk processing in polytetrafluoroethylene-titanium dioxide coated plate heat exchanger. *Journal of Food Process Engineering*, *45*(6), e13836.

Barish, J. A., & Goddard, J. M. (2014). Stability of nonfouling stainless steel heat exchanger plates against commercial cleaning agents. *Journal of Food Engineering*, *124*, 143-151.

Blanpain-Avet, P., Hédoux, A., Guinet, Y., Paccou, L., Petit, J., Six, T., & Delaplace, G. (2012). Analysis by Raman spectroscopy of the conformational structure of whey proteins constituting fouling deposits during the processing in a heat exchanger. *Journal of food engineering*, *110(1),* 86-94.

Caponigro, V., Marini, F., Dorrepaal, R., Herrero-Langreo, A., Scannell, A., & Gowen, A. (2019). Raman and Fourier transform infrared hyperspectral imaging to study dairy residues on different surface. *Journal of Spectral Imaging*, *8(1),* a3.

Changani, S. D., Belmar-Beiny, M. T., & Fryer, P. J. (1997). Engineering and chemical factors associated with fouling and cleaning in milk processing. *Experimental Thermal and Fluid Science*, *14*(4), 392-406.

Crattelet, J., Ghnimi, S., Debreyne, P., Zaid, I., Boukabache, A., Esteve, D., Auret, L., & Fillaudeau, L. (2013). On-line local thermal pulse analysis sensor to monitor fouling and cleaning: Application to dairy product pasteurisation with an ohmic cell jet heater. *Journal of Food Engineering*, *119(1),* 72-83.

Dam Madsen, K. (1994). Vibration Sensor. *Sanitation of Food Processing Plants, Final Technical Report* (Mikkelsen, H.O., ed.), 72-86, Biotechnological Institute, Kolding, Denmark.

Fryer, P. J., Christian, G. K., & Liu, W. (2006). How hygiene happens: physics and chemistry of cleaning. *International journal of dairy technology*, *59*(2), 76-84.

Fysun, O., Anzmann, T., Gschwind, P., Rauschnabel, J., Kohlus, R., & Langowski, H.-C. (2019). Biofilm and dairy fouling detection in flexible tubing using low-field NMR. *European food research & technology*, *245(11),* 2579-2590.

Fysun, O., Khorshid, S., Rauschnabel, J., & Langowski, H.-C. (2020). Detection of dairy fouling by cyclic voltammetry and square wave voltammetry. *Food Science & Nutrition*, *8(7),* 3070-3080.

Gillham, C. R., Fryer, P. J., Hasting, A. P. M., & Wilson, D. I. (1999). Cleaning-in-place of whey protein fouling deposits: mechanisms controlling cleaning. *Food and Bioproducts Processing*, *77*(2), 127-136.

Hay, T. R., & Rose, J. L. (2003). Fouling detection in the food industry using ultrasonic guided waves. *Food control*, *14*(7), 481-488.

Lohr, K. R., & Rose, J. L. (2003). Ultrasonic guided wave and acoustic impact methods for pipe fouling detection. *Journal of food engineering*, *56*(4), 315-324.

Mairal, A. P., Greenberg, A. R., Krantz, W. B., & Bond, L. J. (1999). Real-time measurement of inorganic fouling of RO desalination membranes using ultrasonic time-domain reflectometry. *Journal of membrane science*, *159(1),* 185-196.

Merheb, B., Nassar, G., Nongaillard, B., Delaplace, G., & Leuliet, J. C. (2007). Design and performance of a low-frequency non-intrusive acoustic technique for monitoring fouling in plate heat exchangers. *Journal of food engineering*, *82*(4), 518-527.

Mérian, T., & Goddard, J. M. (2012). Advances in nonfouling materials: perspectives for the food industry. *Journal of agricultural and food chemistry*, *60*(12), 2943-2957.

O'Sullivan, M. M., Kelly, A. L., & Fox, P. F. (2002). Effect of transglutaminase on the heat stability of milk: a possible mechanism. *Journal of Dairy Science*, *85*(1), 1-7.

Piepiórka-Stepuk, J., Diakun, J., Jakubowski, M., Mierzejewska, S., & Masłowska, S. (2012). Influence of time and the cleaning liquid flow velocity on the effectiveness of cleaning the plate heat exchanger. *Agric. Eng.*, *3*(138), 171-176.

Roscoe, S. G., Fuller, K. L., & Robitaille, G. (1993). An electrochemical study of the effect of temperature on the adsorption behavior of β-lactoglobulin. *Journal of Colloid and Interface Science*, *160*, 243–251.

Rosmaninho, R., Santos, O., Nylander, T., Paulsson, M., Beuf, M., Benezech, T., ... & Melo, L. F. (2007). Modified stainless steel surfaces targeted to reduce fouling–Evaluation of fouling by milk components. *Journal of Food Engineering*, *80*(4), 1176-1187.

Tan-Kintia, R. H., & Fox, P. F. (1999). Effect of various preheat treatments on the heat stability of unconcentrated milk. *International dairy journal*, *9*(3-6), 219-225.

Singh, H., & Tokley, R. P. (1990). Effects of preheat treatments and buttermilk addition on the seasonal variations in the heat stability of recombined evaporated milk and reconstituted concentrated milk. *Australian Journal of Dairy Technology*, *45*(1), 10-16.

Smiddy, M. A., Martin, J. E., Kelly, A. L., De Kruif, C. G., & Huppertz, T. (2006). Stability of casein micelles cross-linked by transglutaminase. *Journal of dairy science*, *89*(6), 1906-1914.

Sweetsur, A. W. M., & Muir, D. D. (1980). The use of permitted additives and heat-treatment to optimize the heat-stability of skim milk and concentrated skim milk. *International Journal of Dairy Technology*, *33*(3), 101-105.

Wu, J., Li, H., A'yun, Q., Doost, A. S., De Meulenaer, B., & Van der Meeren, P. (2021a). Conjugation of milk proteins and reducing sugars and its potential application in the improvement of the heat stability of (recombined) evaporated milk. *Trends in Food Science & Technology*, *108*, 287-296.

Wu, J., Li, H., A'yun, Q., Doost, A. S., De Meulenaer, B., & Van der Meeren, P. (2021b). Conjugation of milk proteins and reducing sugars and its potential application in the improvement of the heat stability of (recombined) evaporated milk. *Trends in Food Science & Technology*, *108*, 287-296.

Zouaghi, S., Barry, M. E., Bellayer, S., Lyskawa, J., André, C., Delaplace, G., ... & Jimenez, M. (2018). Antifouling amphiphilic silicone coatings for dairy fouling mitigation on stainless steel. *Biofouling*, *34*(7), 769-783.

Zouaghi, S., Bellayer, S., Thomy, V., Dargent, T., Coffinier, Y., Andre, C., ... & Jimenez, M. (2019). Biomimetic surface modifications of stainless steel targeting dairy fouling mitigation and bacterial adhesion. *Food and bioproducts processing*, *113*, 32-38.

Appendix

Fouling rig modifications

Tara R. Murphy, Eoin W. Finnegan, Tom F. O'Callaghan, James A. O'Mahony

School of Food and Nutritional Sciences, University College Cork, Cork, Ireland

Declaration

This appendix was written by author Tara R. Murphy (TRM) and reviewed by all co-authors.

1.1. Introduction

A custom-built fouling rig, used in a previous study involving fouling of whey protein solutions (Hebishy *et al.,* 2019), was used to study the fouling behaviour of concentrated skim milk. As the fouling material in this present study is different to the previous studies using this rig, several modifications were made to the fouling rig set-up in order to optimise its use for concentrated skim milk.

1.2. Original fouling rig set-up

The original fouling rig set-up is shown in Figure 1. It consisted of a stainless steel tubular heat exchanger of length 58.6 cm and internal diameter 2 cm (Liam A. Barry Ltd., Cork, Ireland), heated using water as a heating medium via the connected circulating water bath (Grant, LT ecocool™100, Cambridge, UK). Two pressure transducers (PR-33X, Keller-druck, Dorchester, UK), located before and after the heat exchanger, gave measurements of temperature and pressure in-line. The stainless-steel feed vessel, of height 14.7 cm and width 15.5 cm (reducing down to 1 cm at the base of the vessel) had a capacity of 3.0 L. Connected to the feed vessel was a positive displacement, progressive cavity pump (Torqueflow, Sydex, UK), which pumped the fluid at a flow rate controlled by a variable speed drive to a maximum capacity of 50 Hz. A three way ball valve, located after the pump, allowed for the batch recirculation system to be drained at the end of the run. The pressure of the system could be set using a manual diaphragm throttling valve, with the pressure being measured with an analogue pressure gauge (1107J486, WIKA, Los Angeles, CA, USA). A thermocouple was mounted to the feed vessel as an additional measure of temperature (Digitron 2024T Digital Thermometer Pt100, Port Talbot, UK).

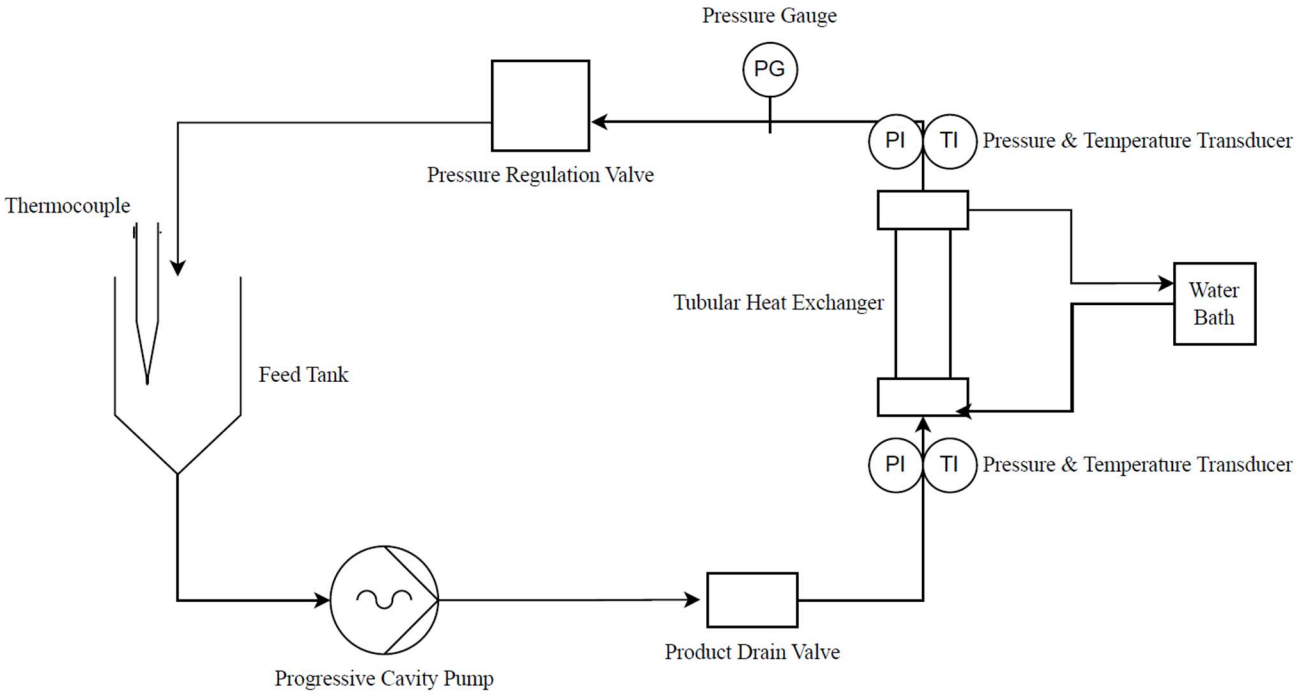

Figure 1.3.: Process flow diagram of fouling rig set up used by Hebishy et al (2019), showing the tubular heat exchanger, feed vessel, positive displacement progressive cavity pump, two electronic pressure transducers, circulating water bath, thermocouple, product drain valve, pressure regulation valve and analogue pressure gauge.

1.3. Modified fouling rig

The modified fouling rig set-up is shown in Figure 2, with the modifications highlighted in red. The first modification was to replace the feed vessel, as the design caused formation of a skin on the surface due to the lack of turbulence in the vessel causing surface dehydration, which was undesirable as this skin could have contained material that would foul the heat exchanger. The newly designed feed vessel (Liam A. Barry Ltd., Cork, Ireland), of height 17 cm and width 15.5 cm (reducing down to 6 cm at the base of the vessel), was rounded at the bottom instead of the original angular design (Figure 3). The feed tube was redesigned to have a tangential entry port, instead of directly down into the vessel as in the original design, with an additional piping inside the vessel at an angle to promote turbulent flow within the vessel without causing aeration or foaming (Figure 4). The new feed vessel also had a clear acrylic lid (with entry points for the thermocouple and pH/conductivity meter (Metler Toledo, SevenGo Duo, SG23, Switzerland)) to prevent evaporation of the material while still being able to take measurements and observe inside the vessel.

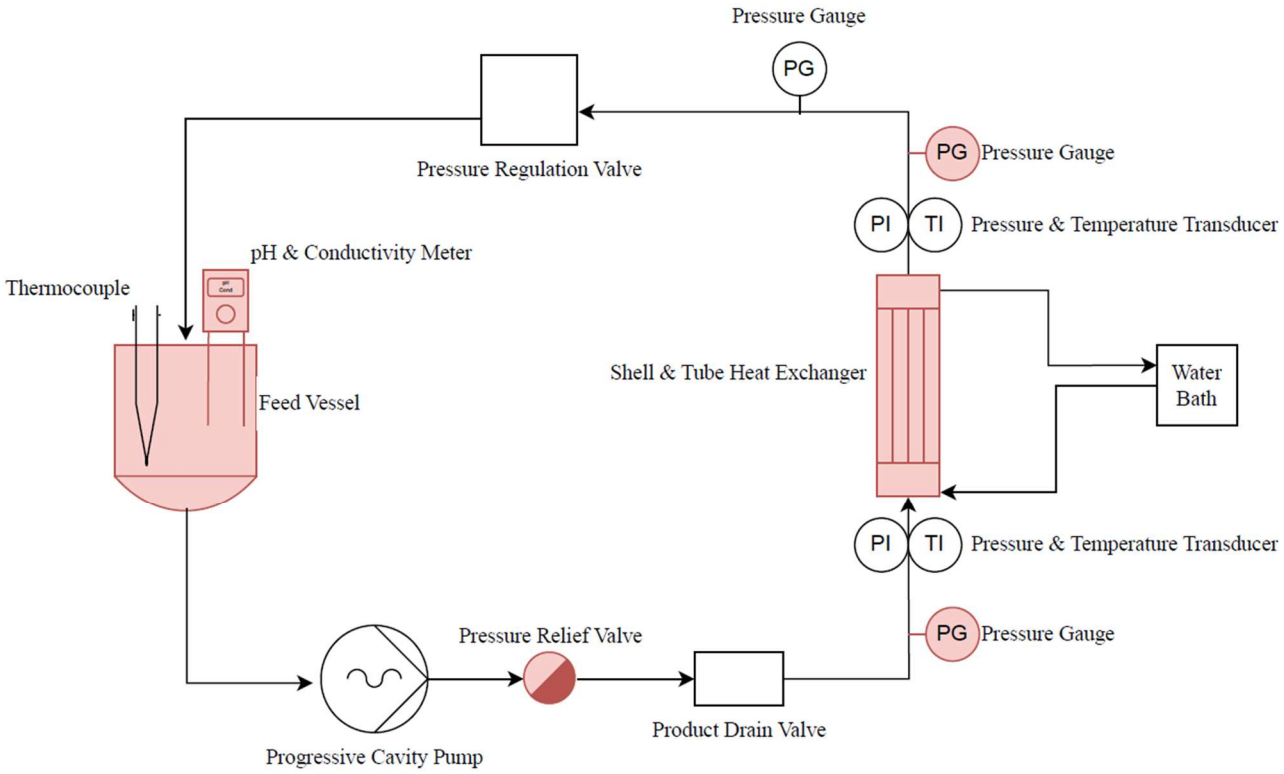

Figure 1.4.: Process flow diagram of modified fouling rig set up, showing the shell and tube heat exchanger, feed vessel, positive displacement progressive cavity pump, pressure relief valve, two electronic pressure transducers, circulating water bath, thermocouple, pH and conductivity meter, product drain valve, pressure regulation valve, and analogue pressure gauges. The areas highlighted in red are the modifications.

Figure 1.3.: The feed vessel from the original fouling rig set-up (left) and the feed vessel from the modified fouling rig set-up (right).

Figure 1.4.: Top down view of the feed vessel from the modified fouling rig set-up, showing the feed tube designed to return product at an angle to promote turbulence without aeration or foaming.

1.3.1. Heat exchanger

The next modification to the fouling rig involved changing the tubular heat exchanger to a shell and tube heat exchanger (Liam A. Barry Ltd., Cork, Ireland), with length of 33.5 cm, internal diameter of 5 cm, and nine inner tubes of diameter 0.8 cm each. The reasoning for the change of heat exchanger due to the greater surface area (766.8 cm^2), when compared to the original heat exchanger (374.5 cm^2), as this promotes heat transfer. As well as this, the design encourages the build up of fouling, as the inner tubes had a narrow diameter and there was a larger surface area for the fouling deposits to build-up on, with Figure 5 showing the fouled versus unfouled heat exchanger.

Figure 5*: Top down view of the inside of the shell and tube heat exchanger, showing the heat exchanger fouled (left) and unfouled (right).*

1.3.2. Safety features

In terms of safety-related components, a pressure relief valve was added between the pump and the product drain valve. Its purpose was to limit the amount of compressed air pressure in the system in order to prevent the pressure building up above 4 bar, which would cause damage to the machinery.

1.3.3. Pressure measurement

The final addition to the fouling rig was two additional analogue pressure gauges on either side of the temperature and pressure transducers as a supplementary pressure measure in case of issues with the transducers.